CHARACTERIZATION OF AGE-RELATED CHANGES IN MOTOR ABILITY AND LEARNING AND MEMORY IN THE 5XFAD MOUSE MODEL OF ALZHEIMER'S DISEASE

by

Timothy Patrick O'Leary

Submitted in partial fulfilment of the requirements
for the degree of Doctor of Philosophy

at

Dalhousie University
Halifax, Nova Scotia
May 2013

DALHOUSIE UNIVERSITY

DEPARTMENT OF PSYCHOLOGY AND NEUROSCIENCE

The undersigned hereby certify that they have read and recommend to the Faculty of Graduate Studies for acceptance a thesis entitled "CHARACTERIZATION OF AGE-RELATED CHANGES IN MOTOR ABILITY AND LEARNING AND MEMORY IN THE 5XFAD MOUSE MODEL OF ALZHEIMER'S DISEASE" by Timothy Patrick O'Leary in partial fulfilment of the requirements for the degree of Doctor of Philosophy.

Dated: May 10, 2013

External Examiner: _____

Research Supervisor: _____

Examining Committee: _____

_____

Departmental Representative: _____

DALHOUSIE UNIVERSITY

DATE: May 10, 2013

AUTHOR: Timothy Patrick O'Leary

TITLE: CHARACTERIZATION OF AGE-RELATED CHANGES IN MOTOR ABILITY AND LEARNING AND MEMORY IN THE 5XFAD MOUSE MODEL OF ALZHEIMER'S DISEASE

DEPARTMENT OR SCHOOL: Department of Psychology and Neuroscience

DEGREE: PhD CONVOCATION: October YEAR: 2013

_____

Signature of Author

TABLE OF CONTENTS

LIST OF TABLES

LIST OF FIGURES

Abstract

The 5XFAD mouse is a double transgenic model of Alzheimer's disease (AD), which harbors a human amyloid precursor protein transgene with three mutations (K670N/M671L, I716V, V717I) and a human presenilin-1 transgene with two mutations (M146L, L286V). These mutations act additively to produce large amounts of amyloid-beta (Aβ) and rapid development of AD-related pathology, including Aβ-plaques, neuroinflammation, synapse loss, impaired synaptic plasticity and death of layer 5 cortical neurons (Oakley et al., 2006, J. Neurosci., 26, 10129-10140). Despite the extensive characterization of neuropathology in the 5XFAD mouse, much less research has been completed characterizing age-related changes in behaviour. Sex, the albinism producing tyrosinase mutation (*Tyr*^{c}), the retinal degeneration phosphodiesterase 6b mutation (Pde6b^{rd1}) and the limb-girdle muscular dystrophy 2B dysferlin mutation (*D*ysf^{im}) are genetic factors present in the background strain (C57BLxSJL) of the 5XFAD mouse and other AD models. However, background genetic factors are rarely controlled, and their influence on AD-related behavioral phenotypes is largely unknown. Therefore, the objectives of this thesis were to characterize age-related changes in behaviour of the 5XFAD mouse, and determine the extent to which background genetic factors influence the expression of AD-related behavioral phenotypes. Male and female 5XFAD and wild-type (WT; C57BL6xSJL F2) mice completed a behavioural test battery at 3-4, 6-7, 9-10, 12-13 and 15-16 months of age in a cross-sectional experimental design. In experiment 1, motor ability was assessed with the open-field (locomotor activity), rota-rod (motor coordination and learning), balance beam (balance) and the wire and grid suspension tests (grip-strength). 5XFAD mice weighed less than WT mice at 9-15 months of age, and also reared less on the open-field and performed worse on the rota-rod. 5xFAD mice also travelled less distance on the open-field, fell faster on the balance beam and showed impaired grip-strength at 12-13 months of age. The *D*ysf^{im} mutation has been previously shown to produce muscular weakness and impair motor function, but mutant *D*ysf^{im} did not impair the motor performance of either WT or 5XFAD mice. In experiment 2, 5XFAD and WT mice were tested on the Morris water maze to assess visuo-spatial learning and memory. 5XFAD mice were impaired in acquisition and reversal learning, but not memory at 6 and 9 months of age. Motor impairments in 5XFAD mice impaired swimming ability and confounded learning and memory performance of mice at 12 and 15 months. Female mice performed worse than male mice, and albino mice performed worse than pigmented mice, demonstrating that background genetic factors influence the performance of mice on the Morris water maze. In experiment 3, olfactory learning and memory was assessed with an olfactory digging discrimination test. 5XFAD mice did not differ from WT mice in memory performance at any age tested. We then examined Aβ plaque pathology in 5XFAD mice and confirmed the presence of Aβ deposits in brain regions associated with motor function and learning and memory. Very few Aβ deposits were present in the cerebellum suggesting plaque pathology in the basal ganglia and/or motor cortex impairs motor function. Extensive Aβ plaque deposition was also found in the olfactory memory system despite the lack of olfactory memory impairment in 5XFAD mice. These results indicate that the 5XFAD mouse is a useful model for Aβ-pathology, cognitive and motor impairments observed in AD, but it is required that sex and albinism are properly controlled in the assessment of cognitive function.

LIST OF ABBREVIATIONS USED

AD Alzheimer's Disease

DSM-IV Diagnostic and Statistical Manual for Mental Disorders 4^{th} edition

NINCDS-ADRDA National Institute of Neurological and Communicative Disorders and Stroke and the Alzheimer's Disease and Related Disorders Association

MMSE mini-mental state exam

Aβ amyloid beta

NFT neurofibrillary tangles

APP amyloid precursor protein

CA cornu ammonis

Il-1β interleukin 1 beta

NO nitric oxide

FAD familial Alzheimer's Disease

SAD sporadic Alzheimer's Disease

PS1 presenilin-1

PS1 presenilin-2

Ca^{2+} calcium

MAPT Microtubule Associated Protein Tau

LTP long-term potentiation

α-CTF alpha c-terminal fragment

sAPPα soluble amyloid precursor protein alpha

AICD APP intra-cellular domain

β-CTF beta c-terminal fragment

sAPPβ soluble amyloid precursor protein beta

$A\beta_{40}$ 40-amino-acid isoform of Aβ

$A\beta_{42}$ 42-amino-acid isoform of Aβ

5'UTR five prime untranslated region

Thy-1 thymus antigen 1

5XFAD five times familial Alzheimer's disease

WT wild-type

cDNA complimentary deoxyribonucleic acid

MMRRC mutant mouse regional resource center

Sw Swedish

Fl Florida

Lon London

$Pde6b^{rd1}$ phosphodiesterase 6b retinal degeneration-1 mutation

PCR polymerase chain reaction

PND post-natal development

GFAP glial fibrillary acidic protein

PSD-95 post-synaptic density 95

Cdk5 cyclin-dependent kinase 5

ChAT choline acetyltransferase

BDNF brain derived neurotrophic factor

Trk-B Tyrosine Kinase B

mRNA messenger ribonucleic acid

CD45 cluster of differentiation 45

COX2 cyclooxygenase 2

LC locus coeruleus

fEPSPs field extra-cellular post-synaptic potentials

AHP after-hyperpolarization

EPM elevated plus maze

OF open-field

MWM Morris water maze

EPM elevated-plus maze

OF open-field

CS conditioned stimulus

UCS unconditioned stimulus

CR conditioned response

BACE1 β-site amyloid precursor protein-cleaving enzyme 1

GAP-43 growth associated protein 43

GAD-67 glutamate decarboxylase 67

eIF2α eukaryotic translation initiation factor-2α

KKT Kamikihi-to

AβpE3 pyroglutamate isoform of amyloid beta

NSAIDs nonsteroidal anti-inflammatory drugs

MCSF-R macrophage colony stimulating factor receptor

PKC Protein kinase C

NA noradrenaline

Dysf dysferlin

Tyr tyrosinase

ANOVA analysis of variance

SEM standard error of mean

OCA2 oculocutaneous albinism II

MOB main olfactory bulb

dH_2O distilled water

PBS phosphate buffer saline

PBTX phosphate buffer with triton-x

DAB 3.3'-diaminobenzidine tetrahydrochloride

PRC parietal cortex

SMC somatosensory cortex

ENC entorhinal cortex

AM amygdala

HIP hypothamus

TH thalamus

PL pyramidal layer

ON oriens layer

DG dentate gyrus

MC motor cortex

PIR piriform cortex

CPU caudate putamen

GP globus pallidus

CRB cerebellum

RN reticular nucleus

STN spinal trigmenial nucleus

VN vestibular nucleus

PT pyramidal tract

AON anterior olfactory nucleus

GR granular layer

AC anterior commissure

ONL olfactory nerve layer

GL glomerular layer

PL internal/external plexiform layers

ML mitral cell layer

LT lateral olfactory tract

TT tenia tecta

OFC orbitofrontal cortex

ACKNOWLEDGEMENTS

I would like to acknowledge my PhD supervisor Dr. Richard Brown for his guidance and support during this thesis. His dedication and passion for science is inspiring, and I am grateful for the time and opportunities I have had to learn from him during my PhD degree. Thanks to Dr. Ian Weaver , Dr. Sultan Darvesh and Dr. Leslie Phillmore for sitting on my thesis committee and for their valued guidance concerning the thesis research. Special thanks to Dr. Douglas Wahlsten for taking the time to be the external examiner for my defense, and for his insightful comments concerning the thesis.

I would also like to acknowledge the work completed by members of Dr. Brown's laboratory who helped complete the thesis experiments. Special thanks to Rhian Gunn for help in breeding the mice and organization of the research project. Thanks to Kurt Stover, Hector Mantolino, and Dietmar Hestermann for assistance in completing behavioural experiments. Thanks to Ian MacDonald and Andrew Reid for completing immunohistochemistry experiments and assistance with microscopy. Additional thanks to students who assisted in scoring countless hours of video from behavioural tests, including Mark Bartolacci, Kevin Le, Maximillian Fiander, Stephanie Pelletier, Jocelyne Whitehead, Jessica Soley and Kaitlyn Gordon (apologies to anyone who is omitted).

I would also like to thank all members of the Brown lab for taking the time to discuss research and for creating an overall positive work environment during my graduate training. Thanks to my family, for their support and understanding during this process. I am also forever grateful to my fiancée Emily LeDue, who provided unwavering support and encouragement while I completed this thesis.

CHAPTER 1 INTRODUCTION

1.1 Alzheimer's Disease: A General Review

Alzheimer's Disease (AD) is an age-related neurodegenerative disease that is the leading cause of dementia in adults over the age of 65. The prevalence of AD is increasing with the aging of the growing global population, and longer life-expectancy from advancements in medical care. There were over 35 million cases of dementia worldwide in 2010, and there is estimated to be a three-fold increase in the number of cases (115 million) by 2050 (World Health Organization and Alzheimer's Disease International, 2012). This rapid increase in AD cases will lead to an eventual world-wide epidemic of AD.

AD greatly impairs the quality of life for those affected by the disease, and places considerable financial burden through medical care costs. In Canada, the cost for AD medical care was estimated to be 8 billion dollars in 2008, and is predicted to be 92 billion in 2038 (Alzheimer's Society of Canada, 2010). Over half of all dementia cases world-wide are in developing countries, which may not have sufficient health care systems to meet the needs of the increasing numbers of AD patients (Ferri et al., 2005). Furthermore, considerable time demands, financial burden and psychological stress will be placed on family members who frequently provide direct or indirect care of AD patients (Langa et al., 2001).

Because of the surge of AD patients worldwide, there is an urgency to better understand the etiology of AD and to develop novel treatments for the disease. This chapter provides a brief review of AD, its symptoms, risk factors, proposed causes and

current treatments. Because current treatments do not prevent or slow disease progression, there is a quest to develop novel disease-modifying treatments for AD.

1.2 Behavioural Symptoms

The first documented case of AD was the 51 year-old female patient Auguste D, who displayed a variety of behavioral abnormalities including memory impairments, aphasia, disorientation, paranoia, hallucinations and psychosocial impairment (Maurer et al., 1997). Following diagnosis of AD, symptom progression depends on age; and life expectancy is 8.3 years when AD is diagnosed at 65 years of age, and 3.4 years when AD is diagnosed at 90 years of age (Brookmeyer et al., 2002). However, on average, symptoms typically begin to develop 2.8 years prior to official diagnosis of AD, in a prodromal phase referred to as mild-cognitive impairment. It is currently recognized that the expression of behavioural symptoms among the clinical AD population is highly heterogeneous in prevalence, age of onset, and rate of decline. This chapter provides a brief review of methods for diagnosing AD based on behavioral symptoms from three different domains: cognitive dysfunction, neuropsychiatric symptoms and motor impairments. However, other neurological disorders produce symptoms within these domains, and thus a diagnosis is for "probable-AD", until a definitive autopsy can be completed (Schneider et al., 2007).

1.2.1 Diagnosis Of AD

The diagnosis of probable-AD can be completed by family physicians or specialists through clinical evaluation (Feldman et al., 2008). Diagnosis is determined using criterion from the Diagnostic and Statistical Manual for Mental Disorders 4th edition (DSM-IV) or the National Institute of Neurological and Communicative

Disorders and Stroke and the Alzheimer's Disease and Related Disorders Association (NINCDS-ADRDA). Clinical evaluation typically consists of an interview to obtain patient history, and to determine if risk factors for AD (head trauma, family history of dementia etc.), vascular dementia (stroke, hypertension, diabetes) or other contributing factors (alcohol abuse or renal failure) are present. Interviews with family members are also completed to corroborate cognitive dysfunction, and identify behavioural changes that might not be apparent to the patient, especially changes in ability to complete activities of daily living. A physical examination of the patient is also completed to determine if there is any indication of stroke. Lastly a brief cognitive test is administered, such as the mini-mental state exam (MMSE), which assesses levels of gross cognitive ability. With this information a diagnosis of dementia can be made, although additional tests can be completed to obtain a differential diagnosis relative to other non-Alzheimer's dementias (Feldman et al., 2008). Computed tomography and magnetic resonance imaging can be used to determine if atrophy is present in the brain and to exclude other potential factors such as brain tumors, subdural hematomas and hydrocephalus. Neuropsychological assessment can also be completed to provide a more sensitive assessment of cognitive ability and aid in discrimination of the patient's cognitive profile across dementia sub-types. Several biomarkers have also been proposed to assist with AD-diagnosis, such as measurement of Aβ and tau proteins within cerebrospinal fluid and levels of cerebral glucose with positron emission tomography (Craig-Schapiro et al., 2009). However, these biomarkers are not recommended for routine use in diagnosis of AD until further research is completed validating and standardizing these methods (McKhan et al., 2011).

1.2.2 Cognitive Dysfunction

The cognitive dysfunction most commonly associated with AD is impairment in episodic memory (for review see Weintraub et al., 2012), which consists of memory for information associated with previous personal life experiences (i.e. time, place and details of daily-life events) (Dickerson and Eichenbaum, 2010). This memory impairment is thought to reflect problems with the consolidation of novel information rather than retrieval, and can lead to profound anterograde amnesia. Deterioration of semantic memory networks also occurs, leading to impairments in the retrieval of previously acquired factual knowledge, general concepts and meanings of words. These semantic memory impairments also lead to language impairment due to difficulty in generating contextually appropriate words. Difficulty is also observed in planning and complex problem solving tasks due to impairments in executive functioning, while the active manipulation of information in short-term memory is impaired due to working memory dysfunction. Impairments are also observed in attention, in both the efficient allocation of attention resources in tasks that required divided attention, and in the shifting of attention from one stimulus to another. Impairments are observed in visuo-spatial perceptual skills and navigational ability (Kaskie and Storandt, 1995; Monacelli et al., 2003), which can produce spatial disorientation and cause people with AD to become lost in familiar environments. Lastly, olfactory related cognitive impairment occurs in the ability to identify and discriminate between familiar odours (Mesholam et al., 1998).

1.2.3 Neuropsychiatric Symptoms

Patients with AD often develop neuropsychiatric symptoms, and these neuropsychiatric symptoms are more strongly associated with caregiver distress than

cognitive impairment (Kaufer et al., 1998). Neuropsychiatric symptoms that develop in AD are heterogeneous, and can consist of delusions, hallucinations, agitation, depression, anxiety, euphoria, apathy, disinhibition, irritability, abberant motor behaviour, sleep disturbances and eating disorders (Poncet et al., 2012). Although apathy, depression, anxiety and agitation tend to be more frequent in early stages of AD, most neuropsychiatric symptoms become more frequent in later stages of AD (van Vilet et al., 2012). When eating disorders are present (Poncet et al., 2012), they may cause and/or contribute to body weight loss which is also commonly found in AD (Guerin et al., 2005). Among the neuropsychiatric symptoms, apathy, anxiety and hallucinations are associated with impairment in global functioning and a more rapid decline in global functioning ability (Wadsworth et al, 2012).

1.2.4 Motor Ability

Although impairments in motor function tend to be more common in non-Alzheimer's dementias (Allan et al, 2005), patients with AD are more likely to develop motor impairments than non-demented age-matched controls. These impairments are thought to be due to impaired functioning of the extra-pyramidal motor system and consist of bradykinesia of the limbs or face, rigidity of the limbs and higher-level gait disorders (Mitchell, 1999). Resting tremor can also occur but is less common relative to the other extra-pyramidal symptoms. Although motor symptoms are more common and severe in later stages of the disease, they predict a faster rate of functional decline in AD and are associated with increased risk of physical injury due to falling (Allan et al., 2005).

1.3 Neuropathological Symptoms

The initial characterization of the AD brain revealed the two pathology hallmarks of AD, Aβ plaques and neurofibrillary tangles (NFT) (Maurer et al., 1997). Although Aβ plaques and NFTs also develop in patients without dementia, there is an increased prevalence and abundance of Aβ plaques and NFTs in AD. Aβ plaques consist of extra-cellular fibrils of aggregated Aβ peptides, which are insoluble and resistant to clearance via proteolysis (Galimberti and Scarpini, 2011). Aβ peptides are produced after cleavage from the amyloid precursor protein (APP) via β-secretase and γ-secretase. APP is a transmembrane protein found at the synapses of neurons, and has been proposed to be involved in promoting neurite growth, synaptogenesis and cell adhesion (Muller and Zheng., 2012).

There are three morphologically distinct sub-types of Aβ plaques consisting of (1) diffuse plaques, which have a generally homogenous distribution, (2) fibrillar plaques, with a dense center of aggregated Aβ surrounded by spoke-like extensions and (3) dense-cored plaques, which contain dense central cores of Aβ, located within a region of sparse aggregated Aβ, all of which is surrounded by an outer rim of dense aggregated Aβ (Dickson and Vickers, 2001). Although all three sub-types are found in early and late stages of AD, fibrillar plaques tend to be more common in late stages of AD and more commonly contain dystrophic or degenerating neurites typically associated with senile (neuritic) plaques.

In general, Aβ plaque pathology in AD is greatest in regions of the medial temporal lobe and association cortices, while primary sensory and motor regions have less severe pathology. The temporal pattern of Aβ plaque development in the cortex was

divided into three stages by Braak and Braak (1997), and subsequently revised into five stages (Thal et al., 2002) to include sub-cortical regions. Each stage involves the formation of plaque deposits in new regions, as well as regions from previous stages. In stage 1, small amounts of diffuse Aβ plaques are initially found throughout all lobes of the cortex. In stage 2, the number of plaques within the cortex increases, along with the development of plaques within the entorhinal region, CA1 of the hippocampus, insular cortex and amygdala. In stage 3, Aβ plaques also develop in subcortical regions, including the caudate nucleus, putamen, basal forebrain nuculei, thalamus, hypothalamus etc. In stage 4, plaques are found in brain-stem nuclei, including the substantia nigra, superior and inferior colliculi, red nucleus etc. In stage 5, plaques are then observed in additional brain-stem nuclei (pontine nucleus, raphe nucleus, locus coeruleus etc.) and within the granular layer of the cerebellum. Within the cortex, plaques are distributed across all cortical layers but have larger densities in layers II, III and IV, and tend to be largest in size in layers III and V (Pearson et al., 1985; Rogers and Morrison, 1985).

Neurofibrillary tangles consist of intra-cellular aggregations of hyper-phosphorylated microtubule associated protein tau. Tau is normally bound to microtubules, thus stabilizing the microtubule cytoskeleton and permitting growth through polymerization. Phosphorylation of tau causes the tau protein to detach from the microtubule, leading to destabilization of the microtubule, and aggregation of Tau into filaments. The aggregated tau disrupts normal cellular function, and upon cell death an extracellular “ghost tangle” remains. Like senile plaques, greater levels of NFT pathology are found in regions of the medial temporal lobe and association cortices, with less pathology in primary sensory and motor cortices. The development of NFT within

the cortex can be divided into 6 stages (Braak and Braak, 1997). NFTs are first observed in the temporal lobe in the transentorhinal cortex (stage I), followed by NFTs in the adjacent entorhinal cortex (stage II). NFTs are next observed in the hippocampus and spread throughout the temporal cortex (stage III), before they are found in the adjacent association cortices (stage IV). In later stages NFTs continue to spread superolaterally (stage V), and are eventually found in primary cortical regions (stage VI). Within the cortex, NFTs are often associated with pyramidal neurons in layers III and IV, which form cortico-cortical and cortico-subcortical connections with other brain regions (Pearson et al., 1985).

Neuroinflammation within the brain is also present in AD, and appears to be at least partially produced by the abnormal accumulation of Aβ and Tau in the brain parenchyma (Hensley, 2010). Indeed, increased numbers of microglia are found surrounding Aβ plaques, suggesting the Aβ actively recruits microglia, and that microglia are involved in the phagocytic removal of Aβ and degenerating neurons near plaques. Reactive astrocytes are also found near plaques which show increased local release of inflammatory cytokines and other pro-inflammatory paracrine molecules, thus contributing to the initiation and/or maintenance of the inflammatory response (Hensley, 2010). Although acute inflammatory responses can be neuroprotective, chronic inflammation within the brain has neurodegenerative effects due to the elevated production of neurotoxic agents such as tumor necrosis factor-α, Il-1β and NO from microglia (Block et al., 2007).

Neurodegeneration occurs in the brains of AD patients, and is generally better correlated with cognitive decline than either Aβ plaques or NFTs. Global atrophy of the

cortex is observed in AD, with a 20-25% overall reduction in cortical volume, and the extent of cortical loss is correlated with mini-mental state scores (Mouton et al., 1998). Neurodegeneration is also found within the hippocampus, with cell loss in the subiculum, CA1 and hilus of the dentate gyrus, but not in the CA2-3 or granule layer of the dentate gyrus (West et al., 2004). Increased age-related loss of synapses has also been found within the cortex in AD, and this synaptic loss is correlated with cognitive impairment moreso than Aβ plaques or NFTs (Terry et al., 1991).

1.4 Genetic And Environmental Risk Factors For AD

There are two forms of AD, familial AD (FAD) and sporadic AD (SAD), which differ in the age of onset and risk factors for development of the disease. FAD has an early age of onset (< 60 years of age), accounts for less than 5% of total AD cases, and has a large genetic component. Currently 24 mutations have been identified in the APP gene (21q21.3) (Goate et al., 1991, Mullan et al., 1992; Eckman et al., 1997), 185 mutations in the presenilin -1 gene (PS1) (14q24.3) (Campion et al., 1995; Sherrington et al., 1995) and 14 mutations in the presenilin-2 gene (PS2) (1q31-42) (Rogaev et al., 1995), all of which have been linked to the development of FAD (for review see Tanzi et al., 2012). PS1 and PS2 proteins are located within the transmembrane γ-secretase complex. The majority of these FAD mutations are inherited in an autosomal dominant fashion, are fully penetrant, and influence the proteolysis of APP by increasing the ratio of $A\beta_{42}$ produced relative to $A\beta_{40}$.

SAD has a later age of onset, accounts for the majority of AD cases, and is due to a combination of both environmental and genetic factors. The strongest risk factor for the development of SAD is age, and it is estimated that after 65 years of age the prevalence

of AD doubles every 5 years (Brookmeyer et al., 2007). The most conclusively demonstrated genetic risk factor for SAD is the ε4-allele of the apolipoprotein E gene (19q13.2) (Strittmatter et al., 1993), which confers a 4 to 10 fold risk of developing AD, depending on whether one or two ε4-alleles are inherited. Apolipoprotein E is involved in lipid metabolism and transport, but may also be involved in the removal of Aβ in the brain. Genome-wide association studies have revealed alleles in 15 other genes which confer much smaller risks of developing AD (~1.15 odds ratio), and these alleles have roles in Aβ production, Aβ clearance, lipid metabolism, immune responses and cellular signaling (see Tanzi 2012 for review).

A number of other risk factors have also been linked to the development of SAD, but the evidence in support of these factors is generally weak (for review see Daviglus et al., 2011). Increased risk of developing AD has been associated with head injury, a history of depression, decreased cognitive reserve due to lower education levels, diabetes mellitus, hyperlipidemia and tobacco use (Fleminger et al., 2003; Daviglus et al., 2011). Decreased risk of developing AD has been associated with non-steroidal anti-inflammatory drugs, regular physical exercise, moderate alcohol consumption, a mediterranean-type diet and folic acid intake (Lindsay et al., 2002). AD is also more prevalent in females (62% to cases) than in males, but it is unclear if sex is a reliable risk factor for AD due to lower background mortality rates in females than males (Brookmeyer et al., 2007). There is some evidence that suggests, however, that following diagnosis of AD, symptoms worsen at a faster rate in males relative to females (for review see Dubal et al., 2012).

1.4.1 The Amyloid Cascade Hypothesis For The Development Of AD

The amyloid cascade hypothesis for the pathogenesis of AD suggests that the primary disease mechanism in AD is abnormal processing of APP. The other pathological changes in the disease, such as NFT, cell loss and cognitive impairment, occur as a result of Aβ deposition and potential dysregulation of intra-cellular Ca^{2+} homeostasis (Hardy and Higgins, 1992). There is considerable evidence in support of this hypothesis, including (1) the identification of Aβ as the primary component of senile plaques, (2) localization of APP to chromosome 21, providing a common source for plaque pathology in both AD and Down's syndrome and (3) identification of FAD mutations within APP and other proteases which alter proteolysis of APP and increase aggregation of Aβ into fibrils (Hardy and Selkoe, 2002). Additional evidence also supports Aβ pathology preceding NFT formation, because mutations in the microtubule associated protein tau (MAPT) gene leads to frontotemporal dementia and NFT production, but do not increase Aβ plaque formation. Also, transgenic mice that have both mutant MAPT and APP transgenes show elevated NFT formation, while the plaque pathology remains unaltered (Hardy and Selkoe, 2002).

Limitations of the initial formulation of the amyloid cascade hypothesis have led to revisions concerning the species of Aβ producing cognitive impairment. Aβ plaque load does not correlate well with the extent of cognitive impairment in patients with AD (Terry et al., 1991). Considerable research has now shown that soluble oligomers of Aβ are neurotoxic and lead to synaptic dysfunction in AD, rather than soluble monomers or insoluble fibrils. Indeed, intra-cerebral injection of Aβ oligomers leads to impaired synaptic plasticity measured by long-term potentiation (LTP) and impaired learning and

memory ability (Walsh et al., 2002). Moreover, some transgenic mouse models of AD show cognitive impairment prior to the development of extra-cellular plaques, suggesting that soluble Aβ oligomers can produce synaptic dysfunction leading to cognitive impairment (Mucke et al., 2000).

1.4.2 Proteolysis Of Aβ From APP

Aβ is cleaved from APP through the sequential action of the α-, β- and γ-secretases (for review see Minati et al., 2009). α-secretase cleaves APP at the N-terminal portion of the protein, leaving Aβ attached to the c-terminal fragment (α-CTF) within the plasma membrane, while releasing a soluble extra-cellular portion of APP (sAPPα) (Figure 1.1). After cleavage by α-secretase, APP is then cleaved by γ-secretase near the C-terminus fragment, releasing the non-toxic extra-cellular p3 portion of Aβ, and the APP intra-cellular domain (AICD). β-secretase also cleaves APP near the N-terminal portion, leaving Aβ and the c-terminal fragment (β-CTF) at the plasma membrane, while releasing a soluble extra-cellular portion of APP (sAPPβ). However, following cleavage by β-secretase, γ-secretase then cleaves APP near the C-terminus fragment, producing Aβ 38-43 amino acids in length, and the AICD (Figure 1.2). The 40-amino-acid isoform of Aβ ($A\beta_{40}$) is considered less toxic and is produced in larger amounts than the 42-amino-acid isoform of Aβ ($A\beta_{42}$) which is toxic and more prone to aggregation. The FAD mutations in APP are located near the cleavage sites of both β- and γ-secretase. These mutations increase the production of $A\beta_{42,}$ by either increasing the amount of both $A\beta_{40}$ and $A\beta_{42}$ peptides (i.e. Swedish APP mutation), or by increasing the amount of $A\beta_{42}$ produced relative to $A\beta_{40}$. FAD mutations in PS1and PS2 also increase production of $A\beta_{42}$ produced relative to $A\beta_{40,}$ by influencing γ-secretase activity.

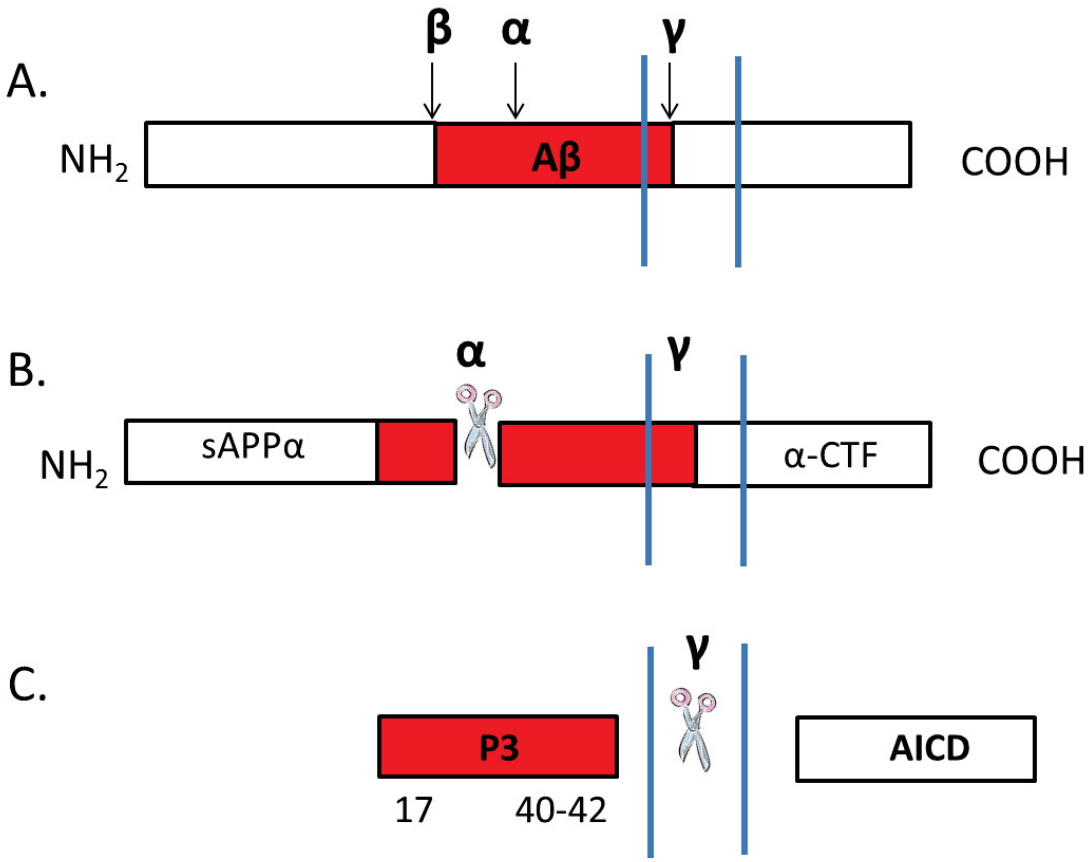

Figure 1.1. Metabolism of APP via α-secretase pathway produces non-amyloidogenic variants of Aβ. (A) APP is located in the plasma membrane (vertical lines) and α-secretase cleaves APP within the Aβ region, near the N-terminal portion. (B) This leaves Aβ and the C-terminal fragment (α-CTF) at the plasma membrane, while releasing a soluble N-terminal fragment (sAPPα). (C) Following cleavage by α-secretase, γ-secretase then cleaves APP near the C-terminal fragment producing the short non-toxic P3 portion of Aβ (17-42 amino acids in length) and the APP intra-cellular C-terminal domain (AICD).

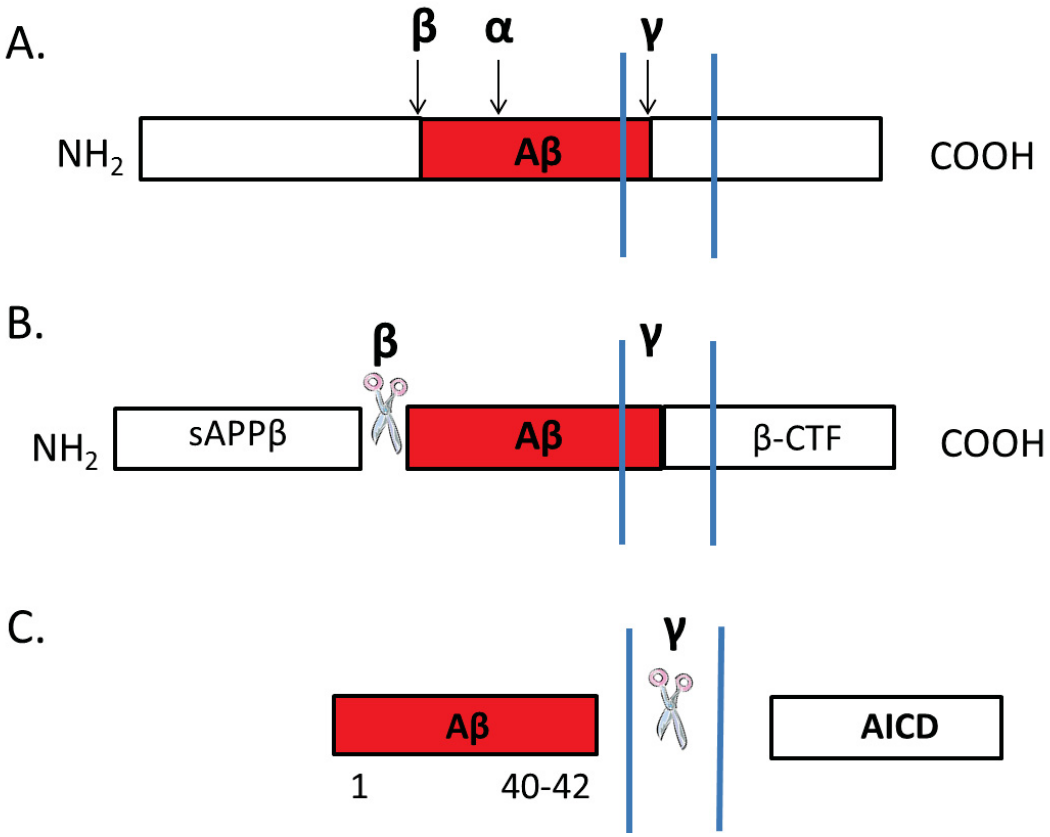

Figure 1.2. Metabolism of APP via β-secretase pathway produces amyloidogenic variants of Aβ. (A) APP is located in the plasma membrane (vertical lines) and β-secretase cleaves APP outside the Aβ region, near the N-terminal portion. (B) This leaves Aβ and the C-terminal fragment (β-CTF) at the plasma membrane, while releasing a soluble N-terminal fragment (sAPPβ). (C) Following cleavage by β-secretase, γ-secretase then cleaves APP near the C-terminal fragment producing the longer Aβ peptide (1-42 amino acids in length) and the APP intra-cellular C-terminal domain (AICD).

1.5 Treatment Of Alzheimer's Disease

The growing numbers of AD cases necessitates the development of novel therapeutics to treat the disease. Brookmeyer et al., (2007) predicts that treatments with a modest effect in delaying AD onset or AD progression will have large effects on reducing the overall number of AD cases, as a large number of cases will die of other causes. Currently approved pharmacological treatments for AD include tacrine, donepezil, rivastigmine and galantamine which are designed to increase levels of acetylcholine in the brain by inhibition of cholinesterase enzymes (Kaduszkiewicz et al., 2005). Memantine is also used to treat moderate and severe AD, and this drug is an uncompetitive glutamate N-methyl-D-aspartate receptor antagonist, designed to protect neurons against excitotoxicity. Currently available treatments, however, show only small effects in ameliorating AD-related symptoms and are not clinically effective in delaying disease onset or progression (Kaduszkiewicz et al., 2005; Gilimberti and Scarpini, 2011).

Therefore, novel treatments for AD have been developed that are designed to modify disease progression through a number of different mechanisms. Although, none of these drugs are currently approved for use with AD, many are undergoing clinical trials (for review see Galimberti and Scarpini, 2011). For example, drugs such as tramiprosate, colostrinin and *scyllo*-inositol are designed to reduce aggregation of Aβ into toxic oligomers. Other drugs have been designed to lower levels of Aβ-42 peptides by either (1) inhibition of γ-secretase activity, (2) modification of γ-secretase activity so that shorter forms of Aβ are produced or (3) increase α-secretase activity to promote proteolysis of APP within a non-amyloidogenic pathway. There are also drugs which may effectively reduce the formation of NFTs, by either reducing aggregation of Tau or

by inhibition of kinases responsible for hyperphosphorylation of Tau. Active immunization against Aβ has also been proposed as a vaccination treatment for AD, promoting increased clearance of Aβ from the brain via the immune system. Although this approach was effective in pre-clinical research with animal models and showed some promise in clinical trials, it produced aseptic meningoencephalitis in a subset of patients with AD, and trials were discontinued. Passive immunization is also currently being examined, as it avoids this complication of T-cell activation during treatment, but this treatment does not reliably produce improvements in cognitive function (for review see Galimberti et al., 2013). Non-steroidal anti-inflammatory drugs have been associated with decreased risk of developing AD, but have shown little efficacy in clinical trials (Galimberti and Scarpini, 2011). Lastly anti-oxidative agents such as folate and vitamins B6 and B12 are also being investigated as potential supplements in the treatment of AD.

1.6 Conclusion

AD is the most common form of dementia in the elderly, and its prevalence is predicted to increase drastically due to the growing aging population. Extensive research has been completed on the behavioural and neuropathological symptoms of the disease, but there are still no treatments which are effective in preventing or slowing the rate of disease progression. Research on the genetic and molecular mechanisms underlying AD has revealed potential targets for pharmacological interventions, some of which inhibit the abnormal aggregation of Aβ and tau. These treatments are commonly evaluated in animal models of AD, to determine if they are potentially efficacious in treating humans. Chapter 2 will discuss animal models of AD, their benefits and limitations, and the use of the transgenic 5XFAD mouse in AD research.

CHAPTER 2 THE 5XFAD MOUSE MODEL OF AD: AGE-RELATED CHANGES IN BRAIN AND BEHAVIOUR AND THEIR RESCUE WITH THERAPEUTIC MANIPULATIONS

2.1 Animal Models Of AD

Given the current lack of disease modifying treatments of AD, extensive pre-clinical research is being completed to assess the effects of novel therapeutics. This research uses primarily animal models of AD, which have been designed to recapitulate many of the disease symptoms. Initial research in the development of cholinesterase inhibitors used aged non-human primates, as they show age-related decline in cognitive function and spontaneously develop AD-related pathology such as Aβ plaques and NFTs (Bartus et al., 2000). Non-human primates are currently used infrequently due to the financial costs, time required for aging and ethical concerns associated with their use in research. Therefore, the majority of current research on AD uses rodent models, despite the decreased translational potential these models may have relative to non-human primates (Balducci and Forloni, 2010).

Rodent models of AD can be created through acute manipulations, such as lesions of brain regions or through the injection of neurotoxic Aβ into the brain (Walsh et al., 2002). However, the most widely used animal models of AD are transgenic mice which express human APP, PS1 or MAPT genes which contain mutations linked to FAD or fronto-temporal dementia (Hall and Robertson, 2012). These transgenic constructs are typically driven with promoter elements (e.g.Thy-1, mouse prion promoter) that enable high levels of gene expression restricted to the central nervous system. For example, the PDAPP mouse was one of the first transgenic mouse model of AD, which contained human APP transgene with the Indian (V171F) mutation (Games et al., 1995). The

Tg2576 mouse model was created shortly after, and contained the human APP gene with the Swedish mutation (K595N/M596L) (Hsaio et al., 1996). These initial animal models recapitulated many AD-related phenotypes including age-dependent development of Aβ-plaques, neuro-inflammation, impaired synaptic plasticity and learning and memory impairments (see Balducci and Forloni, 2010 for review).

Transgenic mouse models of AD have the potential to further our understanding of the etiology of the disease and to provide a platform for the development of novel pharmacological treatments for AD. The increased use of transgenic mice in AD research can be explained by the many advantages associated with their use (Balducci and Forloni, 2010). First, mice can be bred in large numbers and have a fairly rapid gestational period and post-natal neurodevelopment, permitting the rapid completion of experiments. Secondly, both environmental factors (e.g. housing conditions, life history) and genetic factors (e.g. genetic heterogeneity) can be controlled within the laboratory, reducing the influence of non-transgene related factors on neural and behavioural phenotypes. Thirdly, relatively complex cognitive processes can be assessed in mice that cannot be readily assessed in invertebrate models such as the fly (*Drosophila Melanogaster*). Lastly, many AD models are available from central distribution centers such as Jackson Laboratories, allowing researchers to obtain mice relatively easily.

Despite the benefits of transgenic AD model mice, none of these models to date have been successfully used to develop disease modifying therapeutics which are effective and approved for use with the human AD population (Balducci and Forloni et al., 2010). This may be due to several key limitations associated with the use of transgenic AD mice as animal models. In some AD models, Aβ plaques and cognitive

impairment do not develop rapidly, requiring 6-12 months before they can be measured and thus slowing the rate experiments can be completed. In addition, the levels of APP transgene expression required for the development of Aβ pathology in mice is 5-10 fold times higher than normal endogenous mouse and human APP gene expression, suggesting differences in the role of APP in disease progression (Balducci and Forloni et al., 2010). Lastly, none of the AD models fully recapitulates disease symptoms as they occur in humans, because many transgenic mutant APP mice do not develop NFTs or overt cell loss.

Therefore, transgenic mice have been created with multiple transgenes in efforts to overcome the limitations associated with single transgenic mouse models of AD. For example, the APPswe/PS1dE9 and 5XFAD mice produce an accelerated rate of plaque formation, as these mouse models contain both mutant APP and PS1 transgenes which interact to produce larger levels of Aβ (Jankowski et al., 2004; Oakley et al., 2006). The triple-transgenic model has mutant APP, PS1 and MAPT transgenes, and is a more comprehensive model of AD due to the development of both Aβ plaques and NFTs, (Oddo et al., 2003). A large body of research has been completed characterizing the AD-related phenotypes of these models and they are actively being used in the pre-clinical assessment of therapeutics. This thesis will focus specifically on one of these models; the 5XFAD mouse model of AD.

2.2 The 5XFAD Mouse Model Of Alzheimer's Disease

The 5XFAD double-transgenic mouse was created to promote a more rapid, aggressive and complete development of AD-related pathologies relative to other mouse models of AD. While most other transgenic mouse models contain 1-3 familial mutations

(Hall and Robertson, 2012), the 5XFAD mouse expresses the human APP gene with three mutations (Swedish, Florida and London), and the PS1 gene with two mutations (M146L and L286V) (Oakley et al., 2006), with each transgene regulated via the thymus antigen-1 (Thy-1) promoter. Since the 5XFAD mouse was created, its use has increased considerably, and there are now (January 2012) over 35 published papers using this model (Figure 2.1). This chapter summarizes research which has characterized the development of disease-related phenotypes in the 5XFAD mouse, and how these phenotypes have been rescued or exacerbated with genetic, pharmacological and environmental manipulations. Therefore, this chapter serves as a guide for the design of future pre-clinical translational research as it describes the ages at which AD-related phenotypes are present and the replicability of these phenotypes. The phenotypic profile of the 5XFAD mouse is not yet complete, however, and Chapters 3, 4 and 5 will discuss why additional research is needed to fully characterize the AD-related phenotypes in the 5XFAD mouse.

2.3 Creation And Breeding Of The 5XFAD Mouse

The 5XFAD mouse was designed to take advantage of the additive effects of multiple FAD mutations on Aβ production, which occurs when two or more mutations are incorporated into either APP or PS1 (intra-molecular), or when mutations are present in both APP and PS1 (inter-molecular) (Eckman et al., 1997, Oakley et al., 2006). Mutant human APP (695 amino acid isoform) and PS1 cDNA were first generated by site-directed mutagenesis, so that the APP cDNA contained the K6070N/M671L (Swedish), I716V (Florida) and V717I (London) mutations, and the PS1 cDNA contained the M146L and L286V mutations (Moechars et al., 1996). The Swedish mutation has been

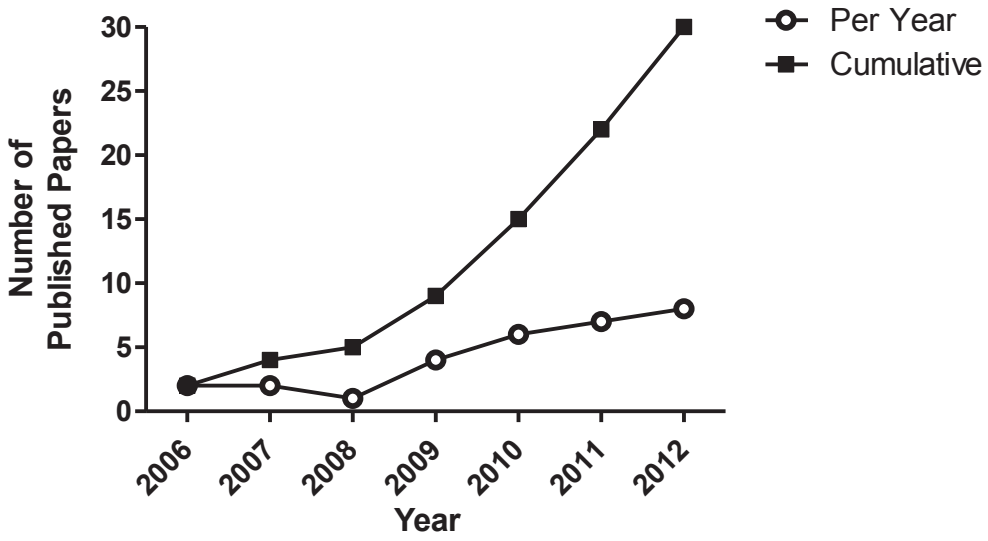

Figure 2.1. The number of published papers using the 5XFAD mouse model of AD. Data are presented based on the number of published papers per year and the cumulative total number of published papers.

shown to increase APP production by influencing β-secretase cleavage, while the Florida, London and PS1 mutations (M146L and L286V) increase the ratio of Aβ-42 to Aβ-40 by influencing γ-secretase cleavage of APP (see Figure 1.1 and 1.2). Mutant APP and PS1 cDNA were then subcloned separately into exon 2 of the Thy-1 transgene cassette (Figure 2.2), replacing thymus-related elements so that expression occurs primarily in the central nervous system (Oakley et al., 2006). The APP transgene also contained the 5' untranslated region containing the putative interleukin-1β translational enhancer element. The transgenes were then purified and equal amounts were injected into the pronuclei of single cell embryos of C57BL/6 x SJL F1 mice. The founder lines were maintained by subsequent breeding to C57BL/6 x SJL F1 mice (Taconic Farms, Gemantown, NY), and the line with the highest expression of APP (line Tg6799) was named the 5XFAD mouse (Oakley et al., 2006). Although the integration site of the APP and PS1 transgenes is not known, both transgenes are inherited together (co-segregation) and show stable germ-line transmission over 10 generations, suggesting co-integration of transgenes at a single genetic locus (Oakley et al., 2006).

Early research using the 5XFAD mice was possible only by obtaining 5XFAD mice from Dr. Robert Vasser, and breeding these mice with wild-type C57BL/6 x SJL F1 mice. The 5XFAD mice (B6SJL-Tg(APPSwFlLon,PSEN1*M146L*L286V)6799Vas/Mmjax, Stock Number :034840-JAX) are now available through the Jackson Laboratories and the Mutant Mouse Regional Resource Center (MMRRC). Colonies of 5XFAD mice are maintained by mating hemizygous transgenic mice with wild-type C57BL/6 x SJL F1 mice. We also recommend that male hemizygous mice be mated with female wild-type mice, to control

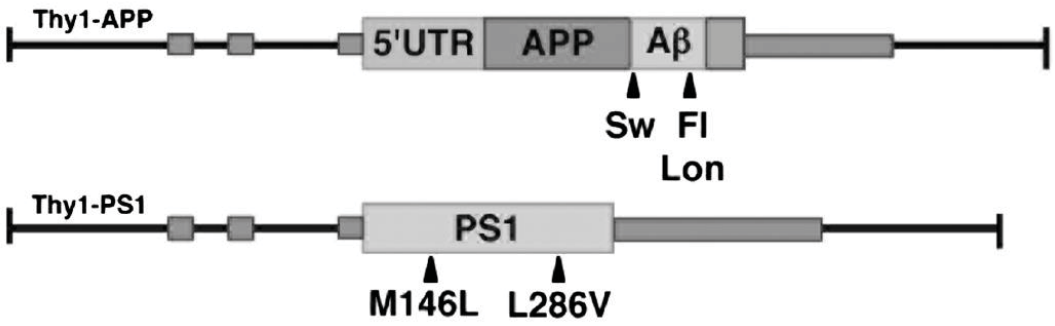

Figure 2.2 The Thy1-APP and Thy1-PS1 transgene constructs which are present in the 5XFAD mouse. The mutant APP and PS1 genes are sub-cloned into Exon 2 of the Thy1 gene. The APP transgene also contains the 5' untranslated region (5'UTR) of the APP gene which contains the IL-1β translational enhancer element. The general locations of the Swedish (Sw), Florida (Fl) and London (Lon) APP mutations, and the M146L and L286V PS1 mutations are indicated by black arrows beneath the transgene cassettes. Modified from (Oakley et al., 2006).

for the potential effects of transgenes on pre-natal development or post-natal maternal behaviour. Although additional breeding of male C57BL/6 x SJL F2 hemizygous and female wild-type mice can be completed, breeding hemizygotes back to F1 mice is desirable to prevent genetic drift between laboratories, and to reduce the probability that deleterious background alleles, such as the blindness-producing $Pde6b^{rd1}$ mutation, are inherited in a homozygous recessive state. The presence of the APP and PS1 transgenes can be detected with polymerase chain reaction (PCR), using protocols available from the MMRRC (http://www.mmrrc.org). Some studies have backcrossed the 5XFAD mice to wild-type C57BL/6 mice for 5-10 generations (Jawhar et al., 2010), but the Aβ-plaque load phenotype in those mice is less than on the C57BL/6 x SJL background (http://www.mmrrc.org/catalog/sds.php?mmrrc_id=34848).

2.4 Neurobiological Phenotype

2.4.1 Transgene Expression And Aβ Load

The development of AD-related pathology in transgenic mouse models of AD is at least partially dependent on the spatial and temporal expression patterns of the APP and PS1 transgenes. Although the expression pattern of APP and PS1 transgenes in the central nervous system of the 5XFAD mouse has not yet been characterized, the expression pattern of the endogenous mouse Thy-1 gene, and the expression pattern of the Thy-1 cassette in other transgenic mice can provide an estimate of the expression patterns of the APP and PS1 transgenes. The expression pattern for the endogenous Thy-1 gene in C57BL/6J mice is complex, as expression occurs in early post-natal development (PND 0-5), and follows different developmental patterns in the eye, spinal cord, and other brain regions (Barlow and Huntley, 2000). Campsall et al., (2002) report

that the Thy-1 transgene cassette can be expressed in the brain as early as embryonic day 11 and can also be detected in non-neuronal tissue at this time. Expression of the endogenous Thy-1 gene in adult C57BL/6J mice using in-situ hybridization data from the Allen Brain Atlas shows variation in Thy-1 expression across brain regions, with highest expression in the cortical subplate and neocortex and lowest expression in the medulla and cerebellum (Figure 2.3). Adult expression levels also vary between cell layers within the cerebral cortex, with higher expression in layers III and V of the sensori-motor cortex compared to other layers (Barlow et al., 2000).

As expected, the brain of the 5XFAD mouse shows elevated expression of both mutant APP and PS1 transgenes. The amount of whole-brain APP expression is 3-4 times higher than endogenous mouse APP (Devi and Ohno, 2010a; Ohno et al., 2006), and is slightly less than the single transgenic Tg2576 mouse with the Swedish APP mutation (Oakley et al., 2006). Increased proteolysis of APP occurs in 5XFAD mice, as indicated by increased levels of β-secretase, the secreted ectodomain of APP and increased levels of c-terminal APP fragments (Ohno et al., 2006; Devi and Ohno, 2010a; Kimura et al., 2010; see Figure 1.2). Unlike the Tg2576 mouse, however, 5XFAD mice produce larger levels of $A\beta_{42}$ than $A\beta_{40}$ in their brains due to the presence of mutations that modulate γ-secretase to bias production of $A\beta_{42}$ over $A\beta_{40}$. The 5XFAD mouse brain accumulates $A\beta_{42}$ peptides as early as 1.5 months of age, and $A\beta_{42}$ levels increase drastically with age. $A\beta_{40}$ peptides also accumulate in the brain of 5XFAD mice, but at a later age (3 months) and at a slower rate than $A\beta_{42}$.

The 5XFAD mouse shows an earlier onset and more rapid development of Aβ-pathology than other mouse models of AD, as demonstrated by both histological

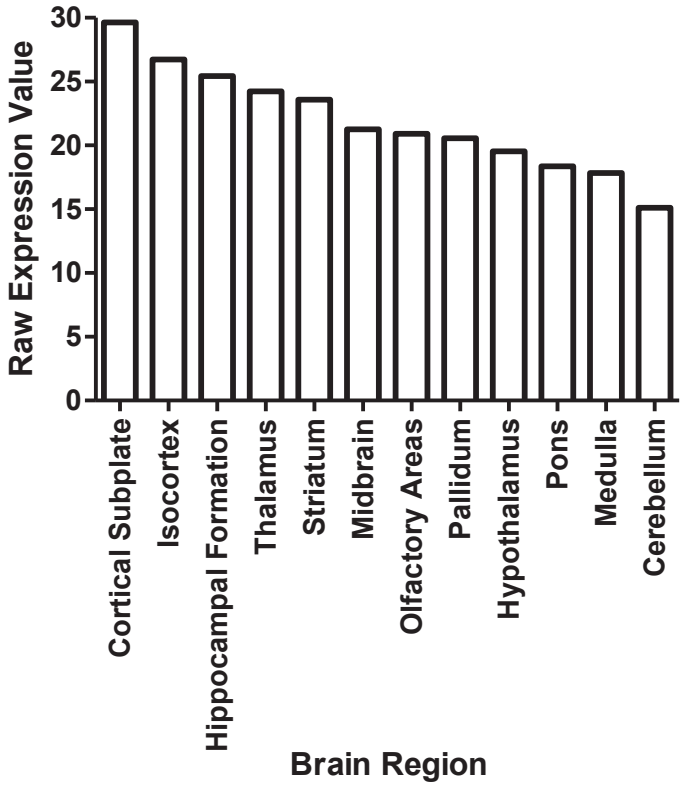

Figure 2.3. Raw expression values (arbitrary values) in different brain regions for the mouse Thy-1 gene in a C57BL/6J mouse. Data is from in-situ hybridization experiments from the publically available Allen Brain atlas database. This data shows that the highest level of Thy-1 gene expression is in the cortical subplate, isocortex and hippocampus.

(Oakley et al., 2006) and in-vivo imaging techniques (Iordanescu., 2011). Punctate Aβ staining is first observed at 1 month of age in an extra-cellular perisomatic pattern, surrounding layer 5 cortical neurons, and in the subiculum and CA1 of the hippocampus (Zhang et al., 2009). The extra-cellular Aβ then begins to aggregate to form small plaques, which tend to be localized near swollen presynaptic terminals. Formation of larger extra-cellular Aβ plaques is first observed in the hippocampus, subiculum, infra-granluar layers of the cortex and spinal cord at 2-3 months, and plaque load increases with age (Jahwar et al., 2012; Oakley et al., 2006). Immunoreactivity in plaques is more pronounced for $A\beta_{42}$ than $A\beta_{40}$, and plaques are also visible using Thioflavin S, indicating that these deposits consist largely of $A\beta_{42}$ in a β-pleated sheet conformational state. Within the cortex, Aβ deposits generally begin in the deep layers and spread to more superficial layers. By 6 months of age, Aβ plaques have also been detected in the insular cortex, cingulate cortex and amygdala (Devi and Ohno, 2010; Kimura et al., 2010). Aβ plaques are also present in the olfactory bulb, thalamus and brainstem, although at lower levels than other brain regions (Oakley et al., 2006; Ohno et al., 2007). In general plaque deposits in 5XFAD mice are smaller but are more numerous than in the single transgenic Tg2576 mice, and Oakley et al., (2006) suggest that this reflects a greater density of plaque "seeds" in the 5XFAD mouse. Despite the wide-spread distribution of Aβ plaques throughout the brains of 5XFAD mice, plaques are not found in the cerebellum and NFTs are not found in the brain (Oakley et al., 2006).

Interestingly, intra-cellular deposits of Aβ have been identified using immunostaining for $A\beta_{40\text{-}42}$ and with Thioflavin-S as early as 1 month of age in the 5XFAD mouse (Oakley et al., 2006; Jawhar et al., 2012; Zhang et al., 2009).Intra-cellular

Aβ is found mainly in large pyramidal cells of the cortex and subiculum, and occurs as punctate staining within the cell soma and neurites, suggesting localization within sub-cellular vesicles. Intra-cellular Aβ is sometimes present as several puncta localized near the axon hillock, and intra-axonal spheroids of Aβ were also detected in the pons and grey matter of the spinal cord in 3 month old mice and increase with age, suggesting the presence of neuronal axonopathy (Jawhar et al., 2012). Intra-cellular Aβ is commonly found in cells with abnormal morphology, which may be in the process of degeneration. Jawhar et al., (2012) observed that the number of cells with intra-neuronal Aβ staining in the cortex of 5XFAD mice was strong at 3 months of age, but the number of cells with intra-neuronal staining and the overall number of cells decreased at 12 months, which together may indicate that intra-neuronal Aβ predicts eventual cell death within the cortex. Oakley et al., (2006) and Jawhar et al., (2012) suggest that the intra-cellular aggregation of Aβ leads to axonopathy, neurodegeneration and the eventual formation and/or contribution of Aβ to extra-cellular plaques, which contributes to the high numbers Aβ plaque deposits in the cortex of 5XFAD mice. Increased levels of intra-cellular β-secretase, APP and Aβ also occur in the nerve terminals of olfactory glomeruli, along with a decrease in size of glomeruli between 6-12 months of age, but without the formation of extra-cellular Aβ deposits (Cai et al., 2012).

2.4.2 Neuroinflammation

An age-dependent increase in activated astrocytes and microglia are present as early as 2 months of age in 5XFAD mice, and by 9 months of age extensive gliosis is present, in the hippocampus and cortex (Oakley et al., 2006; Ohno et al., 2007). The regional distribution of astro- and micro-gliosis follows a spatial pattern similar to Aβ

plaques, and active astrocytes are commonly found surrounding Aβ plaques. The 5XFAD mouse also shows elevated expression of immune-related markers at 6 months of age, including interleukins (β, 6 and 10), members of the toll-like receptor family (2,7 and 9), tumor necrosis factor-alpha, microglia markers (CD11B, F4/80, cathespin etc.) and the astrocyte marker GFAP (Hillman et al., 2012).

2.4.3 Neurodegeneration

Unlike many other mouse models of AD, neurodegeneration is present in the 5XFAD mouse, and occurs through both synapse loss and cell death. Age-dependant decreases in pre-synaptic (synaptophysin) and post-synaptic markers (syntaxin and PSD-95) occur at 4 and 6 months of age respectively, indicating a decrease in synaptic connectivity (Oakley et al., 2006; Shao et al., 2011). In CA1 hippocampal cells, loss of PSD-95 is most prominent in apical dendrites, while a concurrent increase in PSD-95 occurs in the soma, which may reflect a decrease in size of apical dendrites. Cell density and number does not differ between wild-type and 5XFAD mice in the hippocampus (CA1, CA3 or dendate gyrus) or the cortex (frontal, parietal and perihinal) at 6-8 months of age (Joyashiki et al., 2011; Shao et al., 2011). Although the number of neurons in the hippocampus and cortex (all layers) of 5XFAD mice does not differ from wild-type mice at 12 months of age, there is a selective decrease in pyramidal neurons in layer 5 of the cortex (Jahwar et al., 2012). Cell loss is also observable in the subiculum at 9 (Oakley et al, 2006) and 18 months of age (Ohno et al., 2007), but has yet to be quantified. Although the mechanism for cell death is not yet known, elevated levels of Aβ have been shown to increase intra-cellular calcium levels which can lead to activation of the calcium/calpain/cyclin dependant kinase-5 (Cdk5) pathway, which has been linked to

disruption of the neuronal cytoskeleton, abnormal phosphorylation and neurotoxicity. Increased levels of Cdk5 and its activating subunits p25 and p35 are found as early as 2 months of age in the 5XFAD mouse (Sadleir and Vasser, 2012), and p25 levels remain elevated in the cortex at 9 and 12 months of age (Oakley et al., 2006), suggesting a role for the Cdk5 pathway in neurodegeneration within the 5XFAD mouse.

2.4.4 Neurochemical Phenotype

The 5XFAD mice show a number of pathological changes within neurotransmitter systems of the brain. Reduced levels of the enzyme choline acetyltransferase (ChAT) are found in the hippocampus of 5XFAD mice at 4-6 and 15-18 months of age, as well as a reduced number of ChAT positive neurons in the medial septum, suggesting impaired neurotransmission in the septo-hippocampal cholinergic pathway (Devi and Ohno, 2010b). Also, 5XFAD mice show reduced levels of brain derived neurotrophic factor (BDNF) as early as 3 months of age and reduced levels of phosphorylated Tyrosine Kinase B (Trk-B) receptors in the hippocampus at 6 and 15-18 months of age (Kimura et al., 2010; Devi and Ohno, 2012a). It has been shown that levels of mRNA for tyrosine hydroxylase and dopamine beta hydroxylase are reduced in the locus coeruleus of 5XFAD mice. This reduction also corresponds with an increase in the size of tyrosine hydroxylase reactive neurons, and with an increase in mRNA levels of inflammatory markers (CD45, COX2, etc). Taken together, this may reflect neuronal damage in the locus coerculeus of 5XFAD mice (Kalinin et al., 2012).

2.4.5 Neurophysiological Phenotype

Basal synaptic transmission and synaptic plasticity are not impaired in 5XFAD mice before 4 months of age (Kimura and Ohno, 2009). However, the slope of field

extra-cellular post-synaptic potentials (fEPSPs) of neurons in the stratum radiatum layer of CA1 is reduced following stimulation of the Schaffer collateral afferents at 6 months of age (Kimura et al., 2010; Kimura and Ohno, 2009), indicating a decrease in basal synaptic glutamatergic transmission in 5XFAD mice. Despite changes in basal synaptic transmission, no changes were found in short-term plasticity using paired-pulse facilitation at either 4 or 6 months of age (Kimura and Ohno, 2009). However, the fEPSP of CA1 neurons in 5XFAD mice was smaller than that of wild-type mice 35-40 min following the induction of LTP with either 3 or 10 theta burst stimulations, suggesting impaired long-term synaptic plasticity (Kimura et al., 2010; Kimura and Ohno, 2009). Intrinsic excitability was also assessed in CA1 neurons using patch-clamp recordings by measuring post-burst after-hyperpolarization (AHP). AHPs did not differ from wild-type mice at 2 months of age, but were increased in 5XFAD mice at 8 months of age (Kaczorowski et al., 2009), indicating an age-related decrease in hippocampal excitability. Neuronal excitability returned to wild-type levels after administration of the muscarinic acetylcholine receptor-1 agonist carbachol or a Ca^{2+} channel blocker, suggesting impaired excitability in 5XFAD mice is related to cholinergic neurotransmission and/or Ca^{2+} dependent mechanisms.

2.5 Behavioural Phenotype

2.5.1 Gross Physical Appearance And Body Weight

No abnormal observations on gross physical appearance have been reported in 5XFAD mice up to 18 months of age (Devi and Ohno, 2010b; Devi et al., 2012). When provided ad-libitum access to food, body weight in the 5XFAD mice is lower than wild-type mice at 9 and 12 months of age because wild-type mice continue to gain weight

from 6-12 months of age, while 5XFAD mice stop gaining weight after 6 months of age (Jawhar et al., 2012). It is currently not clear why 5XFAD mice show reduced weight gain.

2.5.2 Anxiety And Locomotor Activity

Anxiety-related behaviour has been assessed in the 5XFAD mouse at 3, 6, 9 and 12 months of age using the elevated plus maze (EPM) (Jahwar et al., 2012). Although 5XFAD and wild-type mice did not differ in time spent on the open-arms of the EPM at 3 months of age, 5XFAD mice did spend more time in the open-arms than wild-type mice at 6, 9 and 12 months of age, indicating decreased anxiety levels. In the open-field (OF), however, decreased anxiety was not found at 9 months, but was found at 12 months of age, as 5XFAD mice spent more time in the center of the OF than wild-type mice. The decrease in anxiety on the EPM and OF was not accompanied by changes in locomotor activity, as no differences were found in distance travelled in the OF at 4-7 months (Tohda et al., 2011), 6-8 months (Joyashiki et al., 2011), 7-9 months (Urano and Tohda, 2010), or 12 months of age (Jawhar er al., 2012).

2.5.3 Motor Ability

When held by the tail, 5XFAD mice show an abnormal limb-retraction and clasping response beginning at 9 months of age, and this is thought to reflect neuro-muscular motor impairments and/or weakness (Jawhar et al., 2012). 5XFAD mice also fall faster from the balance-beam and show poor qualitative agility scores on the fore-paw string suspension test at 9 and 12 months of age (Jawhar et al., 2012; Jawhar et al., 2011), suggesting age related impairments in balance and motor coordination beginning at 9 months of age.

2.5.4 Working And Short-term Memory

Age-related cognitive impairments have been found in 5XFAD mice in working memory in the Y-maze and short-term memory in the novel object recognition test. 5XFAD mice exhibit fewer spontaneous alternations than wild-type mice at 4-5 months (Oakley et al., 2010), 6 months (Kimura et al., 2010) and 15-18 months of age (Ohno et al., 2007; Devi and Ohno, 2012). Another study, however, has shown that spontaneous alternation impairments in the Y-maze are not present in 5XFAD mice at 6 months of age (Jahwar et al., 2011). More consistent results tend to be obtained by measuring spontaneous alternation using a plus maze, which is more cognitively demanding than the Y-maze as the mouse must remember the last three arms visited in order to complete an alternation. In this test, 5XFAD mice alternated less than wild-type mice at 6, 9 and 12 months of age (Jawhar et al., 2012; Jahwar et al., 2011). The impairment in spontaneous alternation rates in these studies was not due to decreased levels of locomotor activity or exploration because 5XFAD mice did not differ from wild-type mice in the number of arms entered. Overall, this suggests that 5XFAD mice have an age-related working memory impairment which begins around 4-6 months of age.

Short-term memory has also been assessed in 5XFAD mice with the novel object recognition test using a 30 min delay between sample and test trials. Preference for exploring the novel object over the familiar object was smaller in 5XFAD than wild-type mice at 4-7 and 6-8 months of age (Tohda et al., 2011; Joyashiki et al., 2011). Woo et al. (2010) used a 60 minute delay and found impaired performance in 5XFAD mice at 8.75 months but did not replicate impairments at 4.5 month of age. However, wild-type mice did not show a clear preference for the novel object (50-55%) at 4.5 months of age in this

study, which prevents conclusions concerning short-term memory from being made at this age.

2.5.5 Visuo-spatial Learning And Reference Memory

Visuo-spatial learning and reference memory have been assessed in 5XFAD mice using the Morris water maze (MWM) with a stable escape platform location. At 4-6 months of age, 5XFAD mice take longer to locate the escape platform than wild-type mice (Ohno et al., 2006) indicating impaired learning. This deficit in learning performance was not due to impaired motor coordination at this age, as 5XFAD mice did not differ from wild-type mice in swim speed. During a memory probe trial, both wild-type and 5XFAD mice at 4-6 months of age spent more time near the escape platform's location than expected by chance, indicating that they remembered the location of the escape platform (Ohno et al., 2006). Although performance of 5XFAD and wild-type mice was not directly compared in this study, wild-type mice spent more time in the correct quadrant than the opposite quadrant of the maze during the probe trial, while there was no difference between time spent in each quadrant by 5XFAD mice. Overall, this suggests that 5XFAD mice remembered the location of the escape platform, albeit not as well as wild-type mice.

Other studies using the MWM have found large impairments in visuo-spatial learning in 5XFAD mice at 5 months (Hongpaisan et al., 2011), 6 months (Kalinin et al., 2012), and 7-9 months of age (Urano and Tohda, 2010). In these studies 5XFAD mice showed little (Hongpaisan et al., 2011) or no learning (Urano and Tohda, 2010; Kalinin et al., 2012) as performance did not significantly improve with training. The 5XFAD mice also completed fewer annulus crossings over the escape platform location during the

probe trial than wild-type mice, suggesting impaired memory for the location of the escape platform. Taken together, these results indicate that the 5XFAD mice have impaired visuo-spatial learning and memory on the MWM by 4-6 months of age, and that the size of this deficit is highly variable.

2.5.6 Cued And Contextual Fear Conditioning

Memory in 5XFAD mice has been assessed with both cued and contextual fear conditioning, but impairments are dependent on the amount of training given, and the length of the interval between training and the memory test. In contextual fear conditioning, a mouse is placed into a unique context (CS) and one or more aversive shocks (UCS) are administered so that the mouse associates the context with exposure to shocks. Memory for the context-shock pairing is assessed by measuring freezing behaviour (CR) when mice are returned to the context in which shocks were previously given. When 5XFAD mice were trained at less than four months of age and when one (Kimura and Ohno, 2009) or two context-shock training trials (Ohno, 2009; Devi and Ohno, 2010) were administered, they did not differ in freezing behaviour from wild-type mice when tested 24 hours after training. However, when longer-term (remote) retention was assessed 30 days after training, 5XFAD mice displayed less freezing than wild-type mice, indicating impaired memory. At 6-7, 10-15 and 12-13 months of age, 5XFAD mice were impaired when one (Kimura and Ohno, 2009) or two (Kimura et al., 2010; Devi and Ohno, 2010; Ohno, 2009) context-shock trials were administered and the memory test was given 24 hours later. Although Kaczorowski et al., (2009) found impaired contextual memory in 5XFAD mice at 8 months of age when training was increased to four context-shock pairings, other studies have not replicated this impairment when three or five

shocks are given at 6-7 or 10-12 months of age respectively (Kimura and Ohno, 2009; Kimura et al., 2010), suggesting that memory impairments were less replicable if additional training was provided beyond 2 context-shock trials. If memory was assessed 30 days after training, however, 5XFAD mice froze less than wild-type mice when increased training was provided (3 or 5 context-shock pairings), suggesting an impairment in long-term retention of the shock-context association (Kimura and Ohno, 2009; Kimura et al., 2010). Impairments in the reconsolidation of contextual fear memories in 5XFAD mice also occurred at 10-12 months of age, when reconsolidation was induced by a short (3 min) re-exposure period to the training context 24hr prior to the contextual memory test (48hr delay). With this paradigm, 5XFAD mice did not differ from wild-type mice when no re-exposure period was given, but showed impaired memory when a re-exposure period was provided prior to the contextual memory test, suggesting that reactivation of the memory occurred but impairments are present in memory reconsolidation (Ohno, 2009).

In cued fear conditioning mice are presented with tone-shock pairings and associate the tone with the administration of shock. Cued fear conditioning can be completed by administering the tone immediately before the shock (delay conditioning) or by introducing a time interval between the tone and the shock (trace fear conditioning). Memory for the tone-shock pairing is then assessed in a memory test, where mice are placed in a novel context, and the amount of freezing is measured before, during and after the presentation of the tone. In delay fear conditioning 5XFAD mice were not impaired at 5-6 months of age when 5 tone-shock pairings were administered (Ohno et al., 2006). However, when trace fear conditioning was completed with a 30 sec interval between the

tone and shock, 5XFAD mice froze less than wild-type mice at 5-6 months of age indicating impaired memory. This deficit in trace fear conditioning in 5XFAD mice, however, was not replicated by Kaczorowski et al., (2009) at 4 or 8 months of age with four tone-shock pairings. Kaczorowski et al., (2009) suggested that the failure to find impaired performance of 5XFAD mice may have been due to increased heterogeneity of memory scores due to the use of only males in this study, and suggested that females may show more consistent impairment in trace fear conditioning than males.

2.5.7 Conditioned Taste Aversion

The conditioned taste aversion test is hippocampal independent, and assesses implicit memory for the association between a specific flavor and aversive malaise. In this test, mice are given a novel sucrose solution to drink and later given a malaise inducing agent (Lithium Chloride). To assess memory, mice are given a choice of unflavored water or sucrose flavored water to determine which type of solution they prefer to drink. At 6-7 months of age 5XFAD mice are not impaired at remembering the sucrose-malaise association, but at 9-10 and 12-15 months of age, 5XFAD mice drink the unflavored water and the sucrose solution in equal amounts, indicating impaired memory for the sucrose-malaise association (Devi and Ohno, 2010a).

2.6 Use Of The 5XFAD Mouse To Assess The Efficacy Of Novel AD Treatments

Research characterizing the neural and behavioural phenotypes of the 5XFAD mouse model has revealed many potential targets for therapeutic intervention, and thus a number of studies have assessed the efficacy of genetic, pharmacological and

environmental manipulations on ameliorating AD-related phenotypes in the 5XFAD mouse.

2.6.1 Inhibition Of β-secretase (BACE1)

The effects of reduced proteolysis of APP on AD-related phenotypes have been investigated extensively in 5XFAD mice using genetic and pharmacological treatments that reduce levels of β-secretase (also known as β-site amyloid precursor protein-cleaving enzyme 1 or BACE1). BACE1 is an aspartic acid trans-membrane protease which is upregulated in humans with AD (Zhao et al., 2007), and is a rate limiting enzyme for Aβ production as it cleaves APP into the cell membrane bound C99 c-terminal fragment and a soluble secreted APP ectodomain (Devi and Ohno, 2010a, b). Initial research showed that 5XFAD mice have age-related increases in BACE1 levels and enzymatic activity at 2-4 months of age, without an increase in BACE1 expression, indicating a post-transcriptional up-regulation of BACE1 levels. Increases in BACE1 tend to be localized in rings surrounding a sub-population of Aβ plaques in humans and the majority of plaques in the 5XFAD mouse. BACE1 is also colocalized with markers for neurons, axon terminals and dystrophic neurites (synaptophysin, GAP-43, GAD-67 etc.) but not dendritic processes (microtubule-associated protein-2) (Zhao et al., 2007; Zhang et al., 2009). Overall these results suggest that constituents of extra-cellular Aβ-plaques, likely $A\beta_{42,}$ increase BACE1 levels within surrounding neurons, causing a positive feedback loop resulting in a localized increase in Aβ production in neurons proximal to Aβ-plaques (Zhao et al., 2007; Sadleir and Vasser, 2012).

To investigate the effects of BACE1 on AD-related phenotypes, 5XFAD mice were bred with BACE1 knockout mice, to produce mice with APP and PS1 transgenes

and non-functional BACE1 alleles. These 5XFAD/BACE1$^{-/-}$ mice do not produce BACE1, and have improved trace fear conditioning, improved learning and memory performance on the MWM, reduced levels of $A\beta_{40}$ and $A\beta_{42}$ and do not show neuronal loss in the subiculum and cortex (Ohno et al., 2006; Ohno et al., 2007). However, non-transgenic mice without homozygous BACE1 mutant alleles (WT/ BACE1$^{-/-}$) have hypo-myelination, increased pain tolerance, reduced muscle strength (Hu et al., 2006) and impaired learning and memory which occur independently of 5XFAD transgenes (Ohno et al., 2006; Ohno et al., 2007). Therefore, 5XFAD mice which have only one functional BACE1 allele (5XFAD/BACE1$^{+/-}$) are now more commonly used as their phenotype does not differ from wild-type mice, and the partial reduction in BACE1 levels more closely reflects the effects of potential pharmacological interventions designed to inhibit BACE1.

The 5XFAD/BACE1$^{+/-}$ mice have similar APP expression as 5XFAD mice, but show (1) reduced expression of BACE1 (~50%), (2) reduced levels of the secreted ectodomain of APP and c99 c-terminal fragments, (3) reduced $A\beta_{40}$ and $A\beta_{42,}$ (4) reduced c99 and full length APP within mitochondria along with mitochondria dysfunction, (5) reduced plaque load in the hippocampus, basolateral amygdala, insular cortex and anterior cingular cortex (6) increased levels of hippocampal ChAT and number of septo-hippocampal cholinergic neurons, (7) increased levels of hippocampal BDNF and TrK-B receptors and (8) improved synaptic plasticity as measured by LTP, all between 6-10 months of age (Devi and Ohno, 2010a,b; Kimura et al., 2010; Devi and Ohno, 2012b). Unlike 5XFAD mice, the 5XFAD/BACE1$^{+/-}$ mice are not impaired relative to wild-type mice in conditioned taste aversion at 9-10 months of age (Devi and Ohno, 2010a), spontaneous alternation at 6 months of age (Devi and Ohno, 2010b), or

contextual fear conditioning at 6 months of age (Kimura et al., 2010). The influence of partial reduction of BACE1 in 5XFAD/BACE1$^{+/-}$ mice shows an age-dependant attenuation, however, and does not rescue spontaneous alternation rates, C99 c-terminal fragment levels, levels of $A\beta_{42,}$ mitochondrial dysfunction, hippocampal ChAT levels or the number of septo-hippocampal cholinergic neurons at 15-18 months (Devi and Ohno, 2010b; Devi and Ohno, 2012a,b). Devi and Ohno (2010b), suggest that the attenuated effect of BACE1 reduction is due to increased levels of the phosphorylated eukaryotic translation initiation factor-2a (eIF2α), which in turn increases BACE1 levels through post-transcriptional up-regulation, and eIF2α is found to be increased in both human AD cases and 5XFAD mouse brains (O'Connor et al., 2008).

2.6.2 Traditional Herbal Medicines

A number of studies have investigated the efficacy of traditional herbal medicines for ameliorating AD-related phenotypes in the 5XFAD mouse. Icarrin is a falvanoid contained in the herb *Epimedii Herba*, and is effective in protecting against $A\beta_{1-42}$ induced atrophy of axons and dendrites in-vitro using primary rat cortical neurons. Icarrin produces a small improvement in learning (but not memory) in 5XFAD mice at 7-9 months of age in the MWM (Urano and Tohda, 2010). Kamikihi-to (KKT) is a traditional Japanese Kempo medicine which also reduces $A\beta_{25-35}$ induced atrophy of axons and dendrites in-vitro. In the 5XFAD mouse, KKT reduces impairments in short-term memory in the novel object recognition test and also reduces plaque number in the frontal cortex and hippocampus (Tohda et al., 2011). Although KKT did not significantly change BACE1 levels, it did reduce the number of abnormal Aβ positive axonal swellings and presynaptic boutons located proximal to Aβ plaques within the cortex. Sominone is a

steroidal saprogenin which protects against $A\beta_{1-42}$ induced atrophy of axons and dendrites in-vitro. Sominone rescued impairments in the novel object recognition test, and increased the length of axons as indicated by phosphorylated neurofilament, but did not decrease plaque load or microglial levels throughout the brain (Joyaskiki et al., 2011).

2.6.3 Inhibition Of Pyroglutamate Aβ

Although the majority of Aβ is 40-42 amino acids in length and begins with aspartate at the N-terminal, other Aβ isoforms are produced which are truncated at the N-terminal by 1-5 amino acids. One such isoform of Aβ begins with pyroglutamate (AβpE3), and this isoform is a stable peptide with a propensity to aggregate and is neurotoxic (Wittnam et al., 2012). AβpE3 is increased in the cortex of humans with AD, and overexpression of AβpE3 in a transgenic mouse model leads to neuron loss and other AD-related phenotypes. In the 5XFAD mouse, the most dominant Aβ isoform is $A\beta_{1-42,}$ followed by $A\beta_{1-40}$, $A\beta_{4-42}$, $A\beta_{5-42}$, $A\beta_{pE3-42}$ and $A\beta_{3-42}$ in descending order of abundance.

Production of AβpE3 is catalyzed with glutaminyl cyclase, which can be successfully inhibited pharmacologically (i.e. with PBD150), suggesting that glutaminyl cyclase may be a useful target for therapeutic interventions (Schilling et al., 2008; Jawhar et al., 2011). 5XFAD mice with either an inserted transgene which over-expresses human glutaminyl cyclase, or knocked out alleles for glutaminyl cyclase can be used to examine how increased and decreased levels of glutamyl cyclase influence AD-related phenotypes in the 5XFAD mouse. At 6 months of age, increased glutaminyl cyclase expression increased plaque load in the cortex as indicated by total Aβ and AβpE3 in 5XFAD mice,

while mice having glutaminyl cyclase knocked-out had the opposite effects. 5XFAD mice over-expressing glutaminyl cyclase also showed impaired motor and spontaneous alternation performance compared to normal 5XFAD mice, whom do not normally differ from wild-type mice at 6 months of age. Interestingly, having knocked-out glutaminyl cyclase alleles corrected the spontaneous alternation impairment commonly found in 5XFAD mice at 6 months of age (Jahwar et al., 2011). Motor impairments, working memory impairments and Aβ plaque load were also increased when 5XFAD mice were crossed with a transgenic line which over-produces AβpE3. Interestingly, in this mouse AβpE3 was found within extra-cellular plaque deposits, and did not show intra-cellular accumulation, suggesting a role for AβpE3 in the seeding of extra-cellular plaques (Whittnam et al., 2012).

2.6.4 Non-steroidal Anti-inflammatory Drugs

Epidemiological studies have shown that nonsteroidal anti-inflammatory drugs (NSAIDs) reduce the risk of developing AD (Vlad et al., 2008). NSAIDs have their anti-inflammatory effects by reducing activity of cyclooxygenase 1 and 2 enzymes that promote inflammation through the generation of prostaglandins. There is also evidence that NSAIDs can reduce Aβ generation through modulation of γ-secretase activity, but the mechanism of action is not yet known. The 5XFAD mouse is a valuable model for assessing the effects of ibuprofen as the PS1 mutations reduce the extent to which γ-secretase activity can be modulated, allowing the anti-inflammatory effects of ibuprofen on the disease phenotype to be more accurately measured. When 5XFAD mice are given ibuprofen (for 3 months) they did not show a decrease in Aβ plaque load in the hippocampus or cortex at 6 months of age, but did show an increase in levels of soluble

$A\beta_{42}$. As expected, reduced levels of astrogliosis and microgliosis were observed in the cortex and dentate gyrus, along with a reduction in mRNA levels for immune-system markers including interleukins (6 and 10), MCSF-R and GFAP. Unexpectedly, Ibuprofen exacerbated behavioral impairments in the 5XFAD mice, leading to impairments in motor ability, locomotor activity and spontaneous alternation relative to untreated 5XFAD mice. Hillman et al., (2012) suggest that Ibuprofen is efficacious in reducing inflammation in the 5XFAD mice, but may be harmful in that reductions in inflammation may reduce clearance of $A\beta_{42}$ by microglia, leading to behavioural impairments.

2.6.5 Improving Synaptic Connectivity And Efficacy

Although currently approved drugs for AD (e.g. donepezil, rivastigmine etc.) have not been tested in the 5XFAD mice, several experiments have tested other treatments designed to protect against synapse loss or to improve synaptic efficacy by increasing levels of neuro-tropic factors or neurotransmitter levels. Protein kinase C (PKC) is involved in synaptogenesis and is reduced by soluble Aβ, suggesting that decreases in PKC isozymes may contribute to loss of synapses in AD. Therefore, PKC may serve as a potential therapeutic target to prevent synapse loss in AD. PKC activators Bryostatin-1 (α and ε isozymes) and DCP-LA (ε isozyme) prevent learning and memory impairments in 5XFAD mice relative to wild-type mice at 5 months of age (Hongpaisan et al., 2011). Administration of DCP-LA also reduced the amount of Aβ-plaques and ameliorated the loss of dendritic spines, and synapses in hippocampal CA1 neurons of 5XFAD mice.

Reductions in BDNF levels and phosphorylated TrkB receptors occur in the 5XFAD mice, which may contribute to cognitive impairments. Administering the TrkB agonist 7,8-Dihydroxyflavone did not alter BDNF levels in the hippocampus, but did

increase phosphorylated TrkB receptors, while reducing levels of BACE1, C99 c-terminal fragments, $A\beta_{40,}$ $A\beta_{42}$ and prevented impairments in spontaneous alternation (Devi and Ohno, 2012a). These results suggest that the reductions in BDNF and TrkB receptors in 5XFAD mice may increase levels of BACE1, thus producing increases in Aβ peptides and accelerating AD pathogenesis.

Disruption of noradrenergic neurons in the LC is found in AD, and the 5XFAD mouse shows evidence of neuronal stress, damage and inflammation in the LC. Therefore, the effect of L-DOPS, a synthetic catecholamino acid that can be used to synthesize noradrenaline (NA), was assessed on AD-related phenotypes in 5XFAD mice (Kalinin et al., 2012). Treatment with L-DOPS increased cortical NA levels, and rescued learning and memory impairments on the MWM at 6 months of age. L-DOPS administration also decreased astrogliosis and plaque load in the cortex and hippocampus, while increasing BDNF protein levels, and mRNA levels for synaptophysin, nerve growth factor and dopamine beta hydroxylase.

2.6.6 The Influence Of Stress On AD-related Phenotypes

Psychological stress (Johansson et al., 2010) and depression (Geerlings et al., 2008) have been shown to increase the risk of developing AD, and in the 3xTG transgenic mouse glucocorticoids increase Aβ and Tau pathology (Green et al., 2006). When 5XFAD mice are exposed to a repeated stressor (6 hr of restraint per day for 6 days), increased levels of $A\beta_{42,}$ BACE1, APP, C99 c-terminal fragments and Aβ-plaque load were found in the hippocampus of females but not males, while no sex differences were found in the cortex (Devi et al., 2010c). Increased levels of BACE1 mRNA and phosphorylated translation initiation factor eIF2α were also present in stressed 5XFAD

females, indicating elevation in BACE1 could due to both increased transcription and translation. These results indicate that stress can increase AD-related pathology in 5XFAD female mice, and suggest that sex differences in AD may be at least partially due to sex differences in BACE1 and APP production caused by environmental stressors.

2.7 Conclusions

Considerable research has now been completed characterizing age-related changes in the AD-related phenotypes in the 5XFAD mouse. This work has shown that the 5XFAD mouse recapitulates many of the behavioural and neuro-pathological symptoms which occur in humans with AD. The usefulness of the 5XFAD mouse has also been demonstrated in many experiments examining the mechanisms underlying Aβ-pathology and in the assessment of potential therapeutic interventions for AD.

Although the 5XFAD mouse is a valuable animal model for AD research, several limitations need to be addressed before future research with this mouse model is completed. First, many of the behavioural phenotypes have not been replicated in multiple studies across different laboratories, and therefore their replicability has not been established. Secondly, age-related changes in the behavioural phenotype of 5XFAD mice has not been well characterized, as most studies examine animals at one age, or use large age-ranges spanning multiple months. Lastly, large variation is observed in the size cognitive impairment in the 5XFAD mouse across studies, which suggest that uncontrolled background genetic factors may influence the development of AD-related symptoms. Of the studies reviewed in this chapter, the sex of the animal was either not reported, only one sex was used, or both sexes were used but not compared. We have also identified three mutant alleles (Pde6b^{rd1}, *D*ysf^{im}, and *Tyr*^{c}) that are present on the

C57BL/6 x SJL F1 backgound that may influence the sensory-motor ability of 5XFAD mice, and thus confound behavioural tests of motor and cognitive function. These background mutations have yet to be examined in 5xFAD mouse, and only the Pde6b^{rd1}mutation has been examined in another AD mouse model (tg2576) (Yassine et al., 2011).

Therefore, the purpose of this thesis is to complete additional research characterizing the behavioural phenotype of 5XFAD mouse. This thesis has three overall aims: (1) to establish the replicability of previously reported behavioural phenotypes of the 5XFAD mouse, and the extend this characterization using additional behavioural tests, (2) to examine behavior of 5XFAD mice at multiple ages to examine age-related decline, and (3) to determine the extent to which age-related changes in behaviour are modulated by sex and background genetic factors.

CHAPTER 3 AGE-RELATED DECLINE IN MOTOR ABILITY IN THE 5XFAD MOUSE MODEL OF AD

3.1 Introduction

The double transgenic 5XFAD mouse model of AD carries the mutant APP gene with three mutations and the PS1 gene with two mutations, each expressed via the Thy-1 promoter (Oakley et al., 2006). These mice show a rapid development of AD-related pathology within the brain, including elevated levels of Aβ peptides, development of extra-cellular plaques, intra-neuronal accumulation of Aβ, astro- and microglosis, as well as cell loss within the subiculum and layer 5 of the neo-cortex (Jawhar et al., 2012; Oakley et al., 2006). Although cognitive impairment has been reliably demonstrated in short-term/working and long-term reference memory tasks by 4-6 months of age, the most conspicuous change in behavior is a pronounced decline in motor ability at 9 months of age, which becomes progressively worse at 12 months of age (Jahwar et al., 2012). These impairments may be analogous to the motor impairments found in humans with AD, which consist of bradykinesia, rigidity, abnormal posture and gait and to a lesser extent, tremors (Mitchell, 1999; see Chapter 2), and may be more common in familial AD cases with PS1 mutations relative to sporadic AD (for review see Larner and Doran, 2006).

The mechanism(s) by which motor impairments develop in 5XFAD mice is not yet clear, but recent research suggests that Aβ-induced dysfunction occurs within the pyramidal and/or extra-pyramidal motor systems of the brain and spinal cord. First, extra-cellular plaques develop in regions associated with motor ability, including the motor cortex, basal ganglia and spinal cord (but not the cerebellum), and likely impair the

function of neurons in these regions (Oakley et al., 2006). Secondly, axonal swellings containing Aβ are present within motor neurons of the spinal cord (Jawhar et al. 2012), which may impede axonal transport and reduce synaptic efficacy. Thirdly, although not specifically demonstrated, death of the major efferent neurons that form the cortico-spinal tract (Betz cells) likely occurs, given decreases in neuron number within layer 5 of the neocortex (Oakley et al., 2006). Further research is needed, however, to determine the relative contribution of these neural phenotypes to the development of motor impairment in the 5XFAD mouse.

Therefore, the 5XFAD mouse may be a useful animal model for examining mechanisms by which elevated Aβ can contribute to the development of motor impairments in AD. This motor phenotype may also be a useful end-point for the assessment of novel therapeutics in 5XFAD mice, in addition to the more commonly used measures of cognitive function. Moreover, the effect size for the motor impairment in 5XFAD mice is large and therefore this phenotype may be robust across different tests of motor function and can be detected with moderate to small sample sizes. Thus far, motor behaviour has been assessed once in pre-clinical research with 5XFAD mice, in which the non-steroidal anti-inflammatory drug Ibuprofen exacerbated rather than improved motor function (Hillman et al., 2012).

Before the 5XFAD mouse is used more extensively to investigate the pathogenesis or treatment of motor impairments, four areas of further research are needed to provide a more detailed characterization of the motor behaviour phenotype. First, the replicability of the motor deficits needs to be established across different tests of motor ability, given that tests of motor behaviour often measure different aspects of motor

function (e.g. balance, endurance, strength etc.) and can differ in their sensitivity to detect impairment (Pallier et al., 2008). Furthermore, motor impairments should be replicated across multiple laboratories, given that the testing site (Mandillo, et al., 2008) and idiosyncratic differences in test procedure can influence performance on tests such as the rota-rod (e.g. amount of training, rod size, acceleration rate) (Rustay et al., 2003). Thus far, motor impairment has been observed in the 5XFAD mice on the balance beam, string-suspension strength/agility test (Jawhar et al., 2012) and the rota-rod (Shukla et al., 2013), suggesting impairments in balance, grip-strength and motor coordination, respectively. However, these deficits have yet to be extensively replicated, and age-related impairment of motor coordination has yet to be examined on the rota-rod. In addition, it is not known to what extent the motor system of the 5XFAD mice remains plastic with age, so that motor learning and memory can occur when training is given at different ages.

Secondly, performance of mice on tests of motor function (i.e. rota-rod) can be influenced by body weight. Typically mice that weigh less perform better than heavier mice, but this relationship is strain specific (McFayden et al., 2003). To our knowledge, the influence of body-weight on motor performance is not known for C57BL/6 x SJL hybrid mice, which are used as the background strain for 5XFAD and other transgenic mouse models of AD. Therefore, the influence of body weight on motor performance should be assessed in the 5XFAD mouse to ensure that it does not confound measures of motor ability.

Thirdly, the robustness of the motor phenotype in 5XFAD mice needs to be established across different genetic backgrounds for both sexes. In previous studies

assessing motor function, the 5XFAD mouse was backcrossed to a C57BL/6J background (Jawhar et al., 2012; Hillman et al., 2012), but the majority of research with the 5XFAD mouse maintains the model on a C57BL/6 x SJL hybrid background (Oakley et al., 2006). The expression of AD-related phenotypes in transgenic mouse models is known to be modulated by genetic background (Ryman and Lamb, 2006). Aβ-plaque load on the C57BL/6 background is reduced relative to C57BL/6 x SJL hybrid background (http://www.mmrrc.org/catalog/sds.php?mmrrc_id=34848), and therefore 5XFAD mice maintained on the hybrid background may have a different age of onset and rate of decline for motor impairments. Sex differences have also been reported in the 5XFAD mouse and other transgenic AD-models, but motor ability has only been assessed in females thus far.

Fourthly, the SJL inbred strain has been proposed as a natural animal model of limb-girdle muscular dystrophy 2B and Miyoshi myopathy, due to an autosomal recessive mutation (*D*ysf^{im}) in the dysferlin gene (Bittner et al., 1999). Dysferlin is a transmembrane protein highly expressed in skeletal muscle tissue, and the *D*ysf^{im} mutation leads to muscular degeneration and progressive muscular weakness. The *D*ysf^{im} mutation consists of a 171bp genomic deletion, which produces abnormal exon-skipping and partial removal of the C2-E domain (Vafiadaki et al., 2001), leading to protein instability and an 85% reduction in dysferlin levels (Bittner et al., 1999). Therefore, when transgenic 5XFAD mice are bred with C57BL/6 x SJL F1 mice, a subset of the progeny may be homozygous recessive for the mutant *D*ysf^{im} allele, and will show muscular weakness independent of APP or PS1 transgenes. Dysferlin is also expressed within the brain, within pyramidal neurons (layers III, IV and V) of the neocortex,

enrohinal cortex (layer II), CA 1-3 hippocampal neurons, and large projection neurons in the amygdala (Galvin et al., 2006). In humans with AD, dysferlin is also found within dystrophic neurites associated with Aβ-plaques, and displays shifts to relatively more insoluble forms in later stages of the disease. Galvin et al., (2006) proposed that dysferlin is involved in membrane repair of neurons, and may aggregate abnormally in neurites proximal to plaques due to an inability to repair damage. Therefore, mutant *D*ysf^{im} alleles may also interact with APP and/or PS1 transgenes in the 5XFAD mouse, and alter the development of AD-related neuropathology and motor impairments.

Therefore, the present experiment was designed to provide a detailed characterization of age related changes in motor ability in 5XFAD mice. We tested both male and female 5XFAD and wild-type mice in a cross-sectional design at 3-4, 6-7, 9-10, 12-13 and 15-16 months of age on a battery motor tests designed to assess locomotor activity, motor coordination and learning, balance and grip strength. The goals for this experiment were: (1) to determine if motor impairments in 5XFAD mice are replicable on multiple tests of motor function; (2) to determine the age of onset and severity of motor impairment on a C57BL/6 x SJL background; (3) to determine the influence of body-weight on motor performance; (4) to determine if sex differences are present in motor function in the 5XFAD mice; and (5) to determine if the mutant *D*ysf^{im} allele impairs motor performance of wild-type and/or 5XFAD mice.

3.2 Materials And Methods

3.2.1 Subjects

Male 5XFAD mice, which are hemizygous for mutant APP (+/-) and PS1 (+/-) transgenes on C57BL/6J x SJL/J FN background, were obtained from Jackson Laboratories (Bar Harbour, Maine), along with wild-type female C57BL/6J x SJL/J F1 mice with no APP (-/-) or PS1 (-/-) transgenes. The hemizygous 5XFAD mice were bred with C57BL/6J x SJL/J F1 mice and the F2 progeny, were used in this experiment. To supplement the sample size, hemizygous 5XFAD males were bred with wild-type F2 females, and the F3 offspring were used as additional subjects for this experiment. Because hemizygotes were bred with wild-type mice, and APP and PS1 transgenes co-segregate, all mice used in this experiment were either hemizygous for both transgenes (+/-), or were wild-type with no transgenes (-/-). Mice were housed in same sex groups of 2-4, in polyethylene cages (30 x 19 x 13 cm) with wood-chip bedding. Each cage contained a small polyethylene tube for enrichment (4 cm diameter, 7.5 cm long), a metal top and was covered by micro-isolator filters. Food (Purina rodent chow, #5001) and tap-water were available ad-libitum. Mice were housed in a colony room at a constant temperature (22 ± 1°C), under a reversed light-dark cycle, with lights off from 9:30 am to 9:30 pm. All testing was completed during the dark phase of the light-dark cycle, and all experimental procedures were approved by the Dalhousie University Committee on Animal Care. All mice were genotyped for the APP and PS1 transgenes, as well as the phosphodiesterase-6b retinal degeneration-1 (Pde6b^{rd1}) and the dysferlin (*D*ysf^{im}) mutations by Dr. Chris Sinal (Pharmacology Department, Dalhousie University) with PCR, using tissue samples obtained from the ears of mice at weaning (PND 21).

3.2.2 Test Battery

Mice were tested on the open-field and rota-rod at 3, 6, 9, 12 and 15 months of age, and the number of mice tested at each age is shown in table 3.1. Following these tests, mice also completed testing on the MWM and the olfactory discrimination task (data presented in Chapters 4 and 5). A subset of these mice then completed testing on the balance beam, wire suspension and grid suspension tests at 4, 7, 10, 13 and 16 months of age (see Table 3.2). A general time-line for completion of the test-battery used in chapters 3-5 is shown in Table 3.3. Body weight was obtained using an Ohaus scout II digital scale, prior to testing on the rota-rod. Mice that were homozygous recessive for $Pde6b^{rd1}$ were tested in this experiment, but the data from the open-field was not used given the potential influence of vision on exploratory activity in a novel environment.

3.2.3 Open-field

Mice were tested in the open-field maze to assess locomotor activity and anxiety-related behaviour in a novel environment. The open-field was constructed from wood, and consisted of an open square box, with a clear Plexiglas floor (Figure 3.1 A). A 4 x 4 grid of lines were drawn on the floor of the maze, along with a central square (18 x 18 cm) to clearly demark the center of the maze from the periphery. The floor and walls (36 cm high) of the maze were painted white and one of the walls was made of transparent Plexiglas to allow mice to be visible when in the apparatus. The test room (1.8 m x 4.6 m) was lit by a single 60-watt light, placed above the maze. The Limelight (Actimetrics) video-tracking system was used to record (5 frames/sec) the position of the mouse in the open field. An additional camera was positioned 1 m away from the maze to record the

Table 3.1.The number of male (M) and female (F), 5XFAD (5X) and wild-type (WT) mice included in statistical analyses on the open-field and rota-rod tests at each age.

Age	**3 months**				**6 months**				**9 months**				**12 months**				**15 months**			
Genotype	5X		WT		5X		WT		5X		WT		5X		WT		5X		WT	
Sex	M	F	M	F	M	F	M	F	M	F	M	F	M	F	M	F	M	F	M	F
Open Field	8	10	11	13	11	11	12	9	9	10	15	13	11	12	12	11	6	14	11	11
Rota-rod	13	14	11	16	12	11	12	9	9	11	19	15	11	12	15	11	6	14	12	11

Table 3.2. The number of male (M) and female (F), 5XFAD (5X) and wild-type (WT) mice included in statistical analyses on the balance beam, wire suspension and grid suspension tests at each age.

Age	**4 months**				**7 months**				**10 months**				**13 months**				**16 months**			
Genotype	5X		WT		5X		WT		5X		WT		5X		WT		5X		WT	
Sex	M	F	M	F	M	F	M	F	M	F	M	F	M	F	M	F	M	F	M	F
Balance Beam	6	7	5	7	6	6	7	8	5	11	12	12	8	10	9	11	6	12	10	10
Wire Suspension	6	7	5	7	6	6	5	5	4	11	11	12	8	10	9	11	6	12	10	10
Grid Suspension	6	7	5	7	6	6	5	5	4	10	9	11	7	5	8	7	3	7	10	10

Table 3.3. The order and general procedure of tests within the test battery completed by wild-type (WT) and 5XFAD (5X) mice (Acq = acquisition, Rev = reversal).

Behavioural Test	Days of testing	Training procedure	WT mice tested		5X mice tested		Days without testing before subsequent test is completed
			Male	Female	Male	Female	
Open-field	1	1 5 min trial	69	63	51	64	0-2
Rota-rod	5	30 trials with 6 trials/day	69	63	51	63	0-2
Morris water maze	8	3 days of Acq training (4 trials/day), 3 days of Rev training (4 trials/day), 1 probe test day (1 trial), 1 day of visible platform training (4 trials)	68	63	49	61	0-2
Olfactory Disc.	8	3 days food restriction, 4 days of training (4trials/day), 1 memory test day (1 trial)	63	58	44	56	5-10
Balance Beam	1	3 trials	45	48	31	46	0-2
Wire-Suspension	1	3 trials	40	45	30	46	0-2
Grid-Suspension	1	3 trials	37	40	26	36	NA

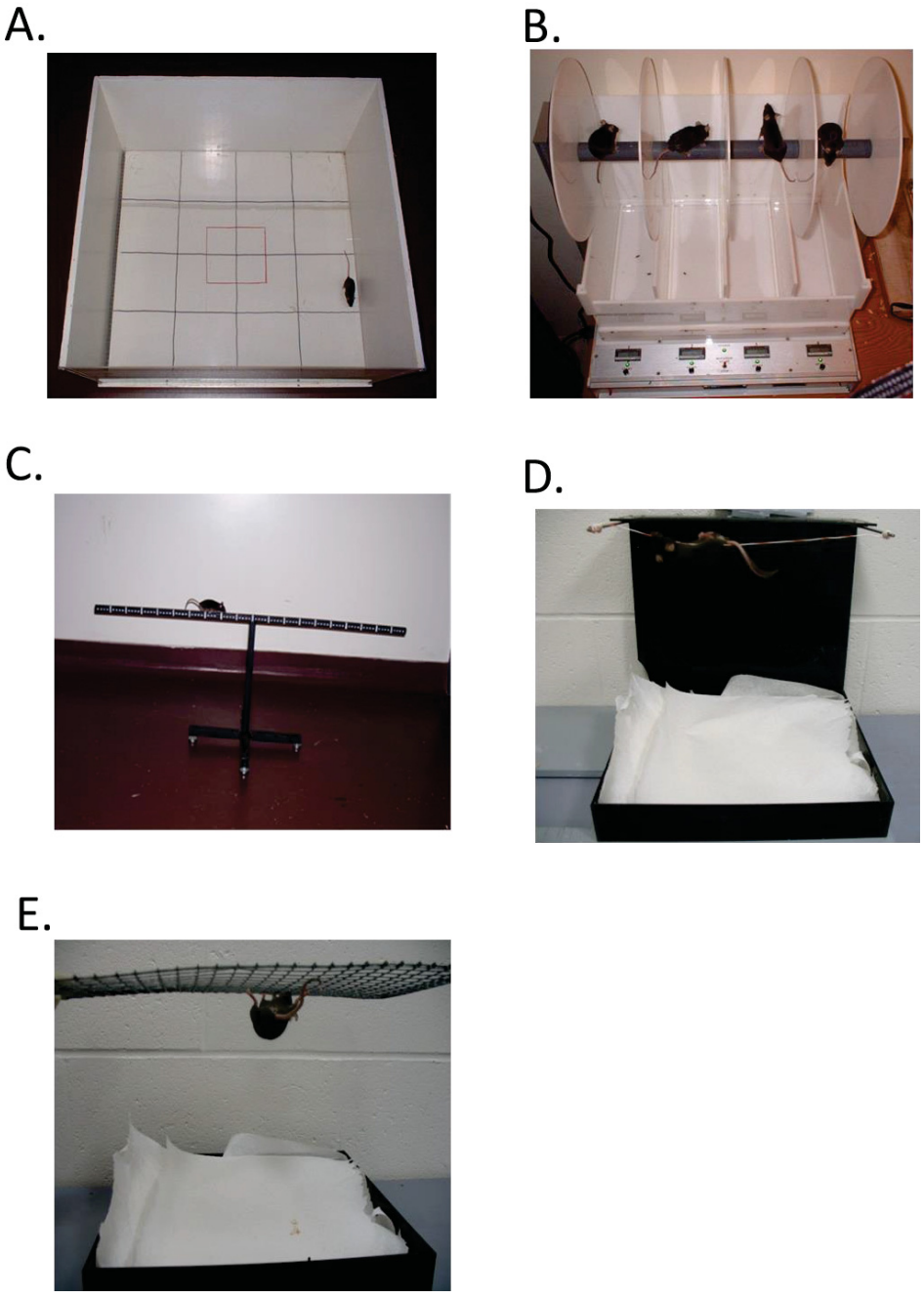

Figure 3.1. Tests of motor ability and coordination used in the present experiment. At 3, 6, 9, 12 and 15 months of age 5XFAD and wild-type mice were tested on the open-field (A) to assess locomotor activity and anxiety, followed by the rota-rod test (B) to measure motor coordination and learning. These same mice were tested at 4, 7, 10, 13 and 16 months of age on the balance beam (C) to assess balance, and on the wire and grid suspension tests (D and E) to assess grip strength.

behaviour of mice for later analysis. The experimenter sat 1.5 m away from the open-field to observe mice during testing.

For each trial, mice were placed into one of the four corners of the open-field using a 500 ml plastic container, and were allowed to explore the open-field for a 5 min trial. Locomotor activity was measured as the distance mice travelled and the total number of rears. To measure anxiety the Ethovision tracking system (Noldus) was used to create a central zone in the open-field, and average proximity to the center of this zone was recorded. The number of defecations was also recorded as a measure of anxiety-like behaviour. The maze was cleaned with 70% ethanol and dried with paper towel after each trial. Because mice were group housed, mice waited in a dark room adjacent to the test room (1.4m x 1.8m), while other mice from their cage completed their respective trials.

3.2.4 Rota-rod

Mice were tested on the AccuRotor accelerating rotarod (Accuscan Instruments Inc. Columbus Ohio) to assess neuro-muscular motor coordination, and motor learning (Brooks and Dunnett, 2009). The rota-rod consisted of an acrylic rod (3 cm diameter) with a rubber covering to assist mice in gripping the rod. The rod was separated into four 11 cm sections by circular Plexiglas dividers (15 cm high), so that up to four mice were tested simultaneously (Figure 3.1B). There were four separate holding chambers 39 cm beneath each section of the rod. Mice completed 5 days of training with 6 trials per day, and the latency to fall was recorded on each trial. The maximum length of each trial was 360 seconds, and during the trial the rod accelerated from 0 to 48 rotations per minute. At the start of each trial the mice were picked up by the base of the tail and placed onto the rod. Mice that resisted being handled, or showed signs of distress were placed on the rod

using a small plastic container. Once all mice were on the rod, the trial was started, and the latency for mice to fall was recorded automatically with sensors in the base of the holding chambers. Mice which showed clear evidence of leaping off of the rod, were immediately retrieved and placed back onto the rotating rod to continue the trial. Although mice have been previously reported to passively hang onto the rod as it rotates (Rustay et al., 2003), we observed the passive rotation behaviour rarely in mice. After all mice fell, they waited in the holding chamber for a minimum of one minute before the next trial was completed. Therefore the inter-trial interval was 1-7 minutes, with mice which had fallen early in the previous trial receiving longer inter-trial intervals than mice that performed well, which in turn reduced fatigue in poorly performing animals. The rota-rod was cleaned with soap and water after each squad of mice (1-4 animals) completed a daily test session of 6 trials. The rota-rod was located in a 112 x 260 cm room, lit by a single 60-watt red light. The experimenter stood directly adjacent to the rota-rod during all testing.

3.2.5 Balance Beam

Mice were tested on the balance beam to assess balance in an apparatus that placed less demand on motor coordination and endurance than the rota-rod (Brooks and Dunnett, 2009). The beam was 2 cm wide, 100 cm in length and was raised 40 cm from the floor. The beam was made of metal and was painted black, with white lines drawn every 1 cm along the beam to allow the distance travelled to be measured (Figure 3.1C). The test room was dimly lit by a single 60-watt light and cloth was placed under the beam to prevent injury to mice when they fell. Testing was completed in the same room as testing on the open-field. Each mouse completed three trials (inter-trial interval of

5-10 min), where they were placed onto the center of the beam and allowed to move along the beam for 120 seconds. The time until the mouse fell was recorded for each trial. Performance may be influenced by locomotor activity on the balance beam, however, as mice that are more active would be expected to have increased chances to slip and fall from the beam. Therefore the average speed (distance travelled/latency to fall) was also recorded for each trial.

3.2.6 Wire Suspension Grip-strength/Agility Test

The wire-suspension grip/agility test was completed to assess grip-strength, but also places demands on motor coordination (Brooks and Dunnett, 2009). The wire suspension test consists of a taught wire attached to two poles 27.5 cm apart (Figure 3.1D). These poles were suspended 30 cm above a small Plexiglass bin filled with paper towel, which prevented injury when mice fell from the wire. Mice completed three trials, where they were held adjacent to the wire, and were released by the experimenter when holding the wire with both fore-paws. The time until each mouse fell from the wire was recorded. If a mouse successfully maneuvered to the end of the wire and climbed onto the poles holding the wire, then the maximum possible score (60sec) was given. We noted considerable variability in performance across trials, and therefore only the trial with the longest duration to fall was used for statistical analyses.

3.2.7 Grid Suspension Grip-strength Test

The grid suspension test was completed to assess grip strength with less demand on motor-coordination than the string-suspension test (Brooks and Dunnett, 2009). The metal wire grid (25 cm x 27 cm, 7 x 7cm grids) was held by the experimenter and the mouse was placed on top of the grid. The grid was then slowly inverted so that the mouse

was suspended beneath the grid (Figure 3.1E). Mice completed three trials and the latency until they fell from the grid was recorded. Mice which moved to the edge of the grid and climbed over to the opposite side received a score of 60 seconds. A holding bin filled with paper towel was placed beneath the wire grid to prevent falling injury, and mice remained in the holding bin during the 1-min inter-trial interval. The mean of all three trials on the grid suspension test were used in statistical analysis.

3.2.8 Statistical Analyses

Statistical analyses were completed with between subject 5 x 2 x 2 factorial ANOVAs (age x sex x genotype). To determine if sex and genotype differences were present at each age, we also completed 2 x 2 ANOVAs separately at each age, with genotype and sex as between subject factors. Effect sizes (ω^2) are reported for these analyses in table 3.3.Throughout this thesis effects sizes are referred to as small ($\omega^2 \sim .06$), moderate ($\omega^2 \sim .12$) and large ($\omega^2 > .20$) based on the guidelines given by Wahlsten (2011). To determine if age-related changes in performance were present, we completed one-way ANOVAs across age, separately for each genotype and sex. For latency to fall from the rota-rod, 5 x 2 x 2 x 5 mixed design ANOVAs, with age, sex and genotype as between subject factors, and day of testing as a within subject factor were conducted. The interaction effects are only reported when significant. Post-hoc tests were completed with simple effects analyses, while Student-Newman-Keuls comparisons were completed for between subject effects of age and within-subject effects of testing day.

Within these analyses, a large number of comparisons were completed given the inclusion of multiple age groups and both sexes, and therefore correction procedures (e.g. bonferroni) for type I error (i.e. false positive effects) based on the overall number of

independent comparisons completed, would lead to an overly conservative level of significance and increased type II error rate (i.e. false negative). Therefore, we used a conservative significance level of $p < 0.01$ to reduce type 1 error, without producing large increases to type II error rate.

3.3 Results

3.3.1 Qualitative Observations

5XFAD mice did not differ from wild-type mice in physical appearance or behavior at 3 or 6 months of age. Males sometimes showed severe aggression which often resulted in mice needing to be housed individually or humanely euthanized due to wounds. As 5XFAD mice reached 12 to 15 months of age, however, they showed signs of abnormal clasping of the limbs when suspended by the tail (Figure 3.2A and B), as previously reported by Jawhar et al. (2012). The clasping behavior in some mice was accompanied by difficulty in returning to an upright position when lying on their sides or back. At 15 months of age, some 5XFAD male mice also showed prolapsis of the penis (Figure 3.2C), which has also been observed in other disease models with motor dysfunction, such as mouse models of amyotrophic lateral sclerosis with super-oxide dismutase mutations (Ijoudjil et al., 2011). At 12 and 15 months of age 5XFAD mice also showed abnormal posture and poor coat condition, which may indicate a lack of normal grooming behaviour (Figure 3.2D and E).

3.3.2 Body Weight

The main effect of genotype ($F(1,227) = 45.8$, $p < .0001$) and the genotype by age interaction ($F(4,227) = 9.06$, $p < .0001$) were significant, because 5XFAD mice weighed

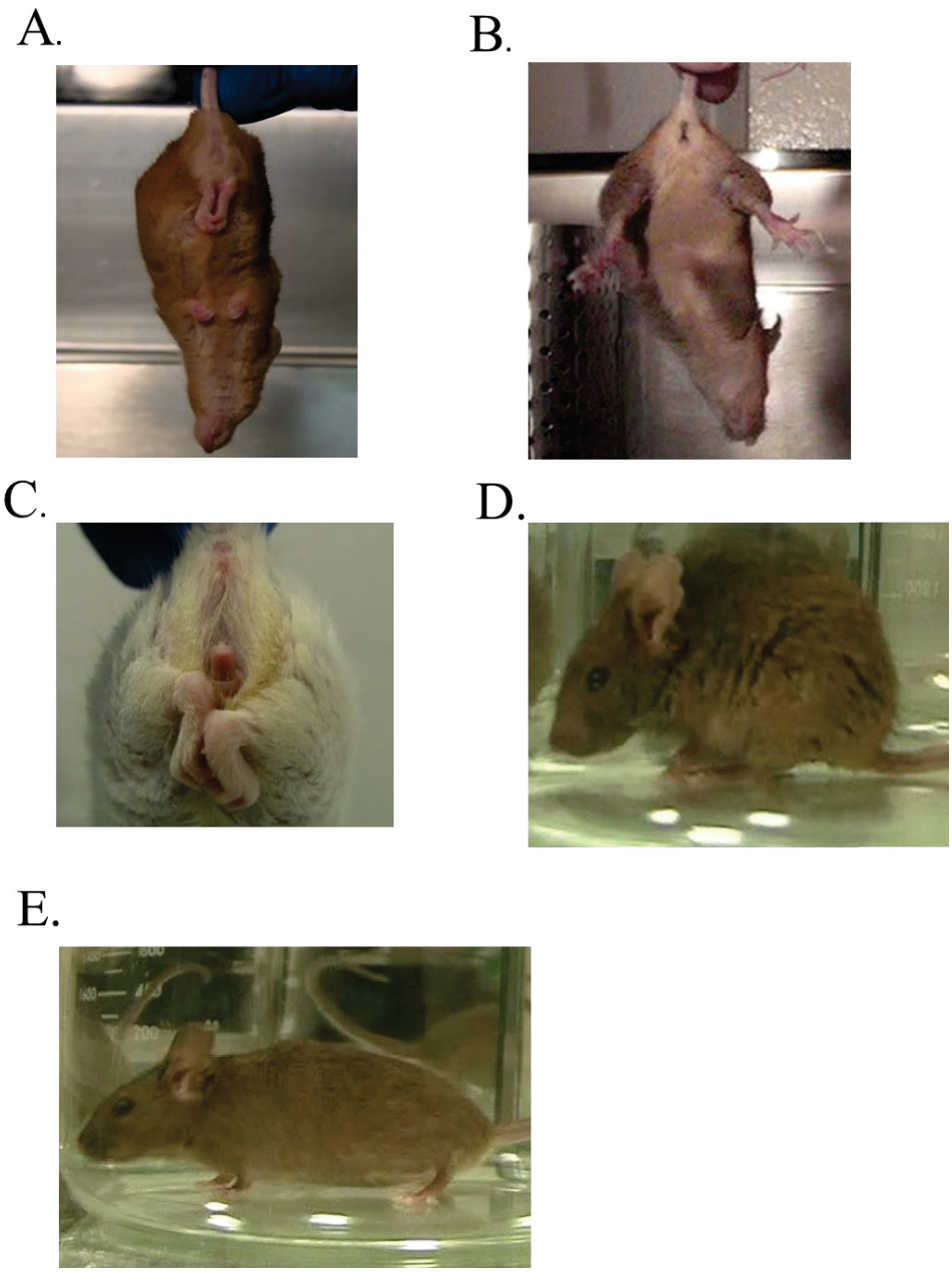

Figure 3.2 Qualitative observations on the gross behaviour and physical appearance of wild-type and 5XFAD mice. (A) After 12 months of age the majority of the 5XFAD mice clasped their hind-limbs and forepaws when suspended by the tail, while wild-type mice splayed their limbs (B). (C) In some cases prolapsis of the penis also occurred in male 5XFAD mice between 12-15 months of age. (D) The fur-coat condition of 5XFAD mice was often in poor condition relative to the coats of wild-type mice (E), and 5XFAD mice also showed abnormal posture after 12 months of age.

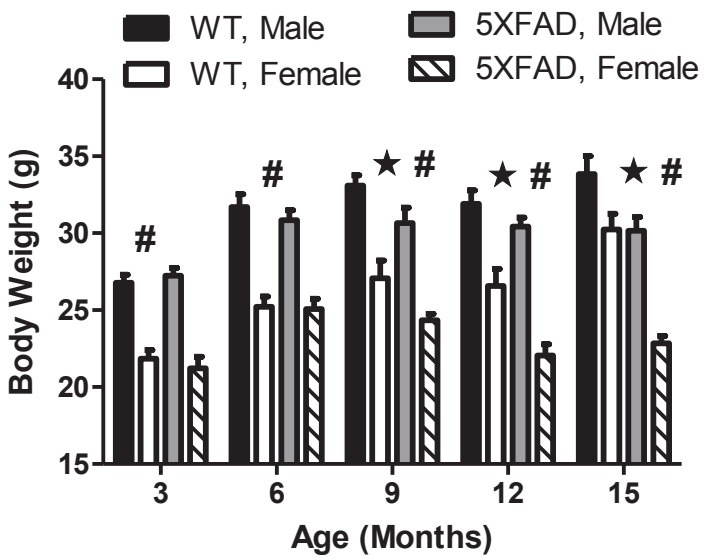

Figure 3.3. Mean body weight (+ SEM) of male and female 5XFAD and wild-type mice at 3, 6, 9, 12 and 15 months of age. # = significant sex difference, ★ = significant genotype difference. See main text for age-related changes in body-weight (section 3.3.2).

Table 3.4. Effect sizes (omega-squared, ω^2) for the genotype effect, sex effect and the genotype by sex interaction, for ANOVAs completed at 3-4, 6-7, 9-10, 12-13 and 15-16 months of age, on the open-field, rota-rod, balance beam, wire and grid suspension tests (M=months).

Open-Field	**Distance Travelled**					**Rearing**				
Age	3M	6M	9M	12M	15M	3M	6M	9M	12M	15M
Genotype	<.010	.037	<.010	.265	.173	<.010	<.010	.253	.383	.454
Sex	<.010	.036	.019	<.010	.059	.029	.020	.018	.103	<.010
Genotype x Sex	<.010	.120	<.010	<.010	<.010	.012	<.010	<.010	<.010	<.010
Rota-rod	**Body Weight**					**Latency to fall**				
Age	3M	6M	9M	12M	15M	3M	6M	9M	12M	15M
Genotype	<.010	<.010	.066	.090	.360	<.010	<.010	.281	.634	.625
Sex	.604	.622	.424	.500	.146	.023	.089	<.010	.011	<.01
Genotype x Sex	<.010	<.010	<.010	.017	<.010	<.010	.026	<.010	<.010	.021
Balance Beam	**Latency to fall**					**Speed**				
Age	4M	7M	10M	13M	16M	4M	7M	10M	13M	16M
Genotype	0.023	<.060	.196	.314	.335	.258	.026	.064	.461	.268
Sex	0.023	<.010	<.010	<.010	<.010	<.010	<.010	.026	.069	.024
Genotype x Sex	0.023	<.010	<.010	<.010	<.010	<.010	<.010	<.010	.092	<.010
Grip-Strength	**Wire-Hang: Latency**					**Grid-Hang: Latency**				
Age	4M	7M	10M	13M	16M	4M	7M	10M	13M	16M
Genotype	<.010	<.010	<.010	.089	.158	<.010	.182	.056	.261	.378
Sex	<.010	.151	.042	.062	<.010	<.010	.287	<.010	<.010	<.010
Genotype x Sex	<.010	<.010	<.010	.058	<.010	<.010	.041	<.010	<.010	<.010

less than wild-type mice at 9 months ($F(1,50) = 7.88$, $p < .01$), 12 months ($F(1,45) = 12.20$, $p < .005$) and 15 months of age ($F(1,41) = 33.68$, $p < .0001$) (Figure 3.3). The effect of sex was also significant ($F(1,224) = 265.47$, $p < .0001$), as males weighed more than females at each age ($p < .0001$).

The effect of age was significant ($F(4,224) = 24.8$, $p < .0001$), as male ($F(4,64) = 9.35$, $p < .0001$) and female ($F(4,58) = 11.33$, $p < .0001$) wild-type mice gained weight between 3 and 6 months of age. Although wild-type males did not gain weight after 6 months, female wild-types continued to gain weight, so that they weighed more at 15 months than all other ages. In 5XFAD mice, males ($F(4,64) = 5.51$, $p <.005$) and females ($F(4,57) = 6.16$, $p < .0005$) increased in body weight from 3 to 6 months of age. In male 5XFAD mice, body-weight did not significantly change from 6-15 months of age, but in 5XFAD female mice body-weight decreased, and was significantly less at 12 and 15 months of age than at 6 months of age.

3.3.3 Open-field

3.3.3.1 Locomotor Activity

For distance travelled, the genotype effect was not significant ($F(1,200) = 3.92$), but the genotype by age interaction ($F(4,200) = 5.67$, $p < .0005$) was significant, as wild-type mice travelled farther than 5XFAD mice at 12 months ($F(1,42) = 17.31$, $p < .0005$) and 15 months of age ($F(1,38) = 10.53$, $p < .005$) (Figure 3.4A). The effect of sex ($F(1,200) = 5.55$, $p = .019$), and the sex x genotype x age interaction were marginally significant ($F(4,200) = 2.74$, $p = .030$). and analyses at each age showed that female 5XFAD mice travelled farther than male 5XFAD mice at 6 months of age ($F(1,39) = 7.39$, $p < .01$), while no sex difference was present in wild-type mice. The effect of age

was significant ($F(4,200) = 4.92$, $p < .001$), as 5XFAD females ($F(4,52) = 6.92$, $p < .0005$) travelled less at 12 and 15 months, than at 3, 6 or 9 months of age.

For rears, the effect of genotype ($F(1,200) = 51.6$, $p < .0001$) and the genotype by age interactions ($F(4,200) = 6.94$, $p < .0001$) were significant, as 5XFAD mice reared less than wild-type mice at 9 months ($F(1,43) = 19.96$, $p < .0005$), 12 months ($F(1,42) = 34.61$, $p < .0001$) and 15 months of age ($F(1,38) = 34.43$, $p < .0001$) (Figure 3.4B). The effect of sex was significant ($F(1,200) = 10.79$, $p < .005$), as males reared more than females overall, but this was largely due to a significant difference at 12 months of age ($F(1,42) = 10.23$, $p < .005$). The effect of age ($F(4,200) = 6.02$, $p < .0001$) was significant, as male 5XFAD mice reared less at 15 months than 3 and 6 months of age ($F(4,40) = 5.44$, $p < .005$), while female 5XFAD mice reared less at 12 and 15 months than at 3 and 6 months of age ($F(4,52) = 8.04$, $p < .0001$).

3.3.3.2 Anxiety-related Behaviour

For average distance from the center of the open-field, the effects of genotype ($F(1,200) < 1$), sex ($F(1,200) < 1$), and all interactions were not significant (Figure 3.5A). The effect of age was significant ($F(4,200) = 3.95$, $p < .005$), as average distances were larger at 15 months than at 9 months, but individual analyses did not reveal age-related differences for 5XFAD or wild-type mice.

For defecations, the effects of genotype ($F(1,189) < 1$), sex ($F(1,189) < 1$) and age ($F(4,189) = 1.67$) were not significant (Figure 3.5B). The sex by age interaction ($F(4,189) = 3.28$, $p = 0.13$) was marginally significant, and individual analyses at each

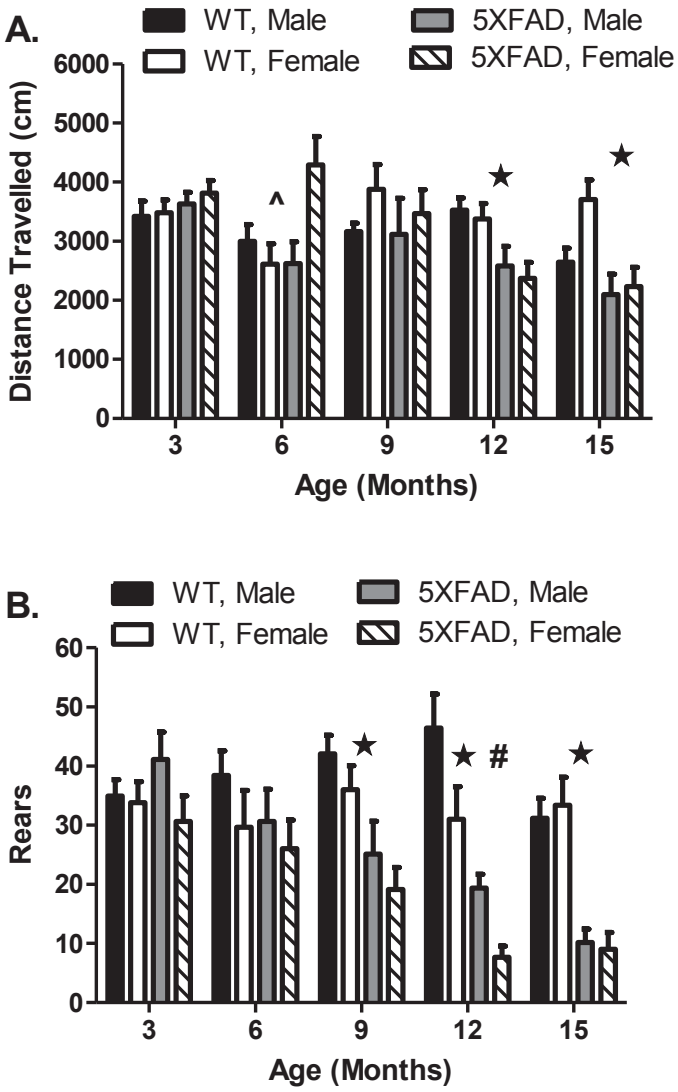

Figure 3.4. Mean (+SEM) distance travelled and rears in male and female, wild-type and 5XFAD mice on the open-field. # = significant sex difference, ★ = significant genotype difference, ^ = genotype by sex interaction. See main text for age-related changes in distance travelled and rears in the open-field (section 3.3.3).

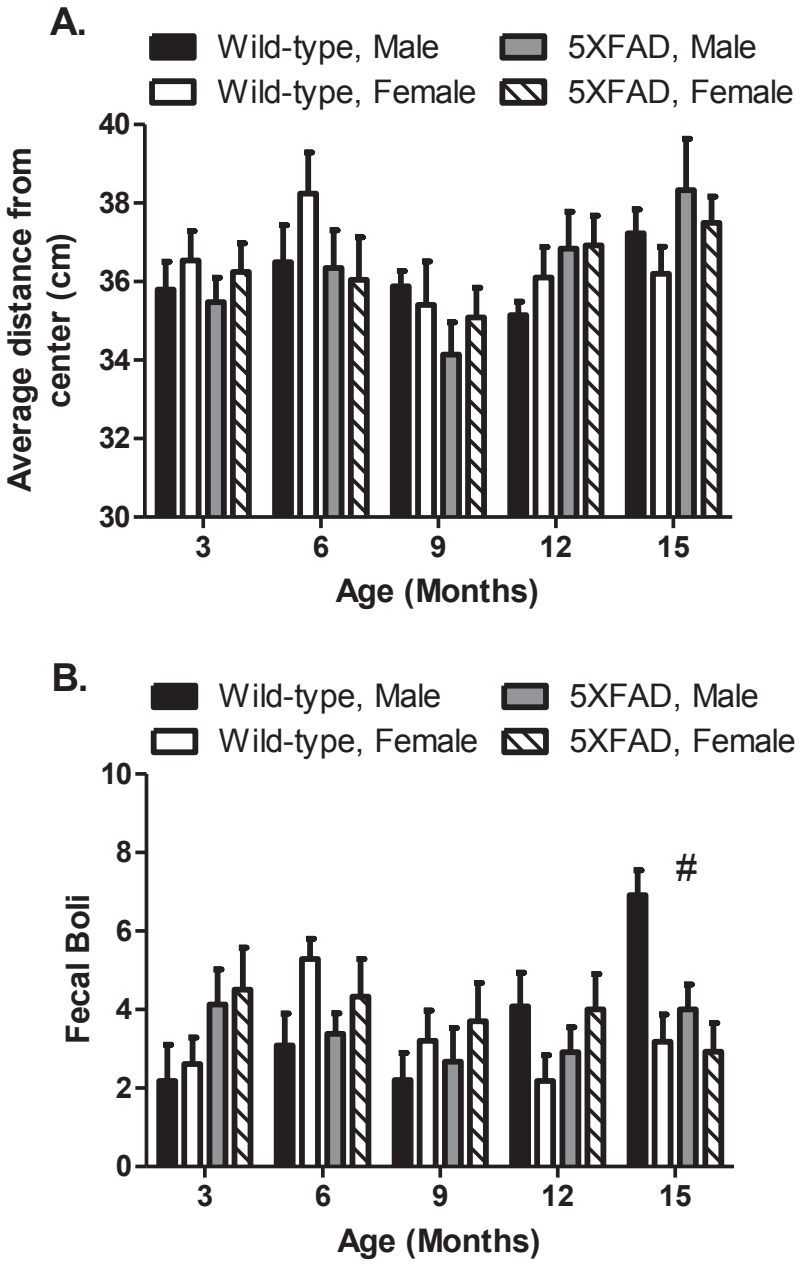

Figure 3.5. Mean (+SEM) average proximity to the center of the open-field (A) and number of fecal boli (B) in male and female, 5XFAD and wild-type mice in the open-field. # = significant sex difference. See main text for age-related changes in proximity to center and defecation in the open-field (section 3.3.3).

age showed that males defecated more than females at 15 months ($F(1,38) = 10.14$, $p < .005$). Significant age-related changes were found only in male wild-type mice, as they defecated more at 15 months than all other ages ($F(4,55) = 5.43$, $p < .001$).

3.3.4 Rota-rod

For latency for fall on the rota-rod (Figure 3.6), the effect of genotype ($F(1,224) = 95.00$, $p < .0001$) and the genotype by age interaction were significant ($F(4,224) = 25.10$, $p < 0001$), as 5XFAD mice fell faster than wild-type mice at 9 months ($F(1,50) = 22.01$, $p < .0001$), 12 months ($F(1,45) = 88.36$, $p < .0001$) and 15 months of age ($F(1,39) = 75.01$, $p < .0001$). The effect of sex ($F(1,224) =2.0$) and interactions involving sex were not significant. The effect of age was significant ($F(4,224) = 17.01$, $p < .0001$), as 5XFAD male ($F(4,46) = 9.73$, $p < .0001$) and female mice ($F(4,64) = 45.54$, $p < .0001$) took longer to fall at 3, 6 and 9 months, than at 12 and 15 months. 5XFAD female mice also took longer to fall at 3 and 6 months than at 9 months.

The within-subject effect of day was significant ($F(4,896) = 206.76$, $p < .0001$), as mice generally improved performance with training. However, the day by genotype ($F(4,896) = 18.27$, $p < .0001$), day by age ($F(16,896) = 2.11$, $p < .01$) and day by genotype by age interactions ($F(16,896) = 2.70$, $p < .0005$) were significant. These interactions were due to greater improvements in performance across training days in wild-type mice compared to 5XFAD mice at 9 months ($F(4,200) = 6.20$, $p < .0001$), 12 months ($F(4,180) = 8.90$, $p < .0001$) and 15 months of age ($F(4,156) = 22.44$, $p < .0001$).

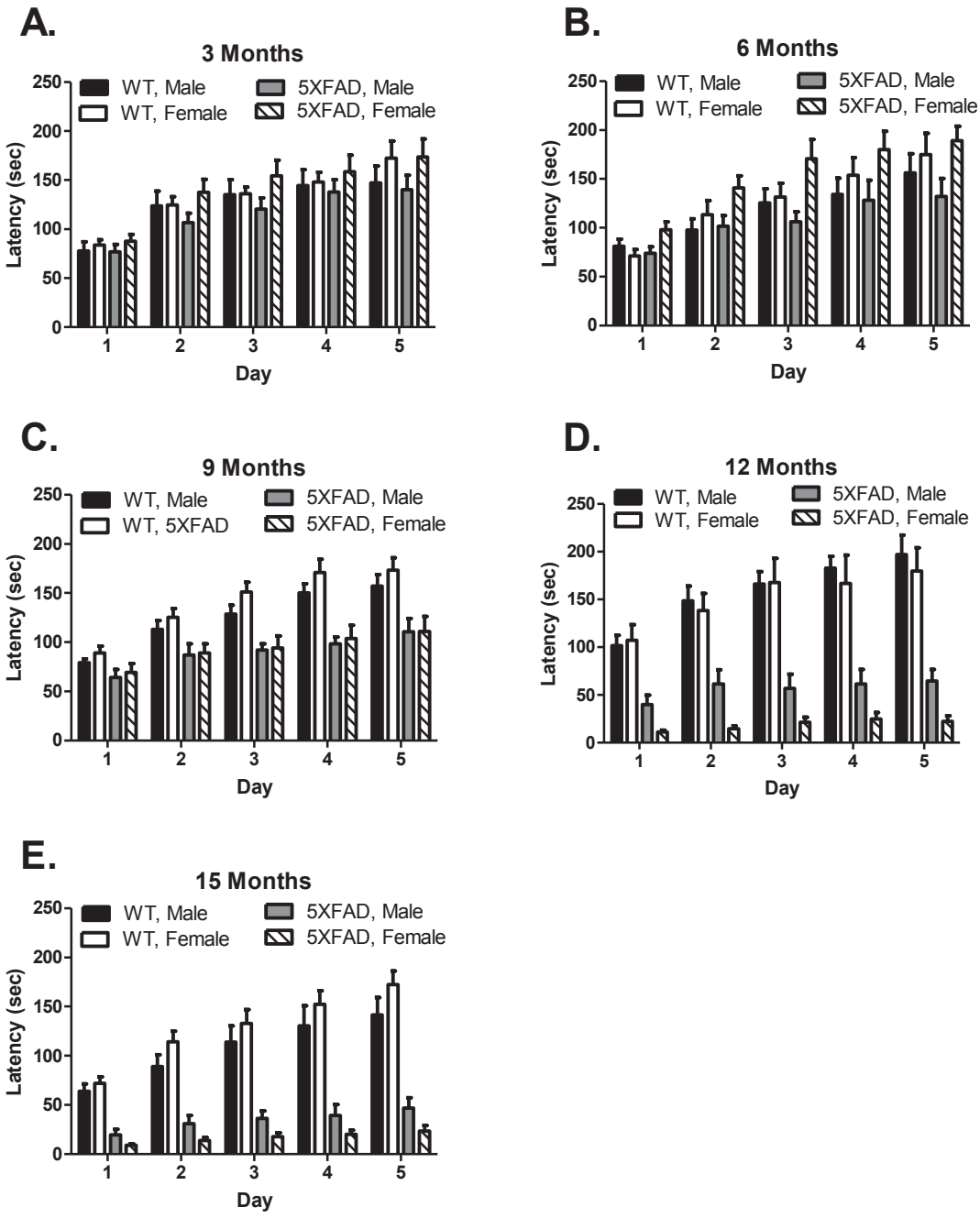

Figure 3.6**.** Mean latency (+ SEM) to fall on the rota-rod by 5XFAD and wild-type mice at (A) 3 months, (B) 6 months, (C) 9 months, (D) 12 months and (E) 15 months of age. See main text for age-related changes in latency to fall on the rota-rod (section 3.3.4).

3.3.5 Balance Beam

For latency to fall from the balance beam, the main effect of genotype ($F(1,148) = 36.56$, $p < .0001$) and the genotype by age interaction ($F(4,148) = 4.83$, $p < .005$) were significant (Figure 3.7A), as 5XFAD mice fell faster than wild-type mice at 10 months ($F(1,36) = 10.39$, $p < .005$), 13 months ($F(1,34) = 17.71$, $p < .0005$) and 16 months of age ($F(1,34) = 19.60$, $p < .0001$). The effect of sex and all other interactions were not significant. The effect of age was significant ($F(4,148) = 12.26$, $p < .0001$), as 5XFAD male ($F(4,26) = 5.48$, $p < .005$) and female mice ($F(4,41) = 5.79$, $< .001$) fell faster at 13 and 16 months than at 4 months of age.

For speed travelled on the balance beam, the effect of genotype was significant ($F(1,148) = 47.39$, $p < .0001$), as wild-type mice moved faster than 5XFAD mice at 4 months ($F(1,21) = 9.15$, $p < .01$), 13 months ($F(1,34) = 47.50$, $p < .0001$) and 16 months of age ($F(1, 34) = 15.23$, $p < .0005$) (Figure 3.7B). The effect of sex was marginally significant ($F(1,148) = 5.1$, $p = .02$), and individual analyses at each age showed that an effect of sex ($F(1,34) = 8.02$, $p < .01$) and a sex by genotype interaction ($F(1,34) = 10.33$, $p < .005$) were present at 13 months of age, with wild-type males travelling faster than females, while no difference was present in 5XFAD mice. The effect of age was also significant ($F(4,148) = 17.73$, $p < .0001$), as 5XFAD and wild-type mice from both sexes moved faster at 4 months than all other ages (all $p<.01$). 5XFAD males also moved faster at 10 months, than at 13 and 16 months of age.

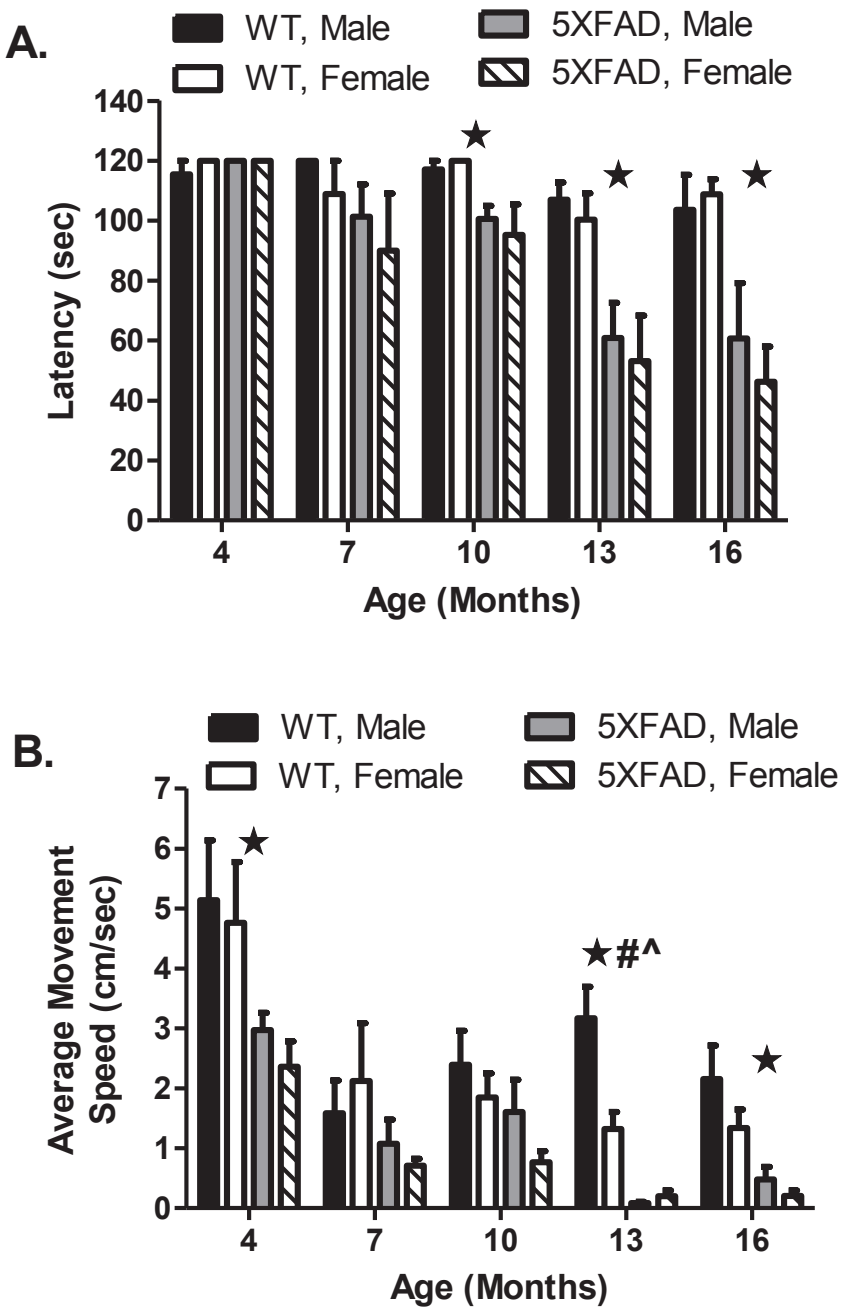

Figure 3.7**.** Mean (+SEM) latency to fall (A) and movement speed (B) on the balance beam in wild-type and 5XFAD mice at 4, 7, 10, 13 and 16 months of age. # = significant sex difference, ★ = significant genotype difference, ^ = significant genotype by sex interaction. See main text for age-related changes in latency to fall and movement speed on the balance beam (section 3.3.5).

3.3.6 Wire Hang Grip-strength/Agility

For latency to fall (Figure 3.8A), the main effect of genotype was significant ($F(1,141) = 7.85$, $p < .01$), as 5XFAD mice fell faster than wild-type mice at 16 months of age ($F(1,34) = 8.02$, $p < .01$). The effect of sex was not significant ($F(1,141) = 5.89$), and none of the interactions were significant. The effect of age was marginally significant ($F(4,141) = 3.41$, $p = .016$), as female 5XFAD mice fell faster at 16 months than at 10, 7 and 4 months of age ($F(4,41) = 4.13$, $p < .01$).

3.3.7 Grid Hang Grip-strength

For latency to fall on the grid-suspension test (Figure 3.8B), the effect of genotype ($F(1,117) = 40.61$, $p < .0001$) and the genotype by age interaction ($F(4,117) = 5.55$, $p < .0005$) were significant, as 5XFAD mice fell faster than wild-types at 7 months ($F(1,18) = 9.19$, $p < .01$), 13 months ($F(1,23) = 10.28$, $p < .005$) and 16 months of age ($F(1,25) = 18.50$, $p < .0005$) . The effect of sex was marginally significant ($F(1,117) = 4.28$, $p = .041$), which was largely because males fell faster than females at 7 months of age ($F(1,18) = 13.93$, $p < .005$). The effect of age was significant ($F(4,117) = 12.39$, $p < .0001$), as 5XFAD males ($F(4,21) = 6.09$, $p < .005$) fell faster at 16 months than at 10, 7 and 4 months of age. Age-related changes in 5XFAD females were marginally significant ($F(4,30) = 3.68$, $p = .015$), as they fell faster at 13 and 16 months, than at 4 and 10 months of age.

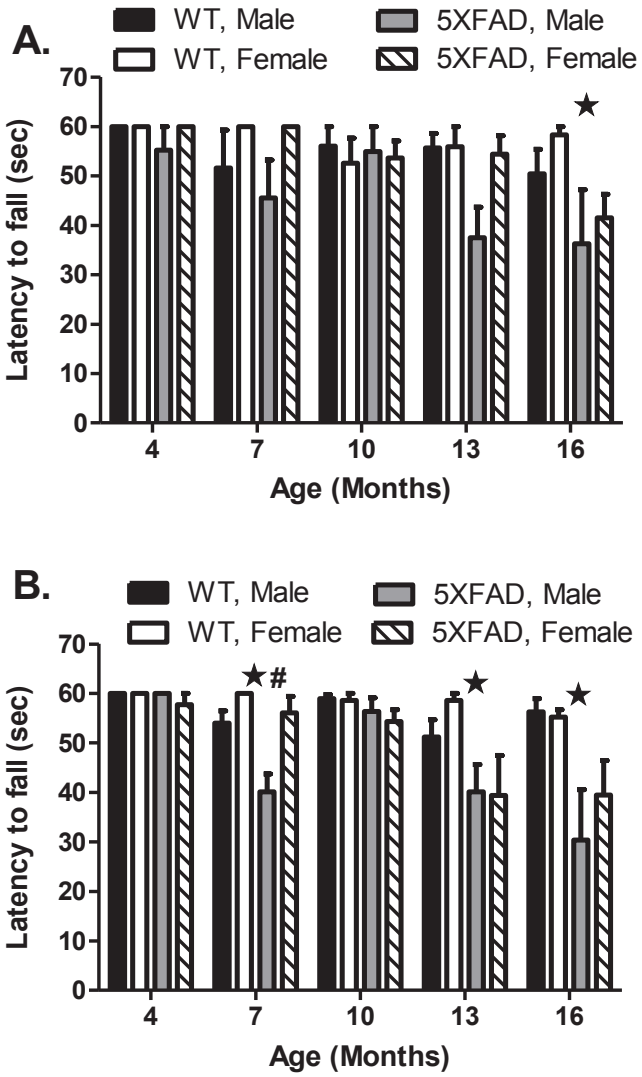

Figure 3.8. Mean (+SEM) latency for wild-type and 5XFAD mice to fall on the wire suspension test (A) and the grid suspension test (B) at 4, 7, 10, 13 and 16 months of age. # = significant sex difference, ★ = significant genotype difference. See main text for age-related changes in latency to fall on the string and grid suspension tests (section 3.3.6 and 3.3.

3.3.8 Performance Versus Body Weight Correlations

Correlations were completed separately for each genotype at each age for the open-field and the rota-rod tests. For the balance beam, wire- and grid-suspension tests, mice were pooled into two age-groups consisting of 7-10 or 13-16 months. Mice that were 4 months were not included due to low sample sizes at this age, and low levels of variability due to near-perfect performance on these tests. Correlations were also completed using animals from all ages, but separately for each genotype. In general, few correlations were significant, and there was no obvious trend for either positive or negative associations between body-weight and performance (Tables 3.5 and 3.6). At 6 months, body-weight correlated negatively with distance travelled in the open-field (r=-.52) in 5XFAD mice. At 9 months body weight correlated negatively with open-field distance (r=-.55) and latency to fall on the rotarod (r=-.49) in wild-type mice. At 12 months 5XFAD mice showed significantly positive correlations between body weight and rears on the OFM (r=.61). Also latency to fall on the rota-rod was significantly positively correlated with body weight at 12 (r=.67) and 15 months (r=.63) in 5XFAD mice. Lastly, body-weight in 7-10 month old 5XFAD mice was negatively correlated with latency to fall on the grid-suspension test (r=-.51). When animals from all ages were used in correlational analyses, body weight was negatively correlated with distance travelled on the OF (r=-.20) and latency to fall on the rota-rod (r=-.21) in WT mice. In 5XFAD mice, body-weight was significantly positively correlated with rearing in the OF (r=.25) and latency to fall on the balance beam (r=.25).

Table 3.5. Correlations between body weight and measures of motor ability on the Open-field (OF) and Rota-rod at 3, 6, 9, 12 and 15 months of age. Significant correlations are indicated by an asterisk (*).

Age	**3 months**		**6 months**		**9 months**		**12 months**		**15 months**		**All Ages**	
Genotype	5X	WT	5X	WT	5X	WT	5X	WT	5X	WT	5X	WT
OF distance	-.46	-.18	**-.52***	.21	-.31	**-.55***	.04	.05	.24	-.07	.09	**-.20***
OF rears	.33	-.09	.01	.04	.41	-.05	**.61***	.02	.19	.31	**.25***	.04
Rota-rod latency	-.24	- .03	-.38	-.22	.12	**-.49***	**.67***	-.20	**.63***	-.27	.07	**-.21***

Table 3.6. Correlations between body weight and measures of motor ability on the balance beam, wire-suspension and grid-suspension tests at 7-10, and 13-16 months of age. Significant correlations are indicated by an asterisk (*).

Age	**7-10 months**		**13-16 months**		**All Ages**	
Genotype	5X	WT	5X	WT	5X	WT
Bal. Beam latency	.08	.14	.25	.04	**.25***	-.02
Wire Susp. latency	.05	.01	-.22	-.14	.07	-.13
Grid Susp. latency	**-.51***	-.01	-.14	-.03	-.03	-.14

3.3.9 Analysis Of The *D*ysf^{im} Mutation

A total of 170 mice were genotyped for the wild-type and mutant *D*ysf^{im} alleles, and from this subset a total of 29 mice were homozygous dominant, 66 heterozygotes and 75 homozygous recessive. The distribution of genotypes deviated significantly (χ^2=33.39, $p < .0001$) from that expected given the mating of heterozygotes (42.5, 85, 42.5), suggesting that some of the breeding pairs contained mice that were homozygous recessive for the mutation. An insufficient number of mice were available at 3-4 months of age to permit inclusion of the sex factor, and therefore mice at this age were excluded from analyses on all tests. To provide increased statistical power, mice were collapsed across age groups, with the first age range (6-10 months) containing mice with prodromal to mild impairment, and the second age range (12-16 months) containing mice with moderate to severe impairment (Tables 3.7 and 3.8). Given the *D*ysf^{im} mutation is transmitted in an autosomal recessive manner, mice that were homozygous dominant and heterozygous were also pooled together for increased statistical power.

Mice that were homozygous recessive for the *D*ysf^{im} mutation did not differ from dominant mice in body-weight (data not shown), distance travelled or rearing in the open-field (Figure 3.9A and B), or in latency to fall on the rota-rod (Figure 3.9C and D). On the balance beam at 7-10 months of age, the effect of mutant dysferlin ($F(1,60) = 4.86$, $p = .032$, ω^2=.043) and the dysferlin by sex interaction ($F(1,60) = 4.88$, $p = .035$, ω^2=.043) were marginally significant, as female dominant mice fell faster than female recessive mice, but no difference was present in males (Figure 3.10 A and B). No difference was present at 13-16 months of age on the balance beam. The effect of *D*ysf^{im} was also not significant for latency to fall on the string-suspension test at 7-10 or 13-16 months of age.

Table 3.7. Number of mice that are homozygous dominant (WT), heterozygous (Het) and homozygous recessive (Mutant) for the *D*ysf^{im} mutation in wild-type (WT) and 5XFAD mice at 6-9 and 12-15 months of age on the open-field and rota-rod.

	Open-field				**Rota-rod**			
Age	**6-9 months**		**12-15 months**		**6-9 months**		**12-15 months**	
Genotype	5X	WT	5X	WT	5X	WT	5X	WT
WT Dysferlin	7	5	6	6	7	6	6	6
Het Dysferlin	6	11	10	18	6	13	11	18
Mutant Dysferlin	17	23	17	13	18	23	18	13

Table 3.8. Number of mice that are homozygous dominant (WT), heterozygous (Het) and homozygous recessive (Mutant) for the *D*ysf^{im} mutation in wild-type (WT) and 5XFAD mice at 7-10 and 13-16 months of age on the balance beam and wire-suspension test.

	Balance Beam				**Wire-suspension test**				**Grid-suspension test**			
Age	**7-10 months**		**13-16 months**		**7-10 months**		**13-16 months**		**7-10 months**		**13-16 months**	
Genotype	5X	WT	5X	WT	5X	WT	5X	WT	5X	WT	5X	WT
WT Dysf	7	6	5	6	7	6	5	6	3	4	5	4
Het Dysf	6	12	9	18	5	10	9	17	2	5	6	15
Mutant Dysf	15	22	17	13	15	17	17	13	13	14	10	12

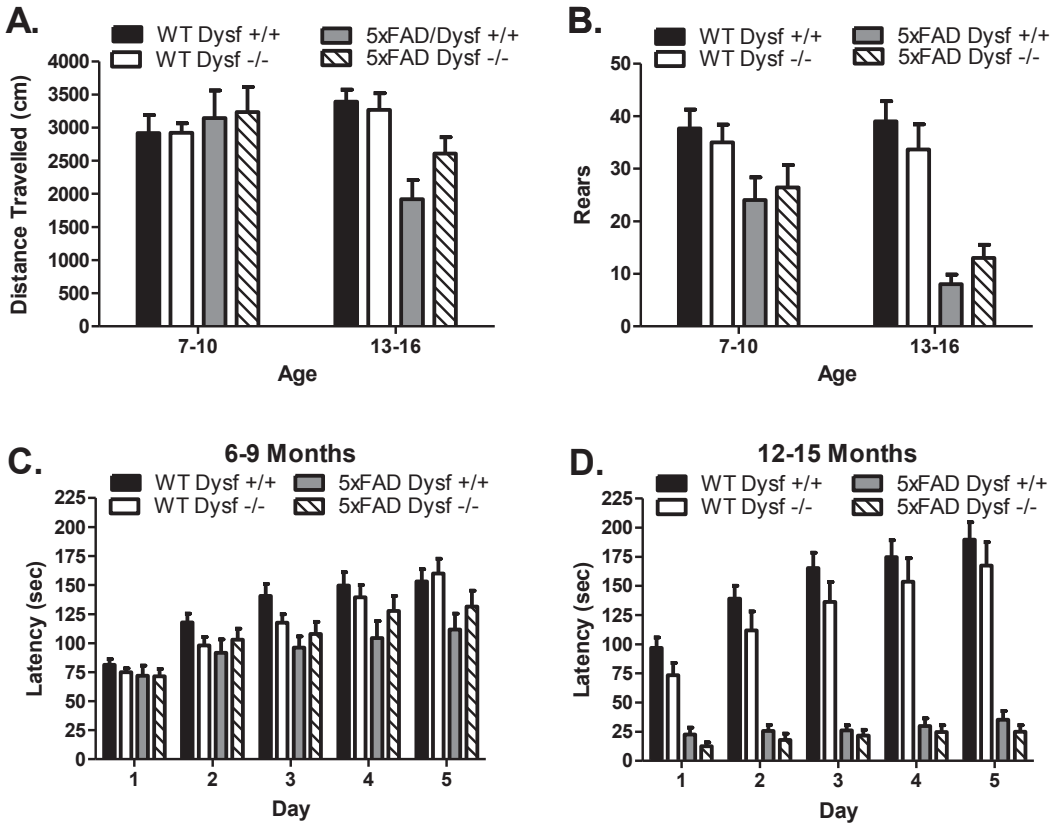

Figure 3.9. Mean (+SEM) performance for wild-type and 5XFAD mice which are either dominant (+/+) or recessive (-/-) for the *D*ysf^{im} mutation on tests of motor function. Data is shown for (A) distance travelled on the open-field, (B) rearing on the open-field, (C and D) and latency to fall on the rota-rod.

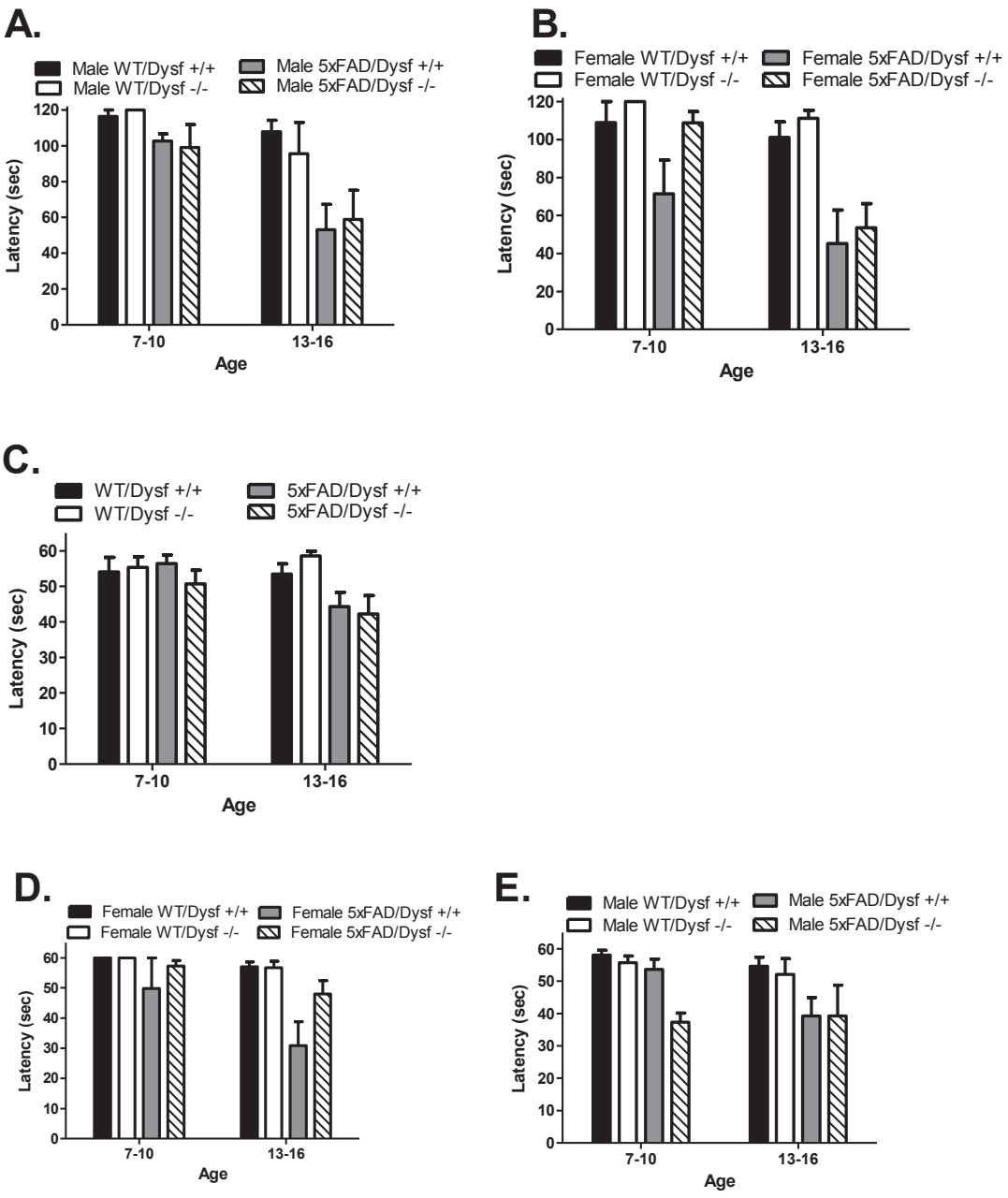

Figure 3.10 Mean (+SEM) performance for wild-type and 5XFAD mice which are either dominant (+/+) or recessive (-/-) for the *D*ysf^{im} mutation on tests of motor function. Latency to fall on the balance beam is presented separately for each sex due to an effect of *D*ysf^{im} in females but not males at 7-10 months of age (A and B). Latency to fall on the string-suspension test is shown in (C). Latency to fall on the grid-suspension test is presented separately for each sex as a *D*ysf^{im} difference is present in male 5XFAD mice at 7-10 months (D and E).

(Figure 3.10 C). On the grid-suspension test at 7-10 months, the effect of dysferlin ($F(1,48) = 7.48$, $p < .005$, $\omega^2=.052$) was significant, along with a significant dysferlin x sex ($F(1,48)=17.92$, $p < .0001$, $\omega^2=.135$) interaction., and a marginally significant dysferlin x sex x genotype interaction ($F(1,48) = 6.30$, $p < .013$, $\omega^2=.045$). The effects were present because 5XFAD *D*ysf^{im} dominant mice took longer to fall than 5XFAD *D*ysf^{im} recessive mice, but only in males and not females (Figure 3.10D and E). There were no differences due to the *D*ysf^{im} mutation at 13-16 months of age on the grid suspension test.

3.4 Discussion

The results of this experiment are discussed through the answers to five questions based on the goals of this experiment.

3.4.1. Are Motor Impairments In 5XFAD Mice Replicable Across Different Tests Of Motor Ability?

Profound age-related impairments were observed in performance of 5XFAD mice on all tests of motor function used in the present study. The age-related changes in performance suggest that the onset of motor impairment may depend on the test and/or the domain of motor function being assessed. 5XFAD mice first displayed impairments in motor coordination on the rota-rod at 9 months of age but still showed evidence of learning, albeit to a lesser extent than wild-type animals. Also at 9 months of age, 5XFAD mice showed less rearing in the open-field, suggesting a difficulty completing this behaviour due to the motor coordination required to stand on the hind-limbs. Smaller impairments were observed on the balance beam, and these impairments could not be explained by increased activity in the 5XFAD mice, suggesting impaired balance. At

12-13 months of age performance on the rota-rod and balance-beam and rearing in the open-field decreased further, and clear impairments were now present in the ability to improve performance with training on the rota-rod. This learning impairment may reflect impaired ability to modify gait to accommodate faster rotation speeds on the rota-rod, and this abnormal gait would also explain the decreased distance travelled on the open-field at this age. At 15-16 months of age, impairments were present on all measures of motor ability, including the string- and grid-suspension tests which rely on grip-strength. The impairments on the suspension tests suggest that motor strength is impaired, possibly due to atrophy of muscles due to low levels species-typical locomotor behaviours within the homecage, or due to synaptic dysfunction and/or peripheral denervation of muscles. However, an alternative and perhaps more parsimonious explanation is that the profound motor coordination impairment causes animals to fall at the onset of attempted movement on the string- and wire-suspension tests. Further research is now needed to determine the exact nature of these motor impairments, by dissociating the impairments among the different domains of motor function.

3.4.2 Are Motor Impairments In 5XFAD Mice Replicable On The C57BL/6 x SJL Hybrid Genetic Background?

Overall, the results of the present study replicate the results of Jawhar et al., (2012), indicating that the motor impairment is replicable when transgenes are present on either C57BL/6 or C57BL/6 x SJL hybrid backgrounds. There were several discrepancies across studies, however, as no difference was detected in locomotor activity in the open-field at 12 months of age by Jahwar et al., (2012), whereas 5XFAD mice travelled shorter distances than wild-type mice at 12 and 15 months of age in the present study. We also did not detect impairments on the string-suspension test until 16

months of age, whereas Jahwar et al., (2012) have detected differences as early as 9 months. It is not clear whether differences across studies are due to SJL alleles modifying the expression of the motor phenotype of 5XFAD mice in the present study, or if differences in apparatus design and test procedure of the open-field and string-suspension tests influenced motor performance. Nevertheless, these differences in motor phenotype across studies should be noted in the design of future studies examining motor function in the 5XFAD mouse.

3.4.3 Does Body Weight Influence The Motor Performance Of 5XFAD Mice?

Age-related decreases in body weight were found in 5XFAD mice, which may suggest abnormal feeding behaviour and/or metabolism is present. The reduced rearing in the open-field may indicate that 5XFAD mice cannot reliably complete this behaviour, and as a result may be unable to reliably access food located on top of the home-cage. In this case, motor dysfunction leads to chronic reduced caloric intake, causing a gradual loss in body-weight which parallels age-related impairments in motor ability. We are currently examining feeding behaviour in more detail and exploring whether hormones influencing feeding and metabolism (e.g. ghrelin and insulin) are abnormal in the 5XFAD mouse, thus contributing to body-weight loss.

Body-weight has previously been shown to influence motor performance on the rota-rod, as lighter mice tend to perform better than heavier mice (McFayden et al., 2003). Thus, body weight may influence the size of the motor impairment observed in 5XFAD mice, and may confound results if not controlled. When analyzed using mice from all ages, increased body weight was associated with poor performance on rota-rod

and decreased locomotor activity in the OF for wild-type mice, replicating the association found by McFayden et al. (2003). In 5xFAD mice, however, increased body weight was associated with better performance on the balance beam and a larger number of rears in the open-field. When examined separately at each age, negative associations were sometimes present, indicating heavier mice performed worse than lighter mice, but these associations were not reliably significant across genotype, age or test. Interestingly, in 5XFAD mice at 12 and 15 months of age, heavier mice performed better than lighter mice on the rota-rod, suggesting that body-weight loss present in 5XFAD mice at these ages is predictive of decreased motor ability. Overall, the results of the present study indicate that body-weight has a small influence on motor ability in the 5XFAD mouse, and does not account for the profound motor impairment observed.

3.4.4 Are There Sex Differences In Motor Performance In 5XFAD Mice?

Sex differences were found in motor function, but were not reliably detected across tests, ages and genotypes. No general trends were observed, with males rearing more than females on the open-field at 9 months and travelling faster on the balance beam at 13 months, whereas females took longer to fall than males on the grid suspension test at 7 months of age. Although these sex differences should be noted in future studies with the 5XFAD mice, further research is required to determine the replicability and mechanism underlying these sex differences.

3.4.5 Does The *D*ysf^{im} Mutation Influence Performance On Tests Of Motor Ability?

When breeding hemizygous 5XFAD mice on a C57BL/6 x SJL FN background with C57BL/6 x SJL F1 wild-type mice, a proportion of the offspring will be

homozygous recessive for the *D*ysf^{im} mutant allele, leading to age-related muscular degeneration and weakness. When the number of animals with this mutation is not controlled, it may confound performance differences due to transgene-effects on tests of motor function. Surprisingly we detected very few differences in motor performance due to the *D*ysf^{im} mutation. When differences were found they were dependent on the test, genotype, age and/or sex, suggesting they are not easily replicated or are spurious. Similar results were found by Rayavarapu et al., (2010), in which SJL mice did not differ from C57BL/6J mice in latency to fall on the rota-rod. Interestingly, SJL mice also showed decreased body-weight, increased grip-strength and decreased locomotor activity on the open-field compared to C57BL/6J, phenotypes which were not replicated in the present study. This suggests that these strain differences may be due to interactions between other alleles on the SJL background and *D*ysf^{im}, given that similar effects were not observed in the mixed genetic background used in the present study. Overall, these results suggest that the motor impairment in 5XFAD mice is not influenced by the *D*ysf^{im} mutation at the ages and tests used in the present study. This finding also suggests it is unlikely that *D*ysf^{im} alters the development of motor impairments found in other AD-model mice (Seo et al., 2010) maintained on a C57BL/6 x SJL background, but this should be confirmed with further research to exclude the possibility of specific transgene by *D*ysf^{im} interactions.

3.4.6 Conclusion

Age related impairments were found in motor performance in the 5XFAD mice which replicate previous findings using this strain (Jawhar et al., 2012). This motor phenotype was most severe and produced the largest effect size ($\omega^2 > .60$) on the

rota-rod, but could also be detected with all of the other tests used in the present study. Given the robustness of this phenotype, impaired motor ability can be used to explore the mechanisms underlying Aβ-induced motor dysfunction with humans, and tests of motor function can also serve as therapeutic end-points in pre-clinical research with 5XFAD mice. The motor impairment, however, can potentially confound performance on tests of cognitive function, and therefore performance on tests of cognitive ability must be examined carefully to determine the influence of motor impairment. Therefore, in chapter 4 we examined visuo-spatial learning and memory in the 5XFAD mouse using the MWM, and determined the ages at which performance is confounded by motor dysfunction.

CHAPTER 4 VISUO-SPATIAL LEARNING AND MEMORY OF 5XFAD MICE ON THE MORRIS WATER MAZE

4.1 Introduction

Impairments in visuo-spatial perceptual skills and cognition are commonly observed in AD (Weintraub et al., 2012), and may be due to the development of Aβ-pathology and neurodegeneration within brain regions associated with visuo-spatial ability, such as the hippocampus (West et al., 2004). The 5XFAD mouse may be a valuable animal model of Aβ-induced dysfunction of visuo-spatial cognition, as it rapidly develops Aβ-plaque pathology within brain regions implicated in visuo-spatial learning and memory. Aβ-plaques are first observed in the subiculum as early as 2 months of age, and are detected throughout the cortex and the hippocampus at 6 months of age (Oakley et al., 2006). 5XFAD mice also show impaired synaptic plasticity within the hippocampus (Kimura et al., 2010) at 6 months, accompanied by impaired visuo-spatial learning and memory on the MWM at 4-6 months of age (Ohno et al., 2006). This impairment in visuo-spatial learning and memory has also been successfully used to assess the efficacy of therapeutic agents, such as Icariin, brytostatin-1 and L-DOPS, in the amelioration of AD-related cognitive dysfunction in the 5XFAD mouse (Urano and Tohda, 2010; Hongpaisan et al., 2011; Kalinin, 2012).

Previous studies which have tested 5XFAD mice in the MWM consistently report visuo-spatial learning and memory impairments, but the size of these impairments varies considerably across studies. For example, some studies report that 5XFAD mice can learn the escape platform location with training (Ohno et al., 2006), albeit not as well as wild-type mice, resulting in modest impairments in learning and memory performance.

Other studies report little or no learning in 5XFAD mice (Hongpaisan et al., 201; Urano and Tohda, 2010; Kalinin et al., 2012), resulting in large impairments in learning and memory performance. The large variability in the performance of 5XFAD mice is problematic, because it results in low replicability of data and questions the validity of cognitive deficits in these mice. This variability also reduces the accuracy of predictions concerning the sample size required to consistently detect performance differences between wild-type and 5XFAD mice. Although a large impairment in the performance of 5XFAD mice is expected, it is unlikely given that other mouse models of AD typically show small or moderately sized impairments on tests of visuo-spatial learning and memory. For example, the Tg2576 mouse model of AD shows small to moderately sized impairments (Cohen's $D < .60$) in memory on the MWM (Reed et al., 2010), while the APPswe/PS1De9 mouse has moderate learning and memory impairment on the Barnes maze (O'Leary and Brown, 2009).

The large variability in visuo-spatial learning and memory performance observed in 5XFAD mice may be due to a number of factors which vary across studies. First, performance of mice on tests of visuo-spatial learning and memory can be influenced by apparatus design and procedural variables (O'Leary and Brown, 2013), and therefore studies which find large impairments in 5XFAD mice may have used experimental parameters that are better optimized to detect learning and memory impairment. Secondly, background strain genetic factors can influence performance of mice on the MWM, and when uncontrolled these factors modify the expression (i.e. size) of the disease-related cognitive impairment. Lastly, the transgene-induced learning and memory deficit in 5XFAD mice may not be reliably detected on the MWM, but experiments

which have failed to show impairment in performance in 5XFAD mice are unavailable due to publication bias in favor of results which demonstrate cognitive impairment. Given the growing number of studies which demonstrate cognitive impairment in the 5XFAD mice, we expect that the first and/or second scenarios are influencing the size of learning and memory impairments on the MWM.

Therefore, the experiment performed herein provides an in-depth examination of age-related changes in visuo-spatial learning and memory in the 5XFAD mouse using the MWM. We explored the potential effects of variations in test procedure by characterizing performance with multiple measures of learning and memory, which differ in their use across studies, and in their sensitivity to detect learning and memory impairment. Previous studies have shown the cumulative search error is a more sensitive measure of learning than the more commonly used measure of latency to find the escape platform (Gallagher et al., 1993). Furthermore, average proximity to the escape platform is a more sensitive measure of memory than the traditionally used measure of time spent in the quadrant that contained the escape platform (Maei et al., 2009). A comparison of these measures has yet to be completed with the MWM in our laboratory, or with the 5XFAD mouse.

We also addressed the issue of background genetic factors, by controlling and/or examining how these factors can influence learning and memory performance. The 5XFAD mouse is typically maintained on a C57BL/6 x SJL hybrid background, and the SJL mouse contributes mutant alleles that may influence performance on the MWM. SJL mice are homozygous recessive for the phosphodiesterase 6b mutant allele ($Pde6b^{rd1}$), which leads to retinal degeneration, functional blindness and poor performance on the

MWM (Brown and Wong, 2007). It is currently not known, however, whether active screening for the Pde6b^{rd1} mutation was completed in previous studies with the 5XFAD mouse. Therefore this study screened all mice for the Pde6b^{rd1} mutation, and actively selected against using homozygous recessive mice during breeding, thus removing the influence of this mutation.

Because SJL mice are inbred, all SJL mice are also homozygous for mutant tyrosinase alleles (*Tyr^{c}*) and are albino, because the tyrosinase enzyme is required for the production of the pigment melanin (Beermann et al., 2004). Albinism results in a large number of phenotypic changes in addition to white coat color, including reduced numbers of rod photoreceptors, abnormal retino-geniculate projections of the optic nerve via the optic chiasm, and reduced visual acuity (Rebsam et al., 2012; Wong and Brown, 2006). In addition, all SJL mice are homozygous recessive for the oculocutaneous albinism II P mutant allele (*OCA2P)*, which reduces melanin pigment production (when present) and leads to lighter coat color and pink eyes (Rosemblat et al., 1994). When the 5XFAD mice are maintained on a hybrid C57BL/6 x SJL background, offspring will consist of three phenotypes: pigmented (*Tyr^{c}* +/+, *OCA2P* +/+, brown, black), pigment reduction (*Tyr^{c}* +/+, *OCA2P* -/-, yellow or grey) or albino (*Tyr^{c}* -/-, white) (heterozygotes produce same phenotype as homozygous dominant mice). It is not known, however, if albinism alters learning and memory performance on the MWM independently or through interactions with APP and PS1 transgenes in 5XFAD mice. Lastly sex differences in visuo-spatial learning and memory in mice have been demonstrated in the MWM, but the effects of sex on visuo-spatial learning and memory performance has yet to be assessed in the 5XFAD mouse (Jonasson, 2005).

We have also demonstrated that motor impairment occurs in the 5XFAD mouse by 9 months of age (see chapter 3), and may therefore impair swimming ability and prevent accurate assessment of visuo-spatial learning and memory. However, examination of the degree to which motor impairment influences performance of 5XFAD mice on the MWM has yet to be assessed. It is not yet known whether subtle deficits in motor ability are present prior to 9 months of age and impair performance of 5XFAD mice on the MWM, or if the deficits at 9-15 months are severe enough to impair swimming ability.

Therefore we assessed visuo-spatial learning and memory in male and female 5XFAD mice at 3, 6, 9, 12 and 15 months of age on the MWM. The goals of this experiment were to (1) characterize the age-related changes in visuo-spatial learning and memory in the 5XFAD mouse, (2) to compare multiple measures of performance in their sensitivity to detect learning and memory impairment, (3) determine when age-related motor impairments in the 5XFAD mouse confound the assessment of learning and memory, (4) determine if sex influences learning and memory performance on the MWM and (5) to determine if albinism influences learning and memory performance on the MWM.

4.2 Materials And Methods

4.2.1 Subjects

Subjects and housing conditions used in this experiment were identical to those described in Chapter 3. In addition to the APP and PS1 transgenes, 5XFAD and wild-type mice were genotyped for the Pde6b^{rd1} mutation, and although all mice that were homozygous recessive for this mutation were tested on the MWM, their data were not

included in statistical analyses. The number of mice which are included in this experiment is shown in Table 4.1.

4.2.2 Morris Water Maze

Mice were tested on the MWM to assess visuo-spatial learning and reference memory. The MWM consisted of a circular pool (110 cm diameter) with 25 cm high walls. The pool was filled with water to a depth of 15 cm, which was made opaque with non-toxic liquid tempera paint. A circular escape platform (9 cm diameter, 14 cm height) was placed in the pool, 1 cm beneath the surface of the water. Small grooves were etched on the top of the escape platform, and a small rubber tube was placed around the escape platform (1cm below top), to assist aged motor-compromised 5XFAD mice in climbing onto of the escape platform. The maze was located in a room which was diffusely lit by two 100W lights pointed towards the ceiling. Extra-maze cues were visible from the water surface, and consisting of two tables upon which a computer and monitor were placed, a large door, a series of cabinets, various cues adhered to the room's walls and the general geometric layout of the test room (5.2 x 2.4 m) (Figure 4.1). The experimenter also served as an extra-maze cue and stood in the same position, 2 m away from the maze for every trial. The WaterMaze (Actimetrics) video-camera based tracking system recorded the movement of mice in the MWM, using a camera positioned above the maze. Mice completed four phases of testing; acquisition training, reversal training, probe trial and visible platform training.

Table 4.1. The number of male (M) and female (F), 5XFAD (5X) and wild-type (WT) mice included for statistical analysis in the MWM at each age.

Age	**3 months**				**6 months**				**9 months**				**12 months**				**15 months**			
Genotype	5X		WT		5X		WT		5X		WT		5X		WT		5X		WT	
Sex	M	F	M	F	M	F	M	F	M	F	M	F	M	F	M	F	M	F	M	F
Morris Water maze	8	10	11	11	11	11	12	9	9	10	15	13	10	11	12	11	5	13	10	12

Table 4.2 The number of male and female, 5XFAD (5X) and wild-type (WT) mice tested on the MWM that were pigmented, showed pigment reduction or were albino at 3-9 months of age.

Sex	**Male**		**Female**	
Genotype	5X	WT	5X	WT
Pigmented	19	24	20	20
Reduction	0	3	4	6
Albino	8	11	7	7

Figure 4.1. The Morris water maze consists of a circular pool with an escape platform hidden beneath the surface of opaque water. Mice are motivated to locate the escape platform because swimming in water is aversive. No proximal intra-maze cues indicate the escape platform's location, therefore to locate the platform, mice use extra-maze visuo-spatial cues. The extra-maze cues consisted of shapes adhered to the walls of the room, a cabinet, tables with computers, and the geometric properties of the test room.

4.2.2.1 Acquisition Training

Mice completed acquisition training over four days with four trials completed each day. For each trial the mouse was released into the pool using a 500 ml plastic container, at one of four positions around the edge of the pool (S, E, N,W). The location that mice were released across trials was determined by a Latin Square design, so that the sequence was not repeated on multiple days, and would therefore prevent mice from learning a motor response to locate the escape platform. Mice were provided a maximum of 60 sec to locate the escape platform, after which they were guided to the platform with the plastic container.

To measure learning performance latency and distance travelled to locate the escape platform were recorded. Cumulative proximity to the escape platform was also measured in order to calculate the cumulative search error measure developed by Gallagher et al., (1993). Cumulative proximity was determined by measuring the distance the mouse was located from the center of the escape platform every second, and then summing these values over the entire trial. The cumulative proximity required for the optimal swim path was also calculated using the average swim speed for the trial, and the distance the mouse was released from to the escape platform. The cumulative proximity for the optimal path is then subtracted from the total cumulative proximity for the entire trial to obtain the cumulative search error measure. Swim speed was also measured to assess swimming ability. Mice were tested in squads of 3-6, and were placed into individual holding cages with beddings of paper towel during daily training sessions. The inter-trial interval was typically 5-10 minutes, but was extended to 10-15 minutes in 12

and 15 month old 5XFAD mice to reduce the possibility of hypothermia due to their lower body weight and slower swim speeds.

4.2.2.2 Reversal Training

Following acquisition training mice completed three days of reversal training, where the escape platform remained hidden, but was moved to the opposite side of the pool. The procedure for reversal training was the same as acquisition training.

4.2.2.3 Probe Trial

A probe trial was completed 24 hours following reversal training to assess memory for the spatial location of the escape platform. In the probe trial, the escape platform was removed and the mouse was released into the pool for 60 sec. The time spent in each of the four quadrants, and the average proximity to the escape platform location in reversal training were recorded to assess memory.

4.2.2.4 Visible Platform Test

The day following the probe trial, visible platform training was completed where the escape platform was placed in a new location, but was rendered visible with a brightly colored top/lid and flag placed on top of the escape platform. Visible platform training was used to determine the extent to which performance in acquisition and reversal training was influenced by non-cognitive confounds, including poor visual ability or reduced motivation to escape from the water. Mice completed four trials, with the same procedure and measures of performance used during acquisition and reversal training.

4.2.3 Statistical Analyses

Analyses using full mixed-design models with age as a factor were completed, but not included due the large number of interactions involving age and trial, thus requiring a large number of post-hoc comparisons. Therefore, analyses completed separately at each age are presented. For measures of learning, we completed mixed design ANOVAs (2 x 2 x 3) separately for each testing phase, with genotype and sex as between subject factors, and day as a within subject factor. Measures of memory performance during the probe trial were analyzed with 2-way factorial ANOVAs (genotype x sex). Age-effects were assessed with simple effects one-way ANOVAs, and were completed separately for each genotype and sex. For all analyses a significance level of $p < 0.01$ was used. Post-hoc tests were completed with simple effects analyses, while Student-Newman-Keuls comparisons were completed for between subject effects of age and within-subject effects of testing day. To compare sensitivity of measures of learning and memory performance, the measure of effect size omega-squared (ω^2) is reported for between subject effects in table 4.3.

4.3 Results

4.3.1 Acquisition Training

4.3.1.1 Latency To Locate Escape Platform

Latency to locate the escape platform did not differ between genotypes at 3 months of age, but the genotype difference at 6 months was marginally significant ($F(1,39) = 6.45$, $p < .015$), with wild-type mice locating the escape platform faster than 5XFAD mice. Wild-type mice also located the escape platform faster than 5XFAD mice at 9 months ($F(1,43) = 9.92$, $p < .005$), 12 months ($F(1,39) = 20.85$, $p < .0001$) and 15

months of age ($F(1,36) = 49.15$, $p < .0001$) (Figure 4.2 A-E). No sex differences were present at any age tested. The effect of training day was significant at all ages tested as mice generally improved with training ($p < .0001$). The day by genotype interaction was marginally significant at 12 months ($F(2,78) = 4.63$, $p = .013$) and significant at 15 months of age ($F(2,72) = 8.84$, $p < .0005$) as wild-type mice improved with training, while 5XFAD animals did not.

Age-related analyses showed that performance of wild-type mice did not change significantly with age, while male ($p < .0001$) 5XFAD mice performed worse at 15 months than at 3 and 9 months, and female ($p < .0001$) 5XFAD mice performed worse at 12 and 15 months than at 3, 6 and 9 months of age.

4.3.1.2 Distance Travelled To Locate Escape Platform

Distance to locate the escape platform did not differ between genotypes at 3 or 6 months of age, but the difference was marginally significant at 9 months ($F(1,43) = 4.86$, $p = .033$), with wild-type mice located the escape platform in a shorter distance than 5XFAD mice (Figure 4.3A-E). This genotype difference was not replicated at 12 or 15 months of age, because 5XFAD mice were frequently unable to locate the escape platform and swam slower than wild-type mice. The effect of day was significant at 3, 6, 9 and 12 months ($p<.01$) and marginally significant at 15 months ($p = .014$) with performance generally improving with training. However, the genotype x trial interaction was significant at 12 months ($F(2,78) = 5.44$, $p < .01$) and 15 months of age ($F(2,70) = 10.44$, $p < .0005$), as wild-type mice improved with training, whereas 5XFAD mice did not. Age-related changes in performance were not significant for either sex in both 5XFAD and wild-type mice.

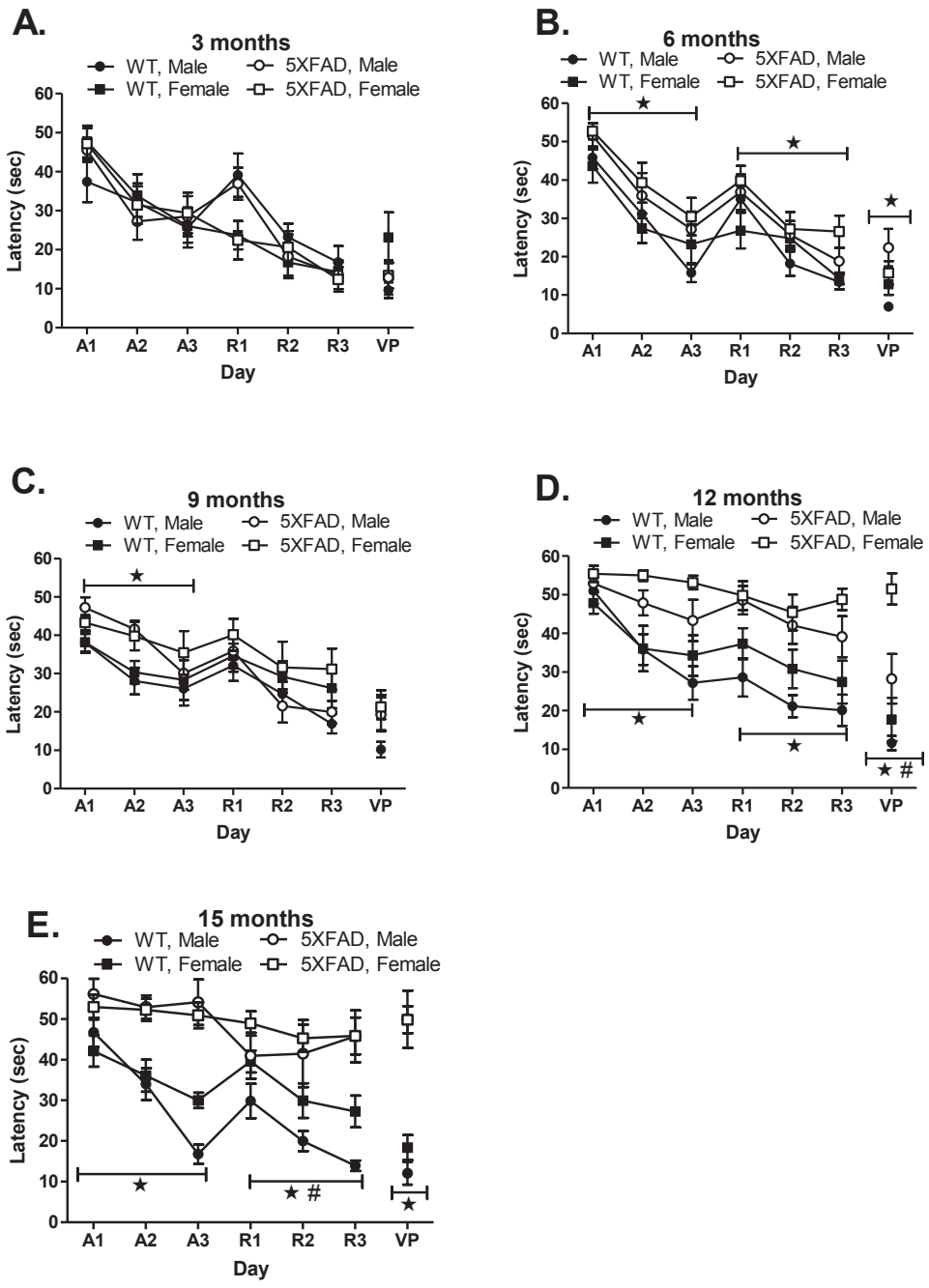

Figure 4.2. Mean (+/- SEM) latency to locate the escape platform in the MWM at 3 months (A), 6 months (B), 9 months (C), 12 months (D) and 15 months (E) of age, in male and female, wild-type and 5XFAD mice. A=Acquisition, R= reversal, VP = visible platform. ★ = significant genotype differences, # = significant sex difference.

Table 4.3. Effect sizes (omega-squared, ω^2) for the genotype effect, sex effect and the genotype by sex interaction, for ANOVAs completed at 3, 6, 9, 12 and 15 months of age, for acquisition and reversal training on the MWM (M=months).

MWM	**Acquisition: Latency**					**Reversal: Latency**				
Age	3M	6M	9M	12M	15M	3M	6M	9M	12M	15M
Genotype	<.010	.117	.165	.312	.551	<.010	.129	<.010	.368	.377
Sex	<.010	<.010	<.010	.016	<.010	.066	<.010	.062	.038	.053
Genotype x Sex	<.010	<.010	<.010	<.010	<.010	<.010	<.010	<.010	<.010	<.010
MWM	**Acquisition: Distance**					**Reversal: Distance**				
Age	3M	6M	9M	12M	15M	3M	6M	9M	12M	15M
Genotype	<.010	<.010	.078	<.010	.032	<.010	.096	<.010	<.010	.167
Sex	.056	.011	<.010	.028	<.010	<.010	.023	.027	.087	.152
Genotype x Sex	<.010	<.010	<.010	<.010	<.010	<.010	<.010	<.010	.026	<.010
MWM	**Acquisition: Cumulative Search Error**					**Reversal: Cumulative Search Error**				
Age	3M	6M	9M	12M	15M	3M	6M	9M	12M	15M
Genotype	<.010	.108	.196	.205	.523	<.010	.074	<.010	.280	.248
Sex	<.010	<.010	<.010	.025	<.010	.062	<.010	.058	.069	.104
Genotype x Sex	<.010	<.010	<.010	<.010	<.010	<.010	<.010	<.010	<.010	<.010
MWM	**Acquisition: Swim Speed**					**Reversal: Swim Speed**				
Age	3M	6M	9M	12M	15M	3M	6M	9M	12M	15M
Genotype	<.010	.033	<.010	.476	.299	<.010	<.010	<.010	.375	.231
Sex	.175	.015	<.010	<.010	<.010	.194	.013	<.010	<.010	<.010
Genotype x Sex	<.010	<.010	<.010	<.010	.034	<.010	<.010	<.010	<.010	.063
MWM	**Probe: % Time in Correct Quadrant**					**Probe: Average Proximity**				
Age	3M	6M	9M	12M	15M	3M	6M	9M	12M	15M
Genotype	<.010	<.010	<.010	<.010	.235	<.010	<.010	<.010	<.010	.277
Sex	<.010	<.010	.105	<.010	<.010	<.010	.062	.032	.026	<.010
Genotype x Sex	.126	<.010	<.010	<.010	<.010	.108	<.010	<.010	<.010	<.010

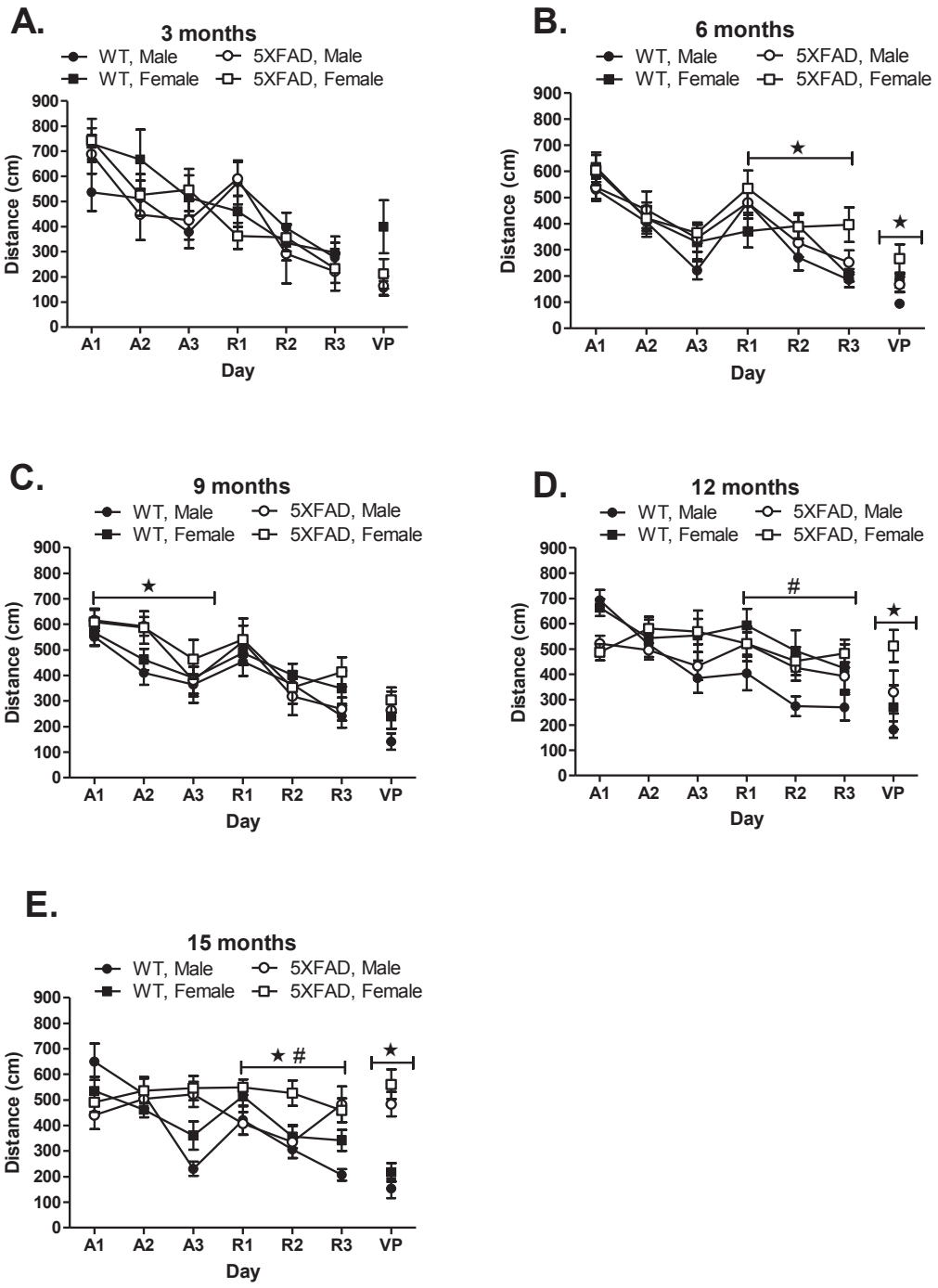

Figure 4.3 Mean (+/- SEM) distance travelled to locate the escape platform in the MWM at 3 months (A), 6 months (B), 9 months (C), 12 months (D) and 15 months (E) of age, in male and female, wild-type and 5XFAD mice. A=Acquisition, R= reversal, VP = visible platform. ★ = significant genotype differences, # = significant sex difference.

4.3.1.3 Cumulative Search Error

Cumulative search error did not differ between genotypes at 3 months of age (Figure 4.4A), but this difference was marginally significant at 6 months, as wild-type mice had smaller search errors than 5XFAD mice ($F(1,39) = 6.01$, $p = .018$). Wild-type mice also had significantly smaller search errors than 5XFAD mice at 9 months ($F(1,43) = 12.03$, $p < .005$), 12 months ($F(1,39) = 12.23$, $p < .005$) and 15 months of age ($F(1,36) = 43.36$, $p < .0001$) (Figure 4.4A-E). Cumulative search error generally decreased across training at all ages ($p < .0001$). The genotype by day interaction was significant at 12 months ($F(2,78) = 4.90$, $p < .01$) and marginally significant at 15 months of age ($F(2,72) = 4.64$, $p = .013$), as wild-type mice showed greater improvements with training than 5XFAD mice. The day by sex interaction was also marginally significant at 15 months of age ($F(2,72) = 4.64$, $p = .013$), as male mice improved with training, whereas females did not.

Age-related analyses showed that performance of wild-type mice did not change significantly with age, while male ($p < .0001$) 5XFAD mice had worse performance at 15 months than 3, 6 and 9 months of age. Female 5XFAD ($p < .0001$) mice performed worse at 12 and 15 months, than at 3, 6 and 9 months of age.

4.3.1.4 Swim Speed

No significant differences in swim-speed were found between genotypes at 3, 6 and 9 months of age (Figure 4.5 A-C), but 5XFAD mice swam slower than wild-type mice at 12 months ($F(1,39) = 39.15$, $p < .0001$) and 15 months of age ($F(1,36) = 18.52$, $p < .0001$). Female mice also swam faster than male mice at 3 months of age ($F(1,36) = 9.21$, $p < .005$), but sex differences were not present at other ages tested.

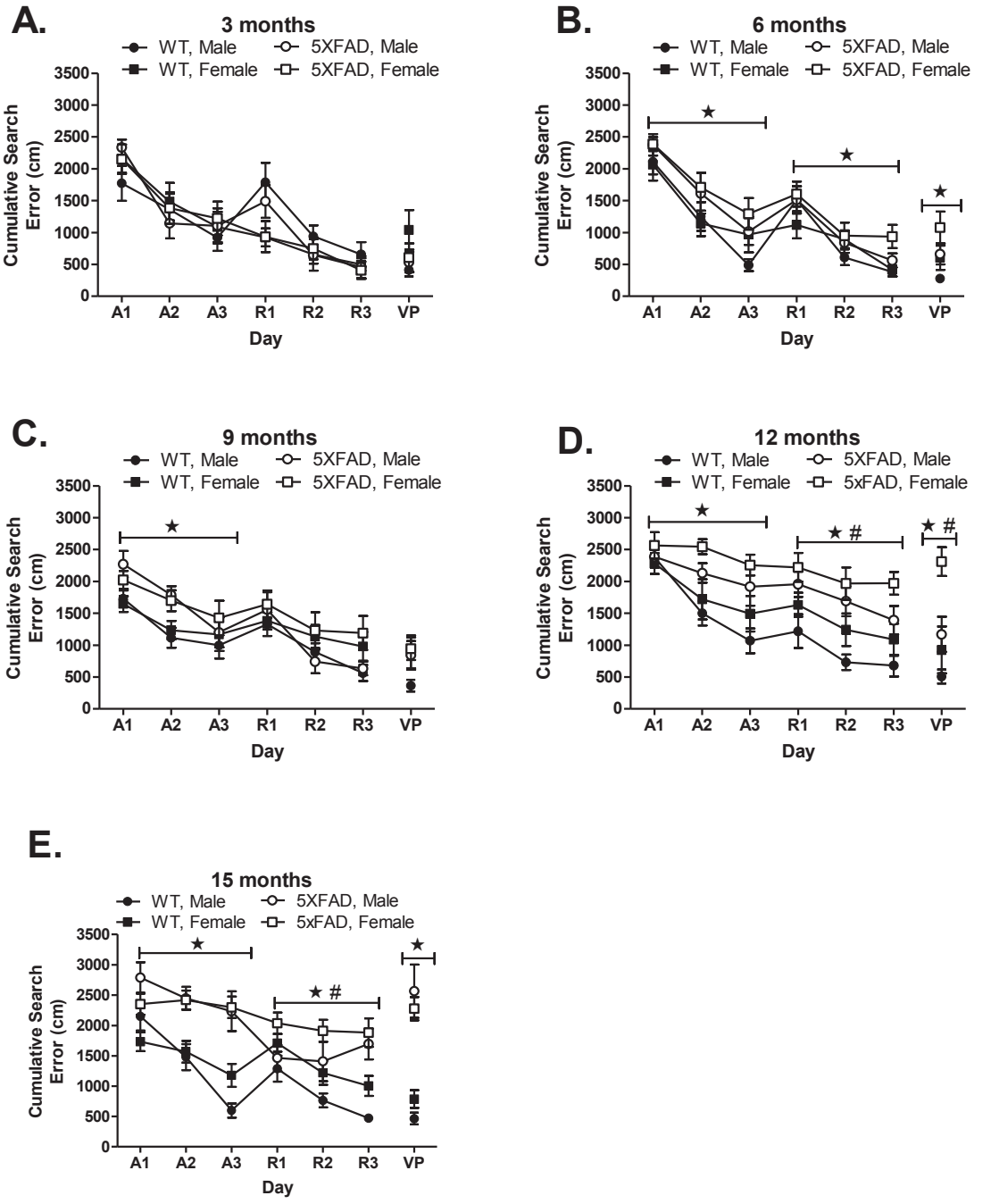

Figure 4.4 Mean (+/- SEM) cumulative search error to locate the escape platform in the MWM at 3 months (A), 6 months (B), 9 months (C), 12 months (D) and 15 months (E) of age, in male and female, wild-type and 5XFAD mice. A=Acquisition, R= reversal, VP = visible platform . ★ = significant genotype differences, # = significant sex difference.

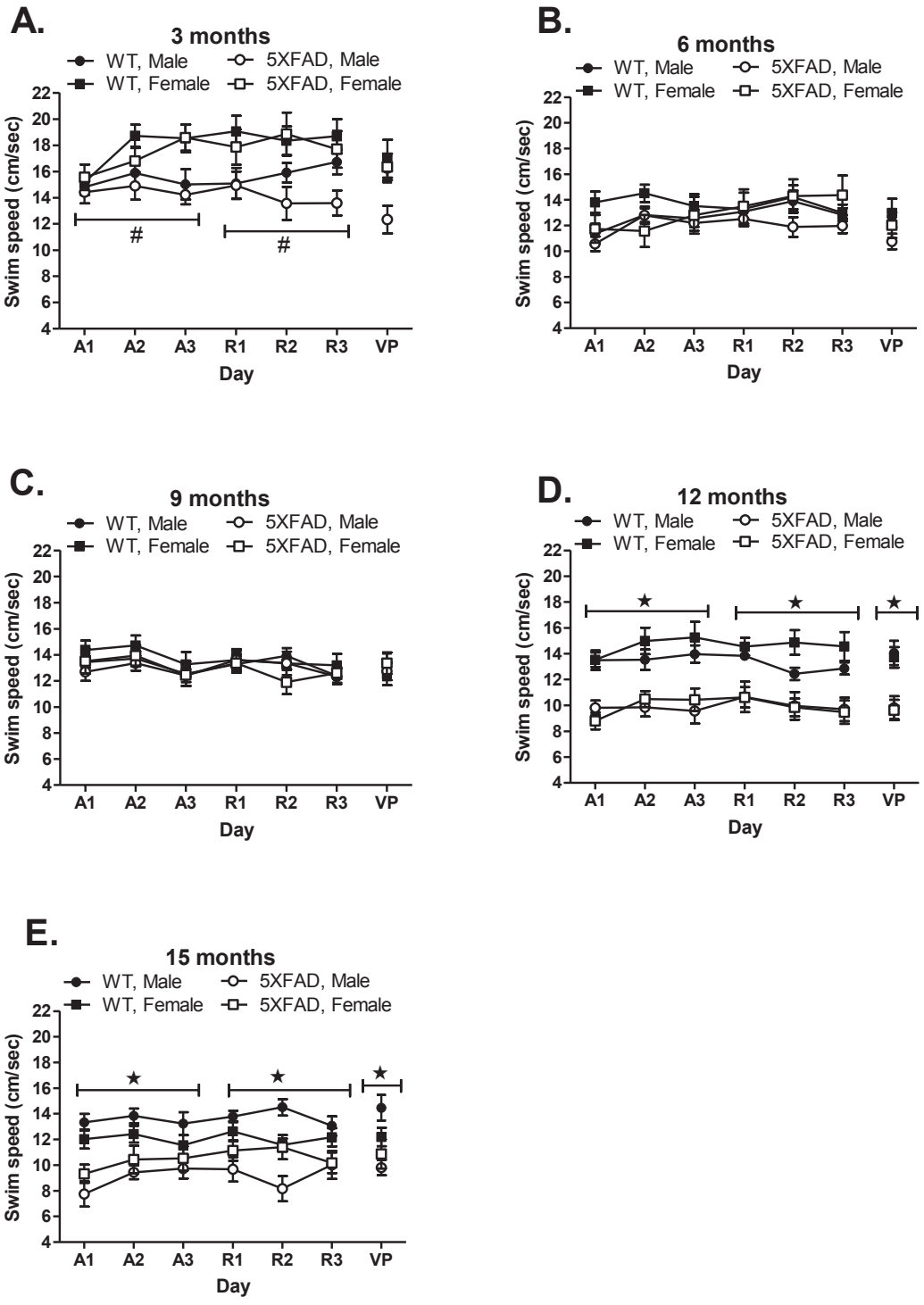

Figure 4.5. Mean (+/- SEM) swim speed in the MWM at 3 months (A), 6 months (B), 9 months (C), 12 months (D) and 15 months (E) of age, in male and female, wild-type and 5XFAD mice. A=Acquisition, R= reversal, VP = visible platform, ★ = significant genotype difference, # = significant sex difference.

The effect of day was significant at 3 months of age as swim speed increased with training ($F(2, 72) = 5.42$, $p < .01$), and at 9 months of age ($F(2,86) = 7.29$, $p < .005$) as swim speed decreased with training..

Age-related analyses showed that wild-type male mice did not significantly differ in swim -speed. Wild-type female mice swam faster at 3 months than at all other ages. In 5XFAD mice, males swam faster at 3 months than at 6, 12 and 15 months, and also swam faster at 6 and 9 months than at 12 and 15 months. 5XFAD females swam faster at 3 months than all other ages, and faster at 6 and 9 months than at 12 and 15 months.

4.3.2 Reversal Training

4.3.2.1 Latency To Locate Escape Platform

Latency to locate the escape platform did not differ between genotypes at 3 months of age, but wild-type mice located the escape platform faster than 5XFAD mice at 6 months ($F(1,39) = 7.27$, $p = .01$) (Figure 4.2 A-E). This difference was not present at 9 months, but was again found at 12 months ($F(1,39) = 21.17$, $p <.0001$) and 15 months of age ($F(1,35) = 26.82$, $p < .0001$). A marginally significant sex difference was present at 15 months of age ($F(1,35) = 4.65$, $p = .038$), with male mice performing better than female mice. The effect of day was significant at all ages tested as mice generally improved with training ($p < .0005$). The day by sex interaction was also significant at 3 months of age ($F(2,76) = 6.79$, $p < .005$), as males took longer to locate the escape platform than females, but only on the first day of reversal training (Figure 4.2 A). The day by genotype interaction was also significant at 15 months of age ($F(2,70) = 6.60$, $p < .005$), as wild-type mice improved with training, while 5XFAD mice did not (Figure 4.2 E).

Age-related analyses showed that performance of wild-type male mice did not change significantly with age, whereas female wild-type mice performed better at 3 months than at 9, 12 and 15 months. In 5XFAD mice, males performed better at 3, 6 and 9 months, than at 12 and 15 months of age. Female 5XFAD mice, however, performed better at 3 months than all other ages, and better at 6 and 9 months than at 12 and 15 months of age.

4.3.2.2 Distance Travelled To Locate Escape Platform

Distance travelled to locate the escape platform did not differ between genotypes at 3 months of age (Figure 4.3A), but this difference was marginally significant at 6 months of age ($F(1,39) = 5.73$, $p = .022$), as wild-type mice had shorter distances than 5XFAD mice. This genotype difference was not replicated at 9 or 12 months of age, but was again found at 15 months ($F(1,34) = 10.11$, $p < .005$). A marginally significant sex difference was present at 12 months of age, as male mice travelled shorter distances than female mice ($F(1,39) = 5.27$, $p = .027$), and this difference was significant at 15 months of age ($F(1,34) = 9.31$, $p < .005$). Distance travelled generally decreased over days at all ages ($p<.0005$). The day by sex interaction was marginally significant at 3 months of age ($F(2,72) = 3.65$, $p = .031$), with male mice performing worse than female mice on day R1 due to larger reversal effects. The day by genotype interaction was also marginally significant at 15 months of age ($F(2,68) = 4.23$, $p = .016$), as wild-type mice improved with training, whereas 5XFAD mice showed no change in performance.

Age-related analyses showed that performance of wild-type male and female mice did not change significantly with age. Performance of 5XFAD male mice also did not

change with age, whereas females performed worse at 9, 12 and 15 months, than at 3 months of age.

4.3.2.3 Cumulative Search Error

Cumulative search error did not differ between genotypes at 3 months of age (Figure 4.4A), but this difference was marginally significant at 6 months ($F(1,39) = 4.37$, $p = .043$) of age, as wild-type mice had smaller search errors than 5XFAD mice. This difference was not replicated at 9 months, but was again found at 12 months ($F(1,39) = 19.11$, $p < .0001$) and 15 months of age ($F(1,35) = 15.54$, $p < .0005$). Marginally significant sex differences were found at 12 months ($F(1,39) = 5.44$, $p = .025$) and 15 months of age ($F(1,35) = 7.13$, $p = .011$), as male mice had smaller cumulative search error than female mice. Cumulative search error generally decreased across training at all ages ($p < .005$). The genotype by day interaction was significant at 15 months of age ($F(2,70) = 8.03$, $p < .001$), as wild-type mice improved performance with training, whereas 5XFAD mice showed no improvement. The day by sex interaction was also significant at 3 months of age ($F(2,72) = 5.86$, $p < .005$), as male mice performed worse than females on day R1, due to larger reversal effects.

Age-related analyses showed that performance of wild-type male mice did not change significantly with age, whereas female mice performed better at 3 months than at 9, 12 and 15 months, and better at 6 months than at 15 months. In 5XFAD mice, males performed better at 3, 6 and 9 months, than at 12 months of age, and better at 9 months than at 15 months of age. Females, however, performed better at 3 months than all other ages, and better at 6 and 9 months than at 12 and 15 months of age.

4.3.2.4 Swim Speed

No significant differences in swim-speed were found between genotypes at 3, 6 and 9 months of age (Figure 4.5 A-C), but 5XFAD mice swam slower than wild-type mice at 12 months ($F(1,39) = 24.21$, $p < .0001$) and 15 months of age ($F(1,35) = 11.75$, $p < .005$). Female mice swam faster than male mice at 3 months of age ($F(1,36) = 10.54$, $p < .005$), but not at other ages tested. The effect of day was marginally significant at 9 months of age ($F(2, 86) = 4.53$, $p = .025$), and 12 months ($F(2,78) = 2.84$, $p < .045$), as swim speed generally decreased across training. The day x genotype x sex interaction was significant at 15 months of age ($F(2,70) = 9.02$, $p < .0005$), as wild-type mice swam faster than 5XFAD mice in males but not females, and only on days R1 and R2.

Age-related analyses showed that swim speed in wild-type male and female mice was faster at 3 months, than all other ages. In 5XFAD mice, males swam faster at 3 and 9 months than at 12 and 15 months. Females swam faster at 3 months than all other ages, and faster at 6 months than at 12 months of age.

4.3.3 Probe Trial

4.3.3.1 Percentage Time In Correct Quadrant

No differences were found between 5XFAD and wild-type mice at 3, 6, 9 or 12 months of age, but wild-type mice spent more time in the correct quadrant than 5XFAD mice at 15 months of age ($F(1,34) = 12.16$, $p < .005$) (Figure 4.6A-E). The sex difference at 9 months of age was marginally significant ($F(1,42) = 6.32$, $p = .016$)., as males spent more time in the correct quadrant than females. The sex by genotype interaction was also marginally significant at 3 months ($F(1,36) = 6.69$, $p = .014$), as males performed better than females in 5XFAD mice, but not in wild-type mice.

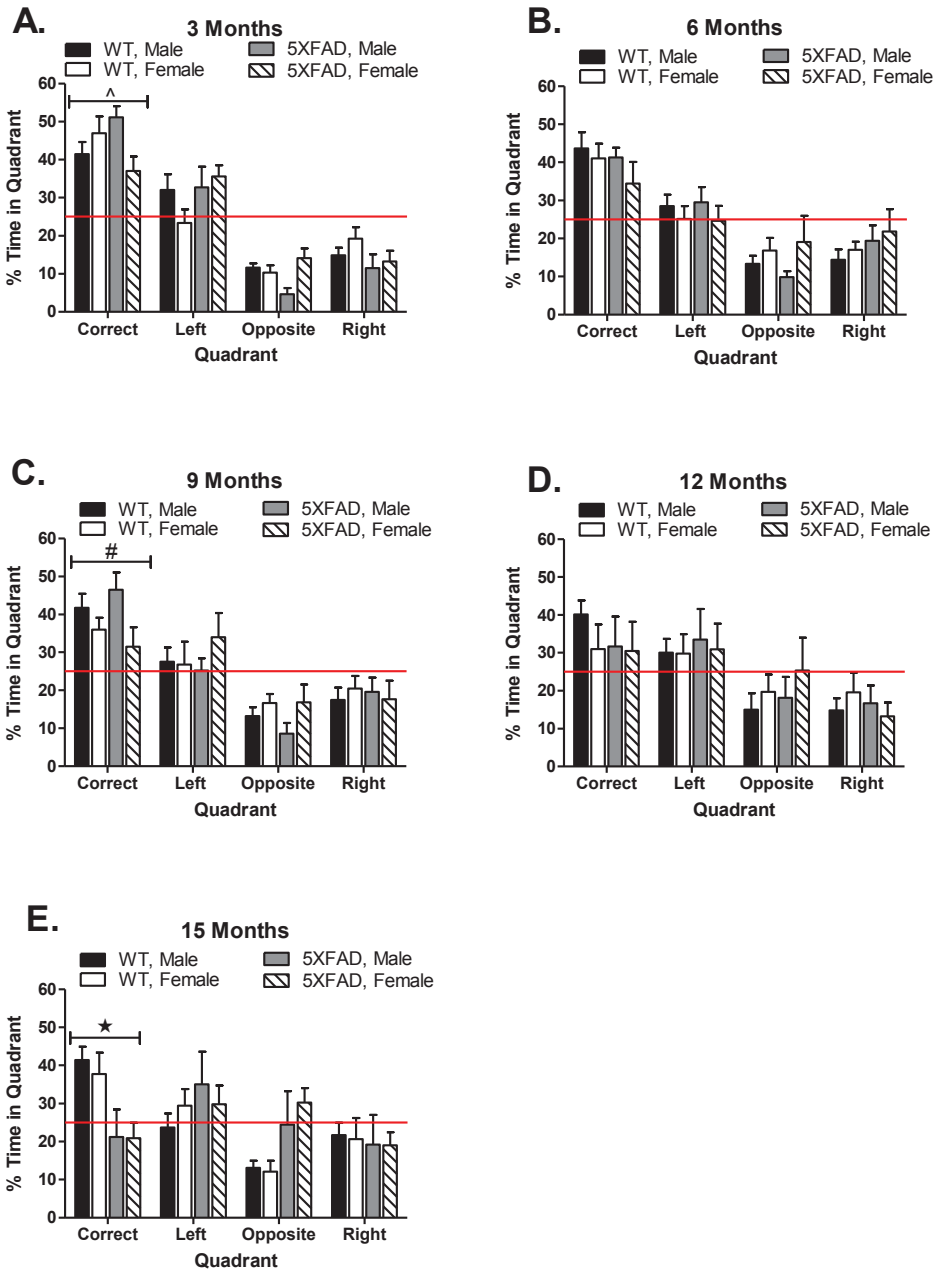

Figure 4.6. Mean (+SEM) time spent in each quadrant in the MWM probe trial at 3 months (A), 6 months (B), 9 months (C), 12 months (D) and 15 months (E) of age, in male and female, wild-type and 5XFAD mice. ★ = significant genotype difference, # = significant sex difference, ^ = significant sex by genotype interaction.

Age-related analysis showed that performance of wild-type male and female mice did not change significantly with age. Performance of 5XFAD female mice also did not change with age, whereas 5XFAD male mice performed better at 3 months than at 12 and 15 months, and better at 6 and 9 months than at 15 months of age.

4.3.3.2 Average Proximity To Escape Platform

No differences were found between 5XFAD and wild-type mice at 3, 6, 9, or 12 months of age, but wild-type mice had smaller average proximity to the escape platform than 5XFAD mice at 15 months of age ($F(1,34) = 14.89$, $p < .0005$) (Figure 4.7). Male mice also had lower average proximity than females at 9 months ($F(1,42) = 7.75$, $p < .01$).

Age-related analysis showed that performance of wild-type male and female mice did not change significantly with age. Performance of 5XFAD female mice also did not change with age, whereas 5XFAD male mice performed better at 3, 6, 9 and 12 months than at 15 months of age.

4.3.4 Visible Platform Training: (All Measures)

Wild-type mice performed significantly better than 5XFAD mice at 6 months for latency to locate the escape platform ($p<.005$), and this difference was marginally significant for distance travelled and cumulative search error ($p<.05$). At 12 months of age, wild-type mice performed significantly better than 5XFAD mice for latency to locate the escape platform ($p<.0001$), and cumulative search error ($p <0005$), and this difference was marginally significant for distance travelled ($p<.05$). At 15 months of age, wild-type mice performed significantly better than 5XFAD mice ($p<.0001$) for all measures of learning performance (Figure 4.2 – 4.4). Males also performed significantly better

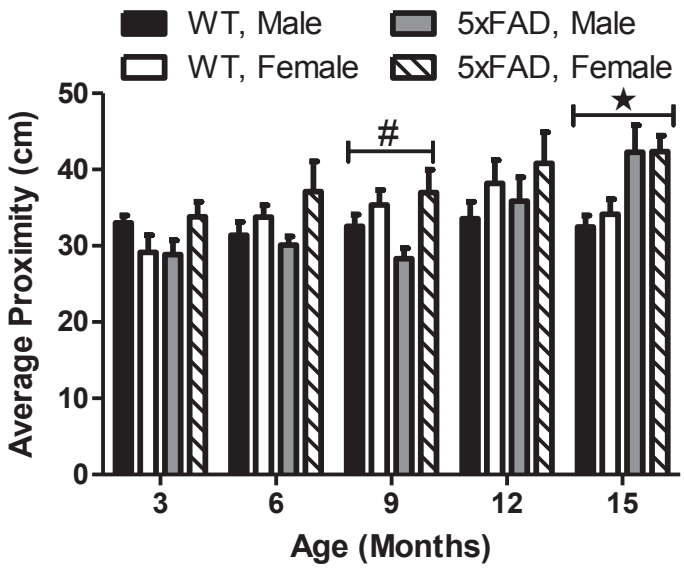

Figure 4.7 Mean (+SEM) average proximity to the escape platform in the MWM probe trial at 3, 6, 9, 12 and 15 months of age, in male and female, wild-type and 5XFAD mice. Note that for average proximity, smaller values indicate better performance. ★ = significant genotype difference, # = significant sex difference.

than females at 12 months of age with both latency ($p<.005$) and cumulative search error ($p<.01$). For swim-speed (Figure 4.5), wild-type mice swam faster than 5XFAD mice at 12 ($p < .0001$) and 15 months ($p<.01$) of age (Figure 4.7).

Age-related analysis showed that performance of male and female wild-type mice did not change significantly with age for any measure of learning performance in the visible platform test (Figure 4.2-4.4). In 5XFAD mice, males performed better at 3, 6, 9 and 12 months than at 15 months of age on each measure of learning performance. Performance of female 5XFAD mice was better at 3, 6 and 9 months, than at 12 and 15 months for each measure of learning. For swim-speed (Figure 4.5), wild-type females swam faster at 3 months than all other ages. No age-related changes in swim-speed were present in 5XFAD male mice, whereas females swam faster at 3 months than all other ages, and faster at 9 months than at 12 months of age.

4.3.5 Analysis Of The Effect Of Albinism On Learning And Memory Performance.

To assess the effects of albinism, data from mice at 3, 6 and 9 months were pooled, given that performance was not compromised by motor ability at these ages. This resulted in 83 animals that were pigmented, 13 animals with pigment reduction, and 33 albino animals (Table 4.2). For all analyses, we pooled animals with pigment reduction and albinism together, to increase statistical power and to ensure enough animals are present in each group for analysis of interactions between sex and genotype factors with albinism. Therefore, we re-analyzed all measures of learning with 2 x 2 x 2 x 3 mixed design ANOVAs (genotype x sex x albinism x day), and measures of memory with 2 x 2 x 2 between subject ANOVAs (genotype x sex x albinism). Because the effects of

genotype and sex are displayed in previous sections, only main effects and interactions involving the albinism factor are reported here. Effect size (ω^2) is reported within the text rather than tables.

4.3.5.1 Acquisition Training

During acquisition training, albino mice performed worse than pigmented mice on latency to locate the escape platform ($F(1,122) = 11.25$, $p < .005$, $\omega^2 = .084$), distance to locate the escape platform ($F(1,122) = 7.85$, $p < .01$, $\omega^2 = .047$) and cumulative search error ($F(1,122) = 7.79$, $p < .01$, $\omega^2 = .045$) (Figure 4.8 A-F). The day by albinism interactions were significant for latency and cumulative search error ($p < .01$), as albino mice performed worse than pigmented mice on days A2 and A3, but not A1. The main effect of albinism was not significant for swim-speed, and interactions involving albinism were also not significant.

4.3.5.2 Reversal Training

During reversal training albino mice performed worse than pigmented mice on latency to locate the escape platform ($F(1,122) = 26.12$, $p < .0001$, $\omega^2 = .159$), distance travelled to locate the escape platform ($F(1,122) = 19.93$, $p < .0001$, $\omega^2 = .129$) and cumulative search error ($F(1,122) = 19.39$, $p < .0001$, $\omega^2 = .123$) (Figure 4.8 A-F). No interactions involving albinism were significant. The main effect of albinism was not significant for swim-speed, and interactions involving albinism were also not significant.

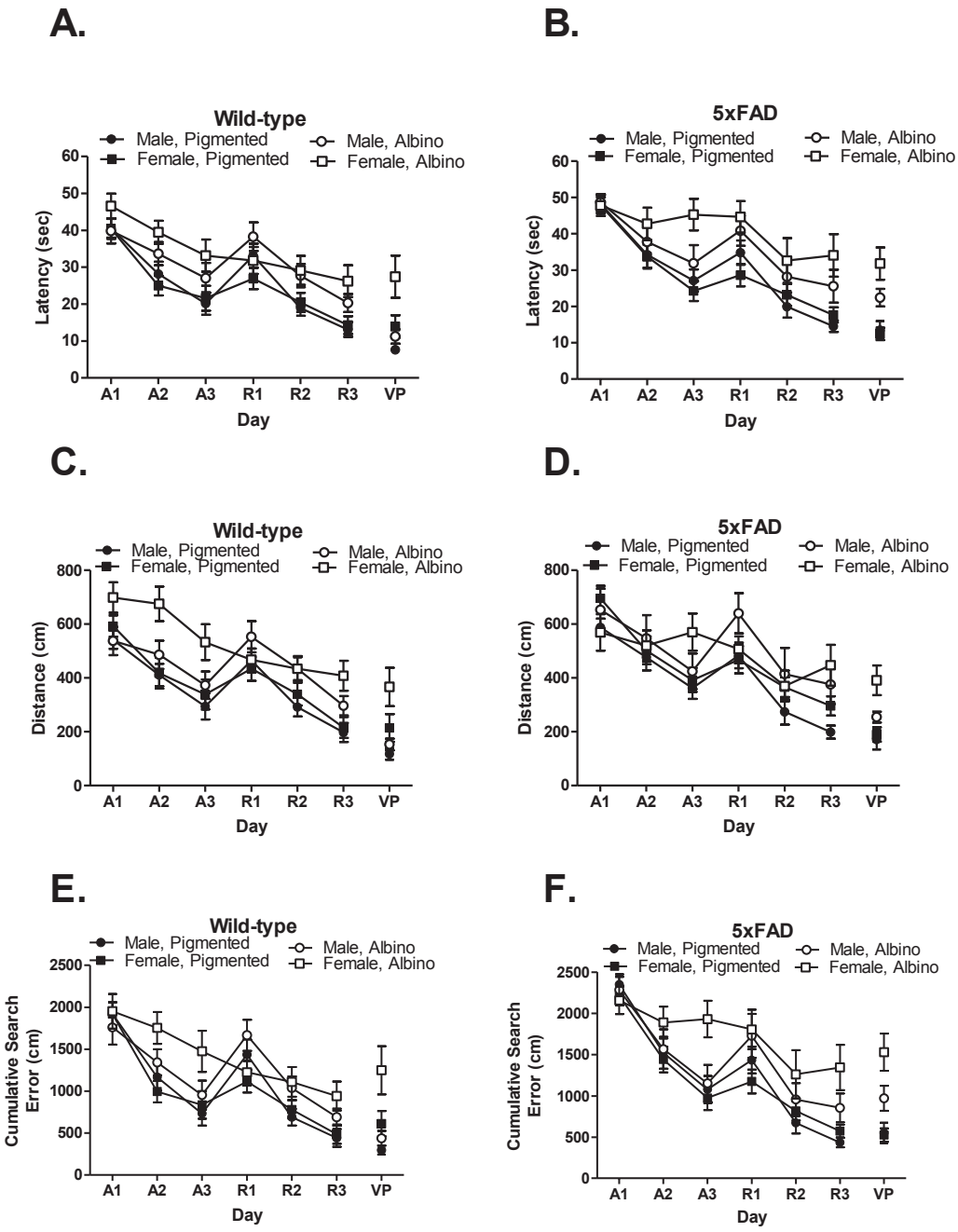

Figure 4.8 Mean (+/- SEM) latency to find the escape platform in the MWM for pigmented and albino mice, displayed separately for wild-type (A) and 5XFAD mice (B) at 3-9 months of age. Distance (C and D) and cumulative search error (E and F) to find the escape platform is also presented for both wild-type and 5XFAD mice. A=Acquisition, R= reversal, VP = visible platform,

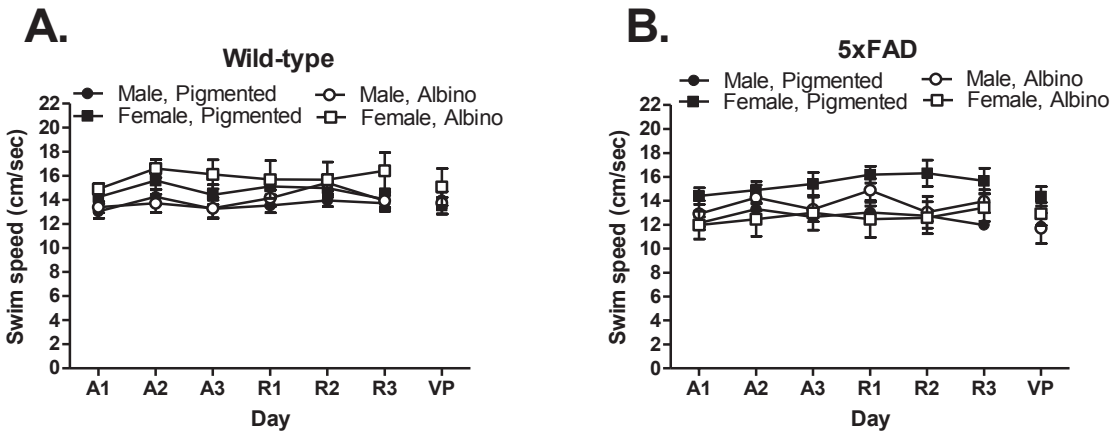

Figure 4.9 Mean (+/- SEM) swim speed in the MWM for pigmented and albino mice, displayed separately for wild-type (A) and 5XFAD mice (B) at 3-9 months of age. A=Acquisition, R= reversal, VP = visible platform.

4.3.5.3 Probe Trial

During the probe trial, no effect of albinism was found for either percentage time in the correct quadrant, or average proximity to the escape platform. (Figure 4.10 A-C)

4.3.5.4 Visible Platform Training

During visible platform training, albino mice performed worse than pigmented animals on measures of latency ($F(1,121) = 28.50$, $p < .0001$, $\omega^2 = .153$), distance ($F(1,121) = 15.08$, $p < .0005$, $\omega^2 = .088$) and cumulative search error ($F(1,121) = 26.97$, $p < .0001$, $\omega^2 = .14$) (Figure 4.8 A-F). The sex by albinism interaction was marginally significant for latency and cumulative search error ($p < .020$, $\omega^2 < .030$), as albino mice performed significantly worse than pigmented mice in females, but not males. No main effect or interactions involving albinism were found for swim speed (Figure 4.9 A and B).

4.4 Discussion

The results of this experiment will be discussed with respect to the four goals described in the introduction.

4.4.1 Are Age-related Deficits In Visuo-spatial Learning Present In The 5XFAD Mice?

Mice received acquisition training on the MWM to assess visuo-spatial learning of the escape platform location over 3 days. At 3 months of age 5XFAD mice were unimpaired in their performance relative to wild-type mice, suggesting that Aβ-induced dysfunction of visuo-spatial learning is not yet present. At 6 months of age, however, 5XFAD mice improved with training on all measures of learning, but showed small,

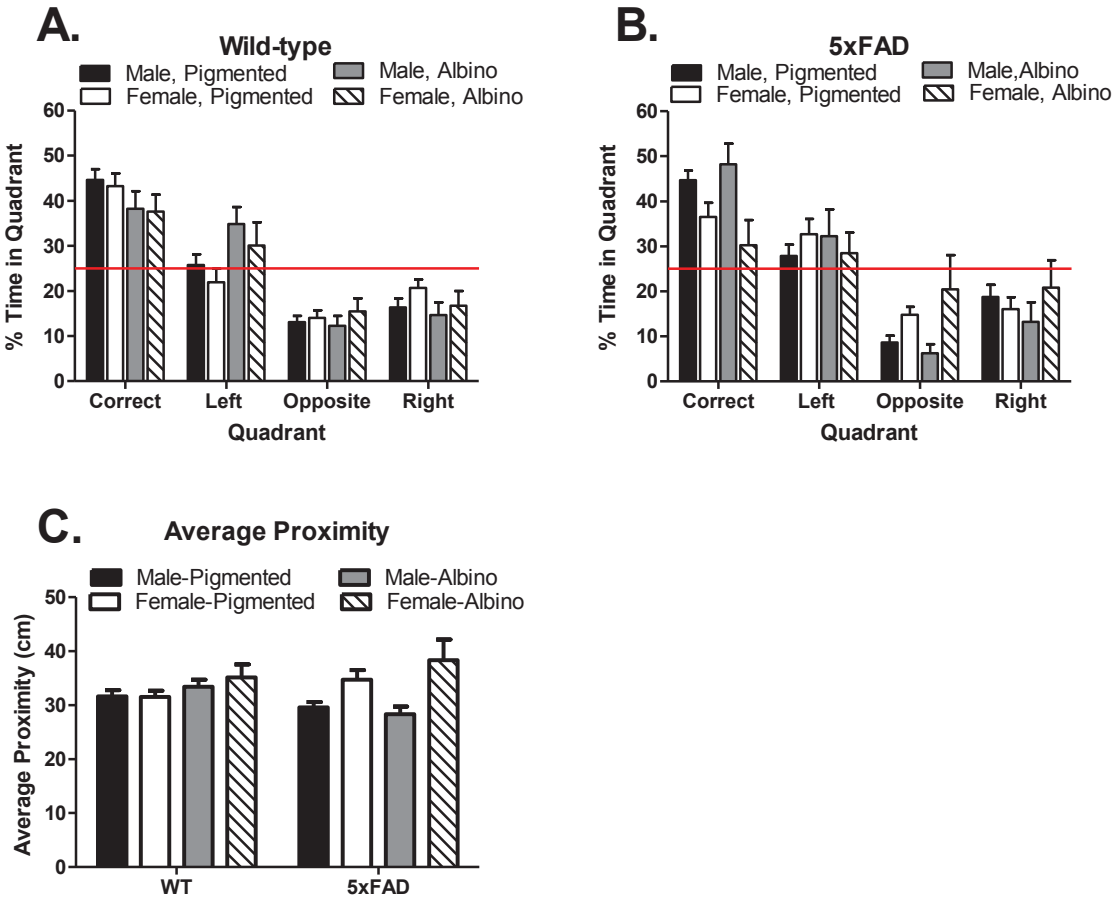

Figure 4.10. Mean (+SEM) time spent in each quadrant in the MWM probe trial for pigmented and albino mice, displayed separately for wild-type (A) and 5XFAD mice (B) at 3-9 months of age. Average proximity to the escape platform is also presented (C).

marginally significant impairments in learning performance relative to wild-type mice ($\omega^2 \sim .11$). These learning impairments were replicated and were moderate in size at 9 months of age ($\omega^2 \sim .18$). Among the measures of learning performance, cumulative search error and latency showed better sensitivity to detect impaired learning than distance travelled. Overall the impairments were small to moderate in size, similar to those reported in the MWM by Ohno et al., (2006) at 4-6 months of age. Larger impairments in acquisition learning were detected at 12 and 15 months of age ($\omega^2 > .20$), but were due to reduced swim-speed present in 5XFAD mice at these ages.

Reversal training was completed to determine if mice could re-learn the location of the escape platform when it was moved to the opposite side of the maze. To our knowledge, this is the first study to examine reversal learning in the 5XFAD mice. 5XFAD mice were not impaired in reversal learning performance at 3 months, but showed small impairments at 6 months of age on all measures of learning performance ($\omega^2 \sim .10$). This deficit, however, was not replicated at 9 months, suggesting that the reversal learning impairments are not as replicable as deficits in the initial acquisition of the escape platform location. Large reversal learning impairments were found at 12 and 15 months ($\omega^2 > .20$), but were again due to reduced swim–speed in 5XFAD mice. Interestingly, impaired performance in 5XFAD mice was not found in distance to locate the escape platform at 12 months, because mice were frequently unable to locate the escape platform within the maximum trial length of 60 sec, thus artificially reducing distance scores.

Despite the impaired learning performance of 5XFAD mice at 6 and 9 months of age, memory was not impaired on either quadrant-based or average proximity measures

during the probe trial. This suggests that although learning was impaired in 5XFAD mice, three days of training (12 trials) was sufficient for mice to learn the escape platform location as well as wild-type mice. Alternatively, 5XFAD mice may have a specific deficit in using extra-maze cues to navigate to the platform, but can remember the location of the escape platform relative to extra-maze cues once the location is reached (Whishaw et al., 1995). Further research is needed, however, to dissociate age-related changes within these two cognitive processes in the 5XFAD mouse. Memory performance was impaired in 5XFAD mice at 15 months of age, which is expected given that very little learning occurred at this age.

Visible platform training was completed to determine if impaired visual ability, motor function or motivation to escape from water potentially confounded learning performance. At six months of age, wild-type mice performed better than 5XFAD mice on all measures of learning, suggesting that impaired performance of 5XFAD mice in acquisition and reversal training is not solely due to visuo-spatial learning deficits. Given that these impairments in visible platform training were not present at 3 or 9 months, the difference in performance in 5XFAD mice at 6 months may not be replicable. However, it may be that the 5XFAD mice have subtle impairments in visual ability, as Aβ-pathology has been shown to be present within the retina of 5XFAD mice (Alexandrov et al., 2011). Therefore, psychophysical assessment of visual acuity in the 5XFAD mouse is warranted to establish if visual acuity is reduced. Impaired performance of 5XFAD mice in the visible platform test was also found at 12 and 15 months of age, which is due to the motor impairment observed at these ages.

4.4.2 Does Motor Impairment Influence Learning And Memory Performance Of Mice On The MWM?

Although impairments in learning and memory performance were detected at 12 and 15 months of age in 5XFAD mice, we cannot conclude that learning is impaired, as 5XFAD mice demonstrated impaired swimming ability due to their motor impairments. During training at these ages, 5XFAD mice generally swam slower than wild-type mice and showed erratic swim-paths, with difficulty turning. These mice also showed abnormal swimming-related behaviours, including difficulty coordinating limbs to initiate swimming at the onset of trials. Furthermore, the tail was often held rigid and showed ballistic movements, rather than the typical flagella-like movement of the tail observed during the swimming of wild-type mice. These behaviours were sometimes observed at 9 months of age in 5XFAD mice, but did not occur frequently enough to produce impairments in swim-speed. These results suggest that motor impairments at 9 months of age produce mild impairments in swimming ability, but at 12 and 15 months swimming ability is considerably impaired, preventing the valid assessment of visuo-spatial learning and memory on the MWM at these ages.

4.4.3 Are There Sex Differences In Visuo-spatial Learning And Memory Performance?

Sex differences were observed in the present study, but were most commonly found in reversal training. Larger impairments in male mice were observed at 3 months of age on day R1, after the location of the escape platform was moved to the opposite side of the pool. This “reversal effect” has been proposed to reflect either a more reliable use of the spatial search strategy by male mice, or increased perseverate search behaviour in male mice at the onset of reversal training (O’Leary and Brown, 2012). This sex

difference was not replicable across ages, however, with either both sexes showing large reversal-effects (i.e. 15 months), or neither sex demonstrating pronounced reversal effects (i.e. 12 months). Further research is required to determine what factors influence the size of reversal effects in female mice, and to determine the nature of this sex difference.

Females also showed small impairments in performance relative to males during reversal training at 12 and 15 months of age ($\omega^2 \sim .10$). This deficit reflects impaired learning rather than motor dysfunction, because no sex differences in swim-speed were observed at these ages. This suggests that the sex difference in learning found in C57BL/6 x SJL mice is reliably detected after 12 months of age, and may reflect a more rapid age-related cognitive decline in female mice than in males. We have previously suggested that this reversal learning impairment is due to slower re-learning of a visuo-spatial search strategy that relies on extra-maze cues in female mice (O'Leary and Brown, 2012).

4.4.4 Does Albinism Influence Learning And Memory Performance In 5XFAD Mice?

During both acquisition and reversal training, albino mice performed worse than pigmented mice, indicating impaired learning performance. However, no differences were observed in memory performance, indicating a specific deficit in the ability to navigate to the escape platform. Albino mice showed impaired performance during visible platform training, which may suggest impaired visual function in these animals, given the lower visual acuity previously found for albino mice (Wong and Brown, 2006).

4.4.5 General Conclusions

This study has shown impaired visuo-spatial learning in 5XFAD mice at 6 and 9 months of age. Memory performance, however, was not impaired in the 5XFAD mice, suggesting a specific impairment in navigating to the escape platform, rather than contextual memory for the escape platform's location. Motor impairment confounded performance on the MWM at 12 and 15 months of age, and therefore assessment of visuo-spatial learning and memory in 5XFAD mice should be completed between 6-9 months of age. The latency and cumulative error measures of learning were slightly more sensitive than distance travelled at detecting impaired performance in 5XFAD mice. Sex differences were observed in reversal learning performance, and were replicable after 12 months of age, potentially due to a faster age-related cognitive decline in female mice. Lastly, albinism impaired learning performance of both wild-type and 5XFAD mice, likely due to reduced visual acuity in albino animals. These results suggest that performance of 5XFAD mice on the MWM can be influenced by both sex and albinism, in addition to other previously documented factors such as retinal degeneration. We propose that the large variation in performance deficits in 5XFAD mice on the MWM, is because these background genetic factors are present but are typically not controlled. Therefore, the learning impairment in 5XFAD mice is small or moderate rather than large in size, and future studies with the 5XFAD mice should ensure a sufficient number of animals are used to detect the learning impairment.

CHAPTER 5 OLFACTORY DISCRIMINATION LEARNING AND MEMORY IN THE 5XFAD MOUSE MODEL OF AD

5.1 Introduction

Olfactory dysfunction is one of the first symptoms reliably detected in early stages of AD, and therefore may be useful in the diagnosis of AD and as a potential biomarker for the disease (Wesson et al., 2010). Although the nature of the olfactory impairment varies across studies, dysfunction has been reliably found in multiple domains of olfaction (Mesholam et al., 1998). One of the earliest cognitive impairments in AD is the poor identification of familiar odors which is thought to reflect impaired semantic memory (Djordjevic et al., 2008; Serby et al., 1991). This olfactory naming impairment is correlated positively with the severity of AD pathology, and predicts a faster rate of subsequent decline in episodic memory (Wilson et al., 2009). Impairments are also present in olfactory discrimination and recognition tasks, in which performance relies to a greater extent on working memory ability (Djordjevic, et al., 2008; Mesholam et al., 1998). Olfactory sensitivity impairments are also found in AD, but typically occur in later stages of the disease (Serby et al., 1991), and do not account for olfactory identification deficits when covariate statistical analyses are used (Djordjevic et al., 2008).

Olfactory dysfunction in AD may result from Aβ plaques and NFTs within the peripheral main olfactory bulb (MOB) and other central brain regions implicated in olfactory cognition, such as the piriform cortex, entorhinal cortex, amygdala and hippocampus (Kovacs, 2013). The development of Aβ plaques and NFTs within the MOB occurs early in the course of AD, and the regional distribution of these pathologies within the MOB differs. Aβ plaques are found throughout the MOB, but are most

abundant in the anterior olfactory nucleus, followed by the glomerular layer and olfactory nerve layer (Kovács et al., 1999). NFTs are also found throughout the MOB, but are most abundant in the anterior olfactory nucleus, followed by the external plexiform and granular layers. These pathologies are also accompanied by neuron loss in the anterior olfactory nucleus and to a lesser extent the mitral cell layer. The extent of Aβ and Tau pathology in the MOB is positively associated with the amount of pathology within the entorhinal cortex (Christen-Zaech, et al., 2003), suggesting that pathology in the MOB and impairments in olfactory cognition may predict the severity of disease progression in AD.

The mechanisms by which Aβ and NFT pathology contribute to olfactory dysfunction in AD can be examined with transgenic mouse models of AD (Wesson et al., 2010). For example, the double transgenic 5XFAD mouse carries mutant human APP (Swedish, Florida and London) and PS1 transgenes (Oakley et al., 2006), and may be a useful animal model for Aβ-induced olfactory impairments, due to rapid development of Aβ-pathology within its olfactory system. Aβ-immunoreactivity is first observed within the glomerular layer as well as the nerve fiber layer within the MOB as early as 1-2 months of age (Cai et al., 2012). In these regions Aβ is co-localized with pre-synaptic markers and often elevated BACE1, suggesting intra-cellular accumulation within pre-synaptic olfactory nerve terminals. At later ages nerve terminals are reduced in number and often have dystrophic morphology, accompanied by a decrease in overall area of glomeruli. Although extra-cellular plaques are not found in the olfactory nerve and glomerular regions, they are observed in other olfactory regions such as the granular cell layer, amygdala and hippocampus between 4-12 months of age

(Cai et al., 2012; Oakley et al., 2006). However, a comprehensive characterization of extra-cellular plaque deposition in the peripheral and central olfactory brain regions has yet to be completed in the 5XFAD mouse.

Despite the development of Aβ-pathology within the 5XFAD olfactory system, very little research has been completed examining olfactory function in these mice. What research that has been completed demonstrates deficits in olfactory sensitivity, olfactory discrimination and decreased exploration of novel odors as early as 2-3 months of age (Österman, 2010). Impairments are also present in an olfactory delayed-response paradigm at 4 months of age in the H-maze, which is a complex rule learning task dependent on frontal cortex function (Girard et al., 2013). Olfactory impairments were not replicated by Roddick (2012), however, who found unimpaired olfactory sensitivity, discrimination, reversal learning and working memory in an operant olfactometer at 6-8 months of age. Similarly, the double transgenic APPswe/PS1de9 mouse shows no age-related impairments in olfactory sensitivity or learning and memory, despite the robust development of Aβ-plaque pathology in the olfactory memory system (Phillips et al., 2011; Stover and Brown, 2012; Darvesh et al., 2012). Therefore it is currently not clear whether olfactory memory is impaired in the 5XFAD mouse, or if the olfactory memory system is robust against the development of Aβ-pathology.

Therefore, the purpose of this experiment was to examine age-related changes in olfactory memory in the 5XFAD mouse from 3-15 months of age. We used the olfactory digging task developed by Schellinck et al (2001), given that this task can be completed despite compromised motor ability which develops in 5XFAD mice at 9 months of age (Jawhar et al., 2012). Both 5XFAD and wild-type mice performed very well on this task,

demonstrating that olfactory memory is not impaired in the 5XFAD mice at any age tested. We also demonstrate that unlike previous experiments with contextual fear conditioning (Kimura and Ohno, 2009), increasing the delay between training and the memory test did not reveal early-onset deficits in long-term remote memory in the 5XFAD mouse. Together, these results indicate that olfactory memory in the 5XFAD mouse is not impaired despite previous reports of Aβ-pathology within the olfactory memory system (Cai et al., 2012; Oakley et al., 2006).

5.2 Materials And Methods

5.2.1 Subjects

Subjects and housing conditions used in this experiment were identical to those described in Chapters 3 and 4. The number of 5XFAD and wild-type mice of both sexes included in this experiment is shown in Table 5.1.

5.2.2 Olfactory Discrimination Training

Three days prior to olfactory discrimination training, mice were placed under food restriction to reduce their body weight to 85-90% of their free-feeding weight. Mice then completed 4 days of training, with 4 trials per day as described by Schellinck et al., (2001). Training trials were completed in polyethylene cages (30 x 19 x 13 cm) similar to the animals' home-cage. The bottom of the cage was covered with pro-chip bedding and top of the cage had a wire lid (Figure 5.1A). Odor pots consisted of a small plastic cup (65 mm diameter) that contained a piece of filter paper (Whatman no. 1; 55mm diameter), upon which liquid odorant was added (0.05 ml). A perforated petri-dish was inverted over the filter paper, within the odor pot (Figure 5.2), which was then filled with

Table 5.1. The number of male (M) and female (F), 5XFAD (5x) and wild-type (WT) mice that completed the olfactory discrimination test at each age.

Age	**3 months**				**6 months**				**9 months**				**12 months**				**15 months**			
Genotype	5X		WT		5X		WT		5X		WT		5X		WT		5X		WT	
Sex	M	F	M	F	M	F	M	F	M	F	M	F	M	F	M	F	M	F	M	F
Olfactory Disc.	12	14	11	16	9	11	10	10	8	11	19	11	9	10	13	11	6	10	10	10

A.

B.

Figure 5.1. (A) The olfactory discrimination training apparatus consists of a housing cage filled with a bedding of pro-chip, and contained a single odor cup with either the CS+ or CS- odor. (B) The preference test apparatus consisted of a rectangular box made of transparent plexiglas, and was divided into three chambers of equal size. Walls between adjacent chambers each contained a small door, and the test apparatus contained a bedding of pro-chip. CS+ and CS- odor pots without sugar reward were placed in chambers at opposite ends of the apparatus.

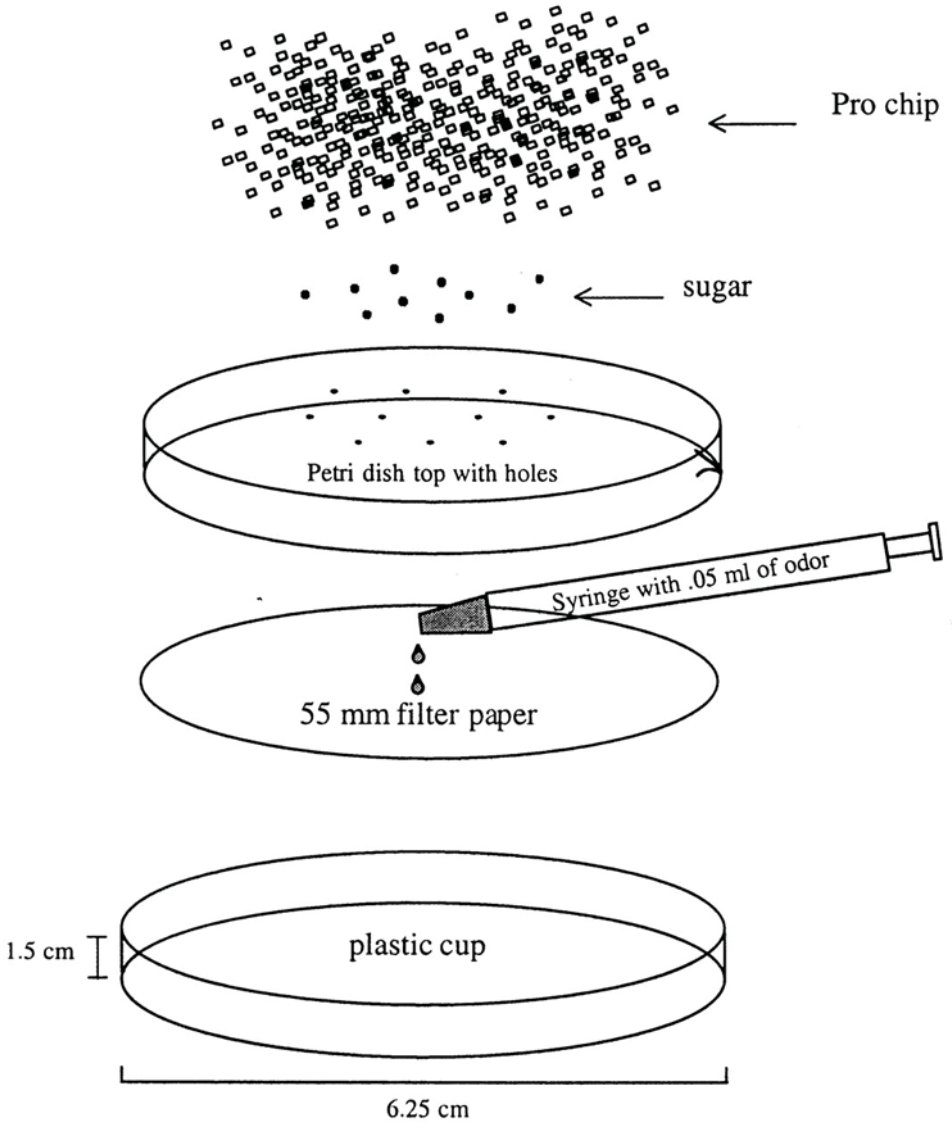

Figure 5.2. The odor cup consisted of a small plastic dish, which contained a piece of filter paper with odorant. The cover to a petri dish was placed within the odor cup, over the filter paper to prevent physical contact with the odorant. Sugar reward was placed on the petri dish, and the remaining area within the odor pot was filled with pro-chip digging medium. Figure is from Schellinck et al., (2001).

pro-chip bedding so that the contents of the odor pot were completely covered. For the majority of mice, odorants consisted of maple and banana, but some 3 month mice received rose (phenyl acetate) and lemon (linalool) instead. Due to experimenter error, some mice could not complete testing with maple and banana, and therefore the orange and cinnamon (7 mice) or lemon and vanilla (6 mice) odor pairs were used. All odorants were produced by Clubhouse (McCormick Canada, London ON), or were purchased from Sigma-Aldrich (linalool and phenyl acetate).

During each day of training mice completed two trials with their respective CS+ odor, and two trials with the CS- odor. The order in which these trials were completed differed across training days and followed a pseudo-random order. On trials with the CS+ odor, 4-5 small pieces of sugar where placed within the odor pot, so that they were located on top of the petri-dish beneath the pro-chip. On the first day of training sugar was also placed on top of the pro-chip during CS+ trials, to encourage mice to dig within the odor pot. On trials with the CS- odor, no sugar was present within the odor pot. For each 10 min training trial, mice were placed in the training cage and were permitted to explore the cage and dig in the odor-pot to locate and eat the sugar. New pro-chip bedding was placed in each training cage, and new odor pots were prepared for each trial. For each mouse, trials with the CS+ odor were completed in a different room than trials with the CS- odor, and mice waited in a room with a neutral odor during the inter-trial interval (15-25 min) to avoid contamination of odorants. Mice were fed a restricted diet each day after training trials were completed, to maintain body weight at 85-90% free-feeding weight.

5.2.3 Olfactory Conditioning Memory Test

Mice completed an odor preference test to assess memory for the odor-sugar association 24 hours following training. The preference test was completed in an apparatus made from clear Plexiglas that was divided into three chambers of equal size, with the floor covered in Pro-chip bedding (Figure 5.1B). Mice first completed a habituation trial, where they were placed into the central chamber of the test apparatus and allowed to explore the apparatus for 2 minutes. During the habituation trial odor pots were placed in the left and right chambers, but these odor pots did not contain odorants or sugar reward. The time spent in the left and right chambers was recorded to determine if mice showed pre-existing preferences for the left or right chamber.

The memory test was completed 5 min following the habituation trial. In the memory test a CS+ odor pot was placed in the less preferred chamber that the mouse spent the lesser amount of time in during habituation, while a CS- odor pot was placed in the opposite chamber. This reduced the extent that pre-existing preferences for specific chambers could confound memory performance by increasing the amount of time spent near the CS+ odor pot. Neither the CS+ nor the CS- odor pots contained sugar during the memory test. Mice were placed into the central chamber and allowed to explore the apparatus for a 3 minute trial. The total time spent digging with the paws or snout in the pro-chip on each of the CS+ and CS- odor pots was recorded for the 3 min trial. Memory for the sugar-odor association was calculated as the percent time spent digging in the CS+ odor [(CS+)/(CS+)+(CS-)]*100].

A subset of 5XFAD (5 males, 6 females) and wild-type (6 males, 7 females) mice tested at 3 months of age also completed a memory test at six months of age, thus

creating a long-term (90 day) retention period for the assessment of remote memory (Wong and Brown, 2007). During the retention period mice were returned to ad-libitum access of food, but underwent restricted access to food three days prior to the memory test as described above. The procedure for the long-term remote memory test was identical to the 24 hour memory test previously used. Following the remote memory test, mice completed training with a new odor pair (Maple and Banana) and a memory test 24hr following training.

5.2.4 Statistical Analysis

For all behavioural measures, 2 x 2 x 5 between-subject ANOVAs were completed (sex x genotype x age). Individual 2 x 2 ANOVAs (genotype x sex) were also completed separately at each age, while age effects were assessed with one-way ANOVAs completed separately for each sex and genotype. As in chapters 3 and 4, a significance level of $p < 0.01$ was used. Effect sizes (ω^2) for genotype and sex effects are reported in table 5.3. Post-hoc tests were completed with simple effects analyses, while Student-Newman-Keuls comparisons were completed for between subject effects of age. Interactions are only reported when significant. Eight wild-type and eight 5XFAD mice were excluded from all analyses as they did not dig for at least 5 seconds during the discrimination memory test.

5.3 Results

5.3.1 Body Weight

In free-feeding weight, males weighed more than females at each age tested ($F(1,201) = 189.30$, $p < .0001$) (Figure 5.3A), and weights generally increased in mice across ages ($F(4,201) = 19.69$, $p < .0001$). The main effect of genotype

($F(1,201) = 28.55$, $p < .0001$) and the genotype by age interaction were significant ($F(4,201) = 5.24$, $p < .0005$), as wild-type mice weighed more than 5XFAD mice at 12 months ($F(1,39) = 8.68$, $p < .01$) and 15 months of age ($F(1,32) = 29.12$, $p < .0001$). Male wild-type and 5XFAD mice significantly increased in weight from 3 to 6 months of age. However, while the weight of male wild-type mice showed no change from 6 to 15 months of age, the weight of male 5XFAD mice decreased at 15 months of age, and was similar to 3 month old mice. Both wild-type and 5XFAD female mice increased in body weight from 3 to 6 months of age, and wild-type mice continued to increase in weight so that they weighed significantly more at 15 months than 3 and 6 months of age. Female 5XFAD mice, however, decreased in body weight at 15 months of age, weighing less than at 6 and 9 months of age.

5.3.2 Percentage Body Weight On Test Day

Following food restriction, the main effects age ($F(4,201) = 1.95$), and sex ($F(1,201) < 1$) on body weight were not significant (Figure 5.3B). The genotype effect ($F(1,201) = 22.19$, $p < .0001$) and the genotype by age interaction ($F(4,201) = 3.87$, $p < .005$) were significant, as wild-type mice weighed more than 5XFAD mice at 12 months ($F(1,39) = 7.63$, $p < .01$) and 15 months of age ($F(1,32) = 13.43$, $p < .001$). Age-related changes in body-weight were not significant for wild-type or 5XFAD mice. Correlations between percentage of free-feeding body-weight on test day with total time spent digging ($r(221) = -.20$, $p < .005$) and percent-digging in the CS+ odor were low but significant ($r(221) = .15$, $p < .05$), indicating that variation in percentage body weight had small effects on digging motivation and memory performance (accounting for 4% and 2% of variance respectively).

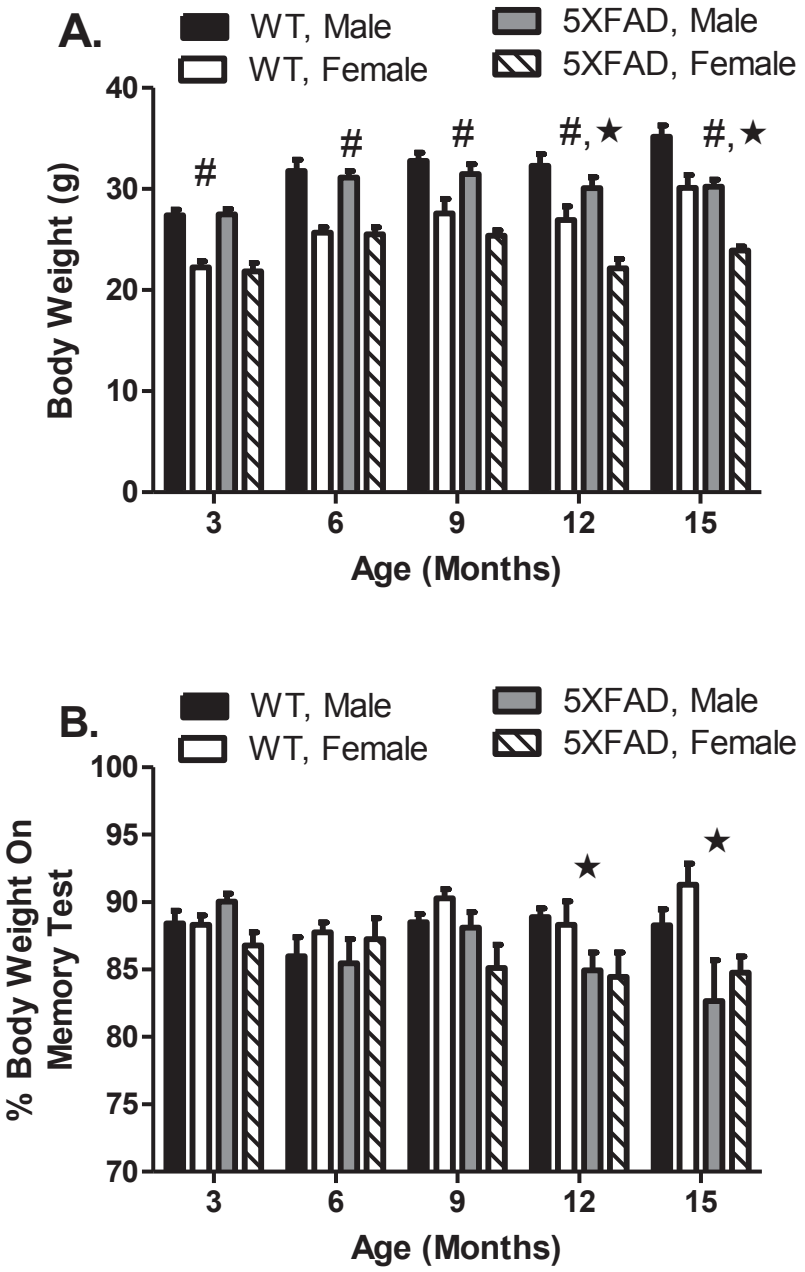

Figure 5.3 Mean (+SEM) body weight (A) and percentage of free-feeding body weight during memory test (B) in male and female, 5XFAD and wild-type mice at 3, 6, 9, 12 and 15 months of age. # = significant sex difference, ★ = significant genotype difference. See main text for age-related changes in body weight and percentage of free-feeding body weight during the memory test (sections 5.1 and 5.2).

Table 5.2. Effect sizes (omega-squared, ω^2) for the genotype effect, sex effect and the genotype by sex interaction, for ANOVAs completed at 3, 6, 9, 12 and 15 months of age in the olfactory discrimination task (M=months, Disc = Discrimination).

Olfactory Disc.	**Body Weight**					**% body weight on memory test**				
Age	3M	6M	9M	12M	15M	3M	6M	9M	12M	15M
Genotype	<.010	<.010	.023	.094	.303	<.010	<.010	.098	.139	.254
Sex	0.554	.594	.367	.378	.315	.052	.016	<.010	<.010	.028
Genotype x Sex	<.010	<.010	<.010	<.010	<.010	.044	<.010	.068	<.010	<.010
Olfactory Disc.	**Time spent digging**					**% time digging in CS+**				
Age	3M	6M	9M	12M	15M	3M	6M	9M	12M	15M
Genotype	.017	<.010	.116	<.010	.015	<.010	<.010	<.010	<.010	<.010
Sex	<.010	.113	.056	<.010	<.010	<.010	<.010	<.010	.010	<.010
Genotype x Sex	<.010	<.010	<.010	.048	<.010	<.010	<.010	<.010	<.010	<.010

5.3.3 Time Spent Digging

Overall 5XFAD mice dug more than wild-type mice ($F(1,201) = 9.26$, $p < .005$) (Figure 5.4A), but there was no significant sex difference ($F(1,201) = 2.48$). The main effect of age ($F(4,201) = 3.31$) was not significant, and sex differences at each age were also not significant. 5XFAD mice, however, did dig more than wild-type mice at 9 months of age ($F(1,45) = 7.75$, $p < .01$).

5.3.4 Percentage Time Digging In CS+ Odor

There were no significant effects of genotype ($F(1,201) < 1$), sex ($F(1,201) <1$), or age ($F(4,201) <1$) and no significant interactions in percentage time digging in the CS+ odor (Figure 5.4B). On average, both 5XFAD and wild-type mice dug over 85% of the time at the CS+ odor. Analyses were also completed with percentage body weight as a covariate within an ANCOVA, but no effects were significant.

5.3.5 Long-term Memory Test And Re-acquisition

A subset of mice completed a 3 month memory test to assess long-term remote memory, and acquisition of a novel odor-sugar association at 6 months of age. There were no genotype ($F(1,20) = 1.24$) or sex differences ($F(1,20) = 3.48$) for time spent digging (data not shown), nor were there significant genotype ($F(1,20) = 1.30$) or sex effects ($F(1,20) < 1$) for percentage time spent digging in the CS+ odour (Figure 5.5). When trained with a new pair of odors and tested 24hr later, there were no genotype or sex differences total time spent digging (genotype: $F(1,20) < 1$, sex: $F(1,20) < 1$) or percentage time digging in the CS+ odour (genotype: $F(1,20) < 1$, sex $F(1,20) < 1$), as mice generally dug over 85% of the time in the CS+ odour.

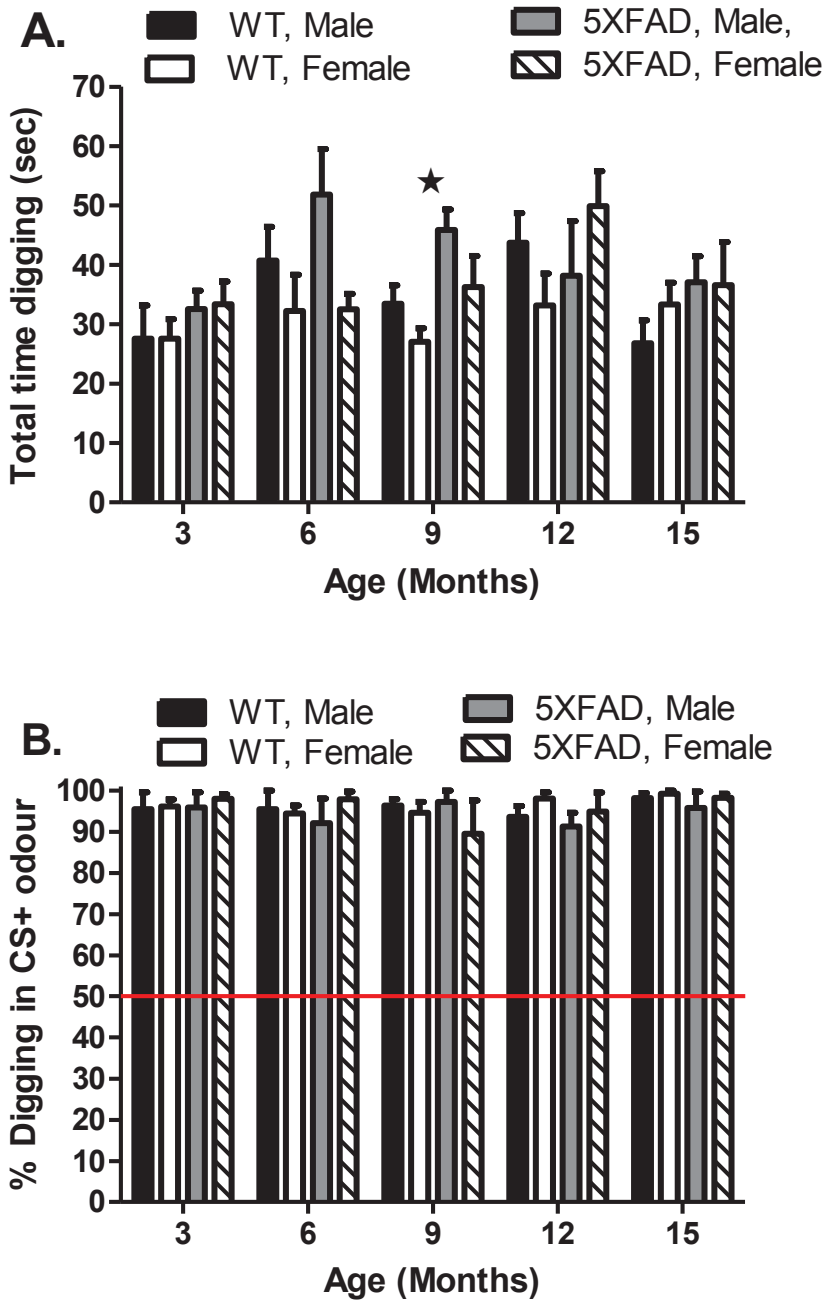

Figure 5.4 Mean (+SEM) total time spent digging (A) and percentage time spent digging in the CS+ odour pot (B) in male and female, 5XFAD and wild-type mice at 3, 6, 9, 12 and 15 months of age. The solid horizontal line indicates performance expected by chance (50%). ★ = significant genotype difference. See main text for age-related changes in time spent digging (sections 5.3).

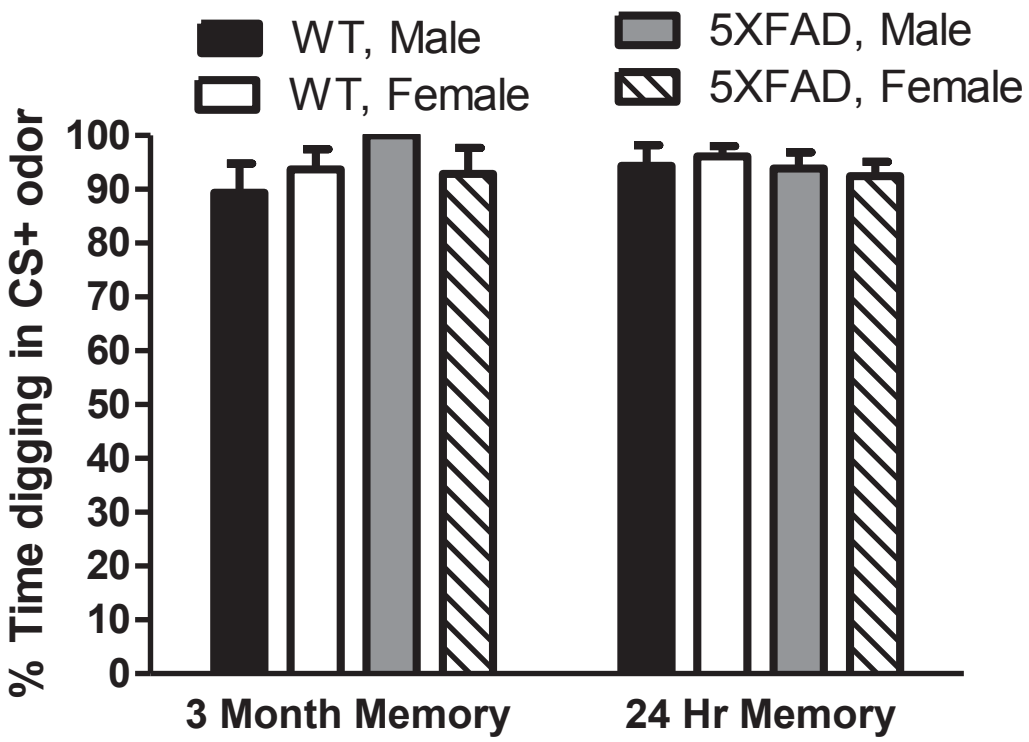

Figure 5.5 Mean (+SEM) percentage time digging in the CS+ odor pot in male and female, 5XFAD and wild-type mice in the 3-month memory test and 24hr memory test after re-training with novel odors at 6 months of age.

5.4 Discussion

The 5XFAD mouse develops Aβ pathology within the olfactory system (Cai et al., 2012; Oakley et al., 2006), but results of experiments examining olfactory learning and memory have not reliably demonstrated an impairment in olfactory ability (Österman, 2010; Roddick, 2012). Therefore, we used the olfactory digging discrimination test (Schellinck et al., 2001) to assess olfactory memory in the 5XFAD mouse from 3-15 months of age. 5XFAD mice were able to complete this task despite the motor impairment observed after 9 months of age (Jawhar et al., 2011), demonstrating this task's usefulness for age-related studies in mice with compromised motor function. The 5XFAD mice did not differ from wild-type mice at all ages tested, indicating that deficits in olfactory learning and memory are not present.

In contextual fear conditioning, memory deficits can be detected in 5XFAD mice at early ages (<4 months) when remote memory is assessed by using long retention periods (30 days) between training and the memory test, but not when recently acquired memories are assessed with short retention periods (24 hr) (Kimura and Ohno, 2009). Remote memory has been proposed to reflect the time-dependent transfer of hippocampal dependent memory traces to cortical networks over longer time periods following training. This suggests that 5XFAD mice have early-onset impairments in the stabilization of remote memories due to impaired cortical function, which may precede dysfunction in hippocampal dependent memory. Given the unimpaired performance of 5XFAD mice at 3 months in olfactory memory in the present study, we increased the difficulty of the task and assessed remote memory 90 days following training. Performance of 5XFAD mice in long-term olfactory memory was not impaired relative to

wild-type mice, suggesting that an early-onset deficit in olfactory remote memory is not present.

Comparisons of the sensitivity of different tasks to detect learning and memory impairments in mouse models of AD have been completed for visuo-spatial tasks (Stewart et al., 2011), but very little information is available for olfactory tasks. Therefore, although performance of 5XFAD mice was not impaired in the present study, it may be that the olfactory digging task lacks the sensitivity to detect olfactory memory dysfunction. Indeed, little change was observed in either 5XFAD or wild-type mice across ages, suggesting age-related decline is also not detected with this task. Stover and Brown (2012) have shown similar results with the APPswe/PS1dE9 mouse model of AD using this task, with unimpaired performance up to 20-26 months of age. This lack of age-related decline and near-perfect performance in both wild-type and 5XFAD mice suggests that the olfactory digging task may not be sufficiently cognitively demanding to detect impairments in olfactory learning and memory in mice. The ease in which this task is completed may result from overtraining during the 8 training trials with each of the CS+ and CS- odors, or because too much odorant is placed on odor pots, thus increasing the salience of the odors. Indeed, Girard et al. (2013) successfully detected olfactory cognitive impairment, but used a relatively complex task with the H-maze in which mice learned multiple rules in a delayed response paradigm. Therefore, we are currently increasing the difficulty of the olfactory digging test by optimizing the test parameters, and by including memory interference with additional odorants.

The body weight of 5XFAD mice was lower than wild-type mice at 12 and 15 months of age, replicating the results of Jawar et al., (2012) (see chapter 3). Maintenance

of body weight within 85-90% of free-feeding weight was required for the digging task, but was more difficult for 5XFAD than wild-type mice after 12 months of age, as the percentage body weight of 5XFAD mice was consistently lower than wild-type mice during the memory test. This genotype difference was likely because mice were group-housed, and when provided with the restricted daily allotment of food, wild-type mice ate more than their 5XFAD cage-mates. Although percentage of free-feeding body weight was not a good predictor of memory performance in the digging task, studies should take additional care in maintenance of body weight in experiments requiring food restriction in the 5XFAD mouse after 9 months of age.

The lack of olfactory memory impairment in 5XFAD mice at 15 months of age suggests that the previously documented Aβ-pathology observed in the MOB and central brain regions was not sufficient to disrupt olfactory memory (Cai et al., 2012; Oakley et al., 2006). This may indicate that pathology not observed in the 5XFAD mice, such as aggregated intracellular Tau and NFTs may contribute to olfactory dysfunction to a greater extent than Aβ-pathology. Alternatively the development of Aβ-pathology in the 5XFAD mouse may follow a different regional pattern relative to humans with AD, thereby not disrupting olfactory memory ability. Further research is needed characterizing Aβ-pathology within the olfactory system of the 5XFAD mouse, to determine the mechanism by which impairments in olfactory cognition are produced in complex olfactory tasks such as the H-maze (Girard et al., 2013). Examination of the regional distribution of Aβ plaque load within olfactory system will be discussed in Chapter 6.

CHAPTER 6 EXAMPLES OF AGE-RELATED CHANGES IN AB-PATHOLOGY IN THE 5XFAD MOUSE MODEL OF AD

6.1 Introduction

The 5XFAD mouse shows a massive increase in the production of Aβ peptides during early adult-hood, leading to the rapid development of extra-cellular plaque pathology within the brain by 3 months of age (Oakley et al., 2006). With age, plaques increase in number and size, and are found in many regions throughout the brain and spinal cord (Oakley et al., 2006; Jawhar et al., 2012; see Chapter 2). Although age-related Aβ-plaque pathology has been reliably shown in the 5XFAD mouse, very few studies have examined variation in plaque distribution throughout functionally distinct regions of the brain. This analysis is warranted to compare the distribution of extra-cellular plaque pathology with the development of AD-related behavioural symptoms in the 5XFAD mouse.

Therefore, we examined age-related changes in the development of extra-cellular Aβ-plaques within brain regions involved in regulating the behavioral phenotypes assessed in chapters 3, 4 and 5. We examined plaque pathology at ages when mice demonstrate normal behaviour (2 months), when impairments are present in visuo-spatial learning (7 months), and when motor impairments are clearly shown (13 months). At each age we examined the extent of plaque pathology in regions involved in motor function (cerebellum, motor cortex, basal ganglia) and visuo-spatial learning and memory (parietal cortex, dorsal hippocampus, subiculum). Given that visuo-spatial learning impairments are present prior to motor dysfunction; we hypothesized that regions involved in visuo-spatial cognition would show earlier and more extensive plaque

pathology than motor regions at 7 months of age, whereas extensive pathology would be present in motor regions at 13 months.

We have shown that the 5XFAD mice do not have age-related impairments in olfactory memory (Chapter 5), which was unexpected given pervious reports of Aβ-pathology within the main olfactory bulb (Cai et al., 2012; Oakley et al., 2006). This may suggest that the olfactory memory system of the 5XFAD mouse is robust against the development of Aβ deposits. To examine this possibility, we examined plaque pathology in the olfactory bulb and related structures at 15 months of age, to determine the extent of plaque pathology that is present despite the absence of impairments in olfactory learning and memory in the 5XFAD mouse.

6.2 Methods

6.2.1 Subjects

Brains were obtained from naïve wild-type and 5XFAD male mice at either 2, 7 or 13 months of age (N = 3-4 mice per genotype and age). For analysis of the olfactory system, images were obtained from naïve female wild-type and 5XFAD mice at 15 months of age. All mice were housed as described in Chapter 3.

6.2.2 Aβ Immunohistochemistry

Mice were anesthetized with a lethal dose of sodium phenobarbital (200mg/kg), and perfused (trans-cardiac) with 25ml of 0.9% saline with 0.1% sodium nitrite, followed by 50 ml of 4% paraformaldehyde dissolved in 0.1M phosphate buffer (pH,7.4). Brains were removed and then post-fixed in 4% paraformaldehyde for 1-2 hours, and subsequently stored in PBS with 0.1% sodium azide. Prior to sectioning, brains were

cryoprotected in PBS containing 30% sucrose for 48 hours. Tissue was sectioned serially on the coronal plane at 30 μm, using a Leica SM2000R microtome (Leica Microsystems Inc., Nussloch, Germany) with Physitemp freezing stage and BFS-30TC controller (Physitemp Instruments, Inc. Clifton, NJ). Tissue was sectioned into four series, with one series stained for Aβ using immunohistochemistry.

All immunohistochemistry experiments were completed by Mr. Andrew Reid and Dr. Sultan Darvesh (Medical Neuroscience, Dahousie University). Free-floating sections were first washed for 5 min in 0.05M PB (pH7.4), followed with distilled water (dH_2O). To improve the Aβ straining, tissue was treated with 90% formic acid for 2 minutes for antigen retrieval. Additional washes of dH_2O (5 x 1 min) and PB (2 x 15 min) were completed before treating tissue with H_2O_2 in PB (30 min) to quench endogenous peroxidase activity. Tissue was then washed in PB (30 min) before incubation in PB with 0.1% Triton X-100 (PBTX), normal goat serum (1:100), and polyclonal rabbit anti-Aβ antibody (1:400; 71-5800, Invitrogen, Camarillo, CA) for 16 hours at room temperature. The anti-body used is specific to 4- to 5kDa Aβ peptide, produced through proteolysis of APP. Following an additional wash in PB, tissue was incubated in PBTX containing biotinylated goat anti-rabbit secondary antibody (1:500), and normal goat serum (1:1000) for 1 hour. Tissue was then washed in PB, and treated with PBTX containing the Vectastain elite ABC kit (1:182, PK-6100, Vector Laboratories, Burlingame, CA), based on manufacturer's instructions for 1 hour. Tissue was then washed in PB containing 1.39 mmol/L 3.3'-diaminobenzidine tetrahydrochloride (DAB) chromagen for 5 min. 50 μL of 0.3% H_2O_2 in dH_2O was added for each ml of DAB solution, and tissue was left to incubate for 10 min. Reactions were stopped through washes of 0.01M acetate buffer

(pH 3.3). Tissue was then mounted onto glass slides, dehydrated in ethanol, cleaned with histo-clear (National Diagnostics, Atlanta, GA) and coverslipped with Permount (Fisher, Scientific).

6.2.3 Imaging Of Brain Tissue

Imaging of Aβ immunolabelling was completed with a bright-field microscope (Zeiss, Axioplan II), with a high-resolution digital camera (Zeiss, Axiocam HRc), and the AxioVision4.6 software (Carl Zeiss Canada Ltd., Toronto, Ontario, Canada). Photomicrographs were assembled with the GIMP (ver 2.6) software, and images were brightness adjusted to keep background similar across images. Areas of interest were identified with a stereotaxic atlas of the mouse brain (Franklin and Paxinos, 2008).

6.3 Results

No immunoreactivity was present in the brains of wild-type mice, as mice do not spontaneous develop Aβ plaques (Figure 6.1). Aβ immunoreactivity within the brains of 5XFAD mice increased from 2-13 months of age, indicating increased Aβ-plaque load with age (Figure 6.2A-C). At 2 months of age, a distinct band of staining was present in the cortex which was more prominent in dorsal (motor cortex) relative to ventral cortical regions (entorhinal cortex). Examination of the cortical staining at higher magnification revealed a staining pattern consistent with intra-cellular accumulation of Aβ, likely within layer 5 pyramidal cells (Figure 6.3A and B). Small amounts of Aβ staining were also present in sub-cortical regions such as the thalamus and amygdala at 2 months of age, but

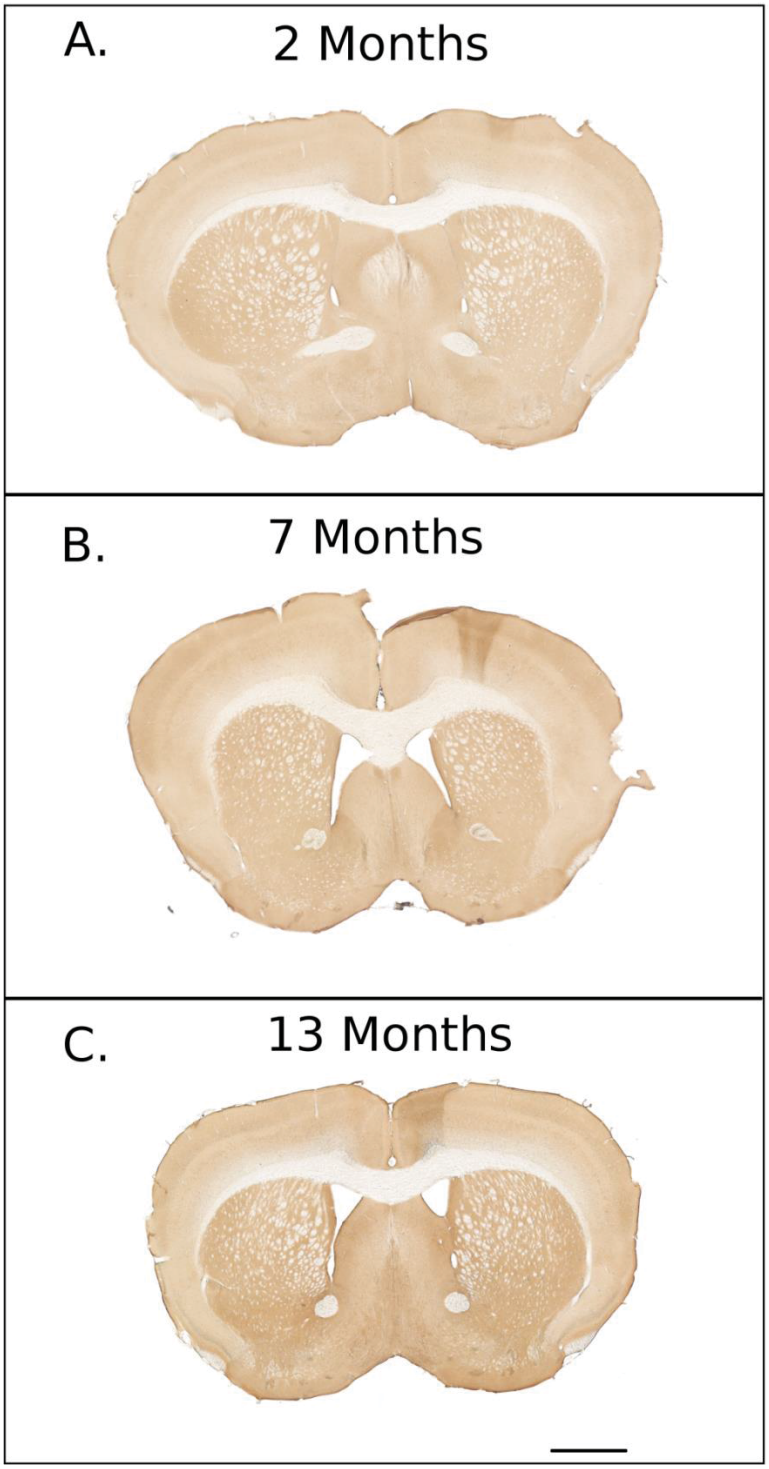

Figure 6.1. Aβ plaque pathology is not present in the brains of wild-type mice at 2 months (A), 7 months (B) and 13 months (C) of age. Images were obtained between -1.18 and 0.98 mm from bregma, at 25x magnification. Scale bar represents 1mm.

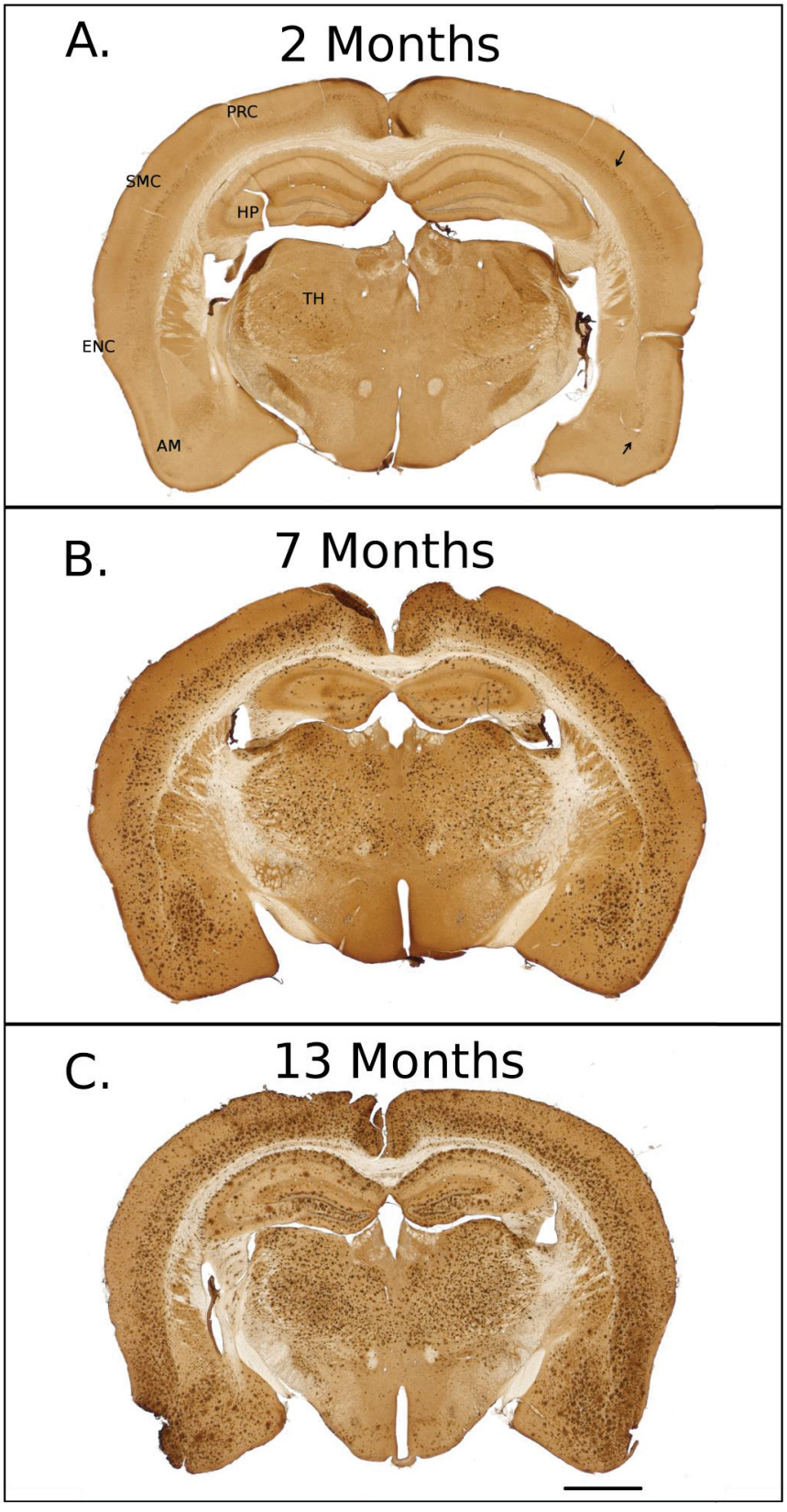
A.
2 Months
PRC
SMC
HP
TH
ENC
AM
B.
7 Months
C.
13 Months

Figure 6.2. Aβ-plaque pathology in cortical and subcortical regions within the 5XFAD mouse at 2 months (A), 7 months (B) and 13 months (C) of age. At 2 months of age a distinct band of immunostaining was found within the cortex (indicated by arrow). The position of this staining was consistent with cortical layer 5, and showed a punctate pattern, characteristic of intra-cellular deposits rather than extra-cellular Aβ deposits. Cortical staining was found in the primary motor cortex (MRC), somatosenory cortex (SMC), but was less pronounced in the entorhinal cortex (ENC), suggesting that intra-cellular accumulation of Aβ progresses in a dorsal to ventral fashion throughout the cortex with age. Additional sparse staining was observed in the amygdala (AM) (shown by arrow) and thalamus (TH) at this age, but was absent in the hippocampus (HIP). At 7 months of age Aβ plaque load increased in all aforementioned brain regions, and was now present within the hippocampus. This distinct band of intra-cellular immunostaining in the cortex was replaced by larger extra-cellular deposits, mainly within layers 5 and 6. At 13 months of age massive amounts of Aβ immunostaining was observed in both cortical and subcortical brain regions. Images were obtained between -1.46 and -1.82 mm from bregma, at 25x magnification. Scale bar represents 1mm.

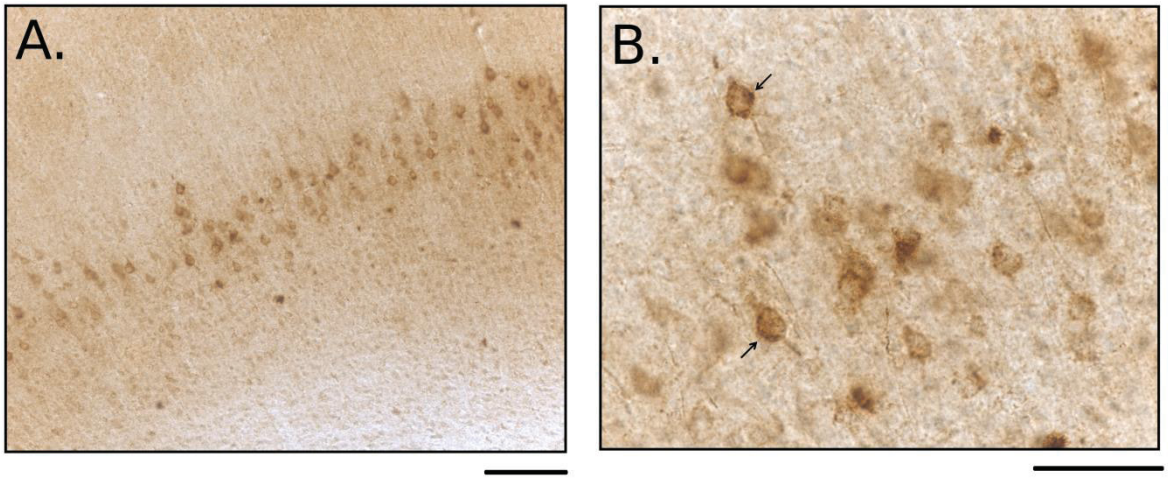

Figure 6.3. Aβ immunoreactivity in layer 5 of the cortex at 2 months of age (400X) (A). When viewed at a higher magnification (640X), the pattern of staining is consistent with intra-cellular accumulation with the soma of neurons (indicated by an arrows) (B). Darker staining was often present surrounding an area of less immunoreactivity, which may suggest localization of Aβ within the cytoplasm, but exclusion from the nucleus. Scale bars represent 50 μm.

was absent from the hippocampus. At 7 months of age, extra-cellular Aβ deposits were present throughout cortical layers 5 and 6, and to a lesser extent in cortical layers 1-4 (Figure 6.2B). Aβ deposits were now present in the hippocampus at this age, although at lower levels than the thalamus and amygdala. At 13 months of age massive levels of Aβ deposits were present throughout the cortex and aforementioned subcortical regions.

6.3.1 Aβ-pathology In Regions Involved In Visuo-spatial Learning And Memory

We examined the regional distribution of plaque pathology in the parietal cortex, subiculum and hippocampus given that each region is involved in visuo-spatial ability and/or learning and memory. The subiculum contained a considerable amount of extra-cellular plaque deposits at 2 months of age, indicating a rapid development of Aβ pathology within this region (Figure 6.4A-C). Interestingly, plaque load increased from 2 to 7 months of age, but little change was present from 7 to 13 months of age. This may indicate that given the rapid accumulation of Aβ deposits, plaque load in the subiculum is saturated at seven months of age and does not increase further with age.

Within the parietal cortex, intra-cellular Aβ is present within layer 5 at 2 months of age (Figure 6.4 D-F). Plaque load increased at 7 months of age primarily in layers 5 and 6, with fewer deposits present in layers 1-4. Large amounts of Aβ deposits are present at 13 months of age, with again fewer deposits in layers 1-4.

In the hippocampus, plaque deposits were not present at 2 months of age (Figure 6.5A-C). At 7 months however, plaques are present, but tend to be localized within the dentate gyrus and oriens layer of the hippocampus. At 13 months of age, plaques are

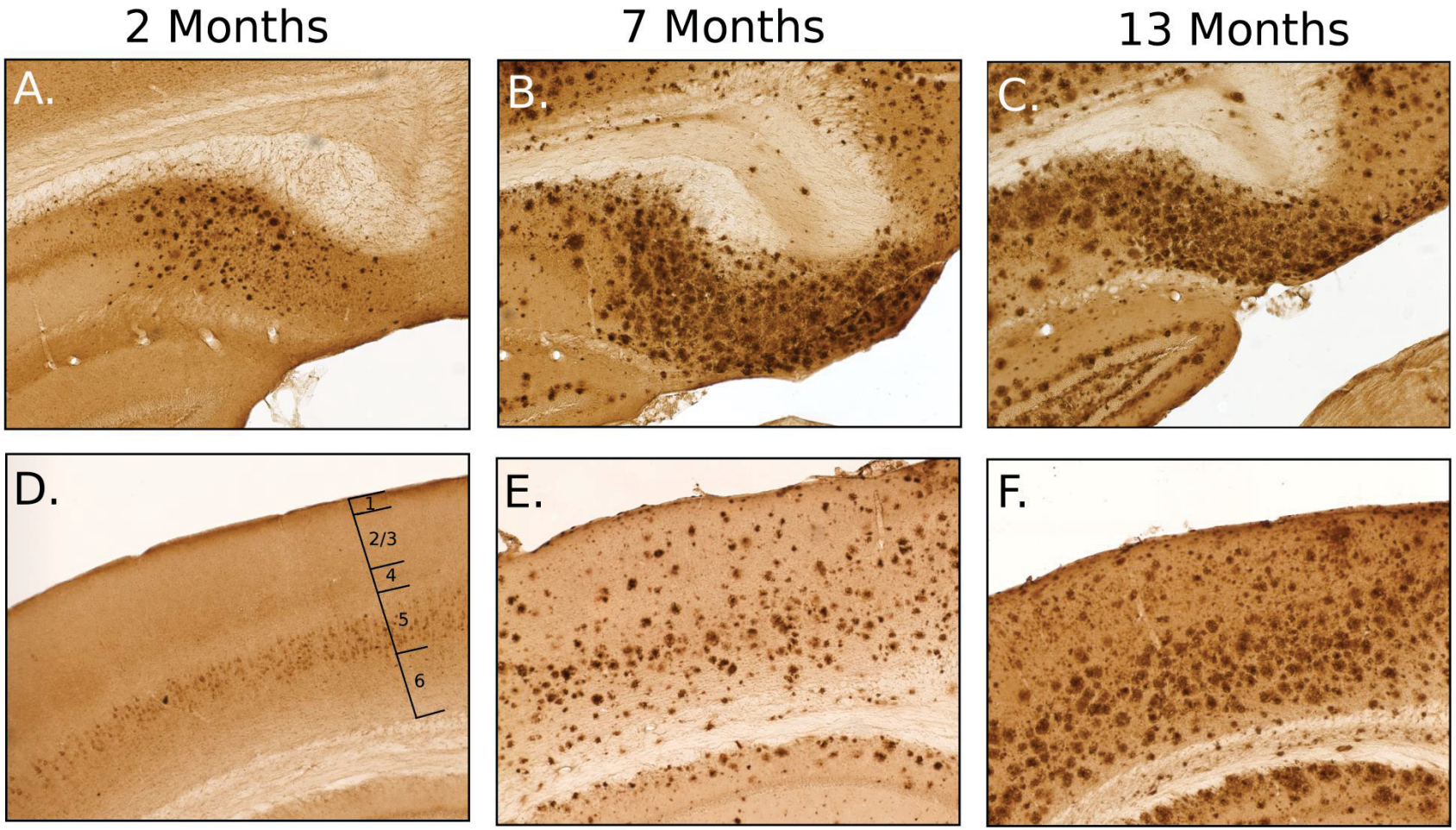
2 Months
7 Months
13 Months
A.
B.
C.
D.
E.
F.
1
2/3
4
5
6

Figure 6.4. Aβ-plaque pathology in the subiculum and parietal cortex within the 5XFAD mouse at 2 months (A and D), 7 months (B and E) and 13 months (C and F) of age. For the subiculum considerable amounts of immunostaining was already present at 2 months of age (A). At 7 months of age plaque load increased further (B), but showed little change from 7 to 13 months of age (C). For the parietal cortex, the approximate divisions between cortical layers are shown in panel D. At 2 months of age intra-cellular labelling is present within layer 5 of the cortex, located beneath a band of dark background straining characteristic of the granular layer (layer 4). At 7 months of age, Aβ plaque load increases throughout the cortex, especially within layers 5 and 6. At 13 months of age, plaque deposits increase in all layers, and remain more abundant in layers 5 and 6. For panels (A-C) images were obtained between -2.54 and -2.80 mm from bregma, and for panels (D-F) between -1.82 to -1.94mm from bregma. All images were obtained at 100x magnification. Scale bar represents 200μm.

A. 2 Months

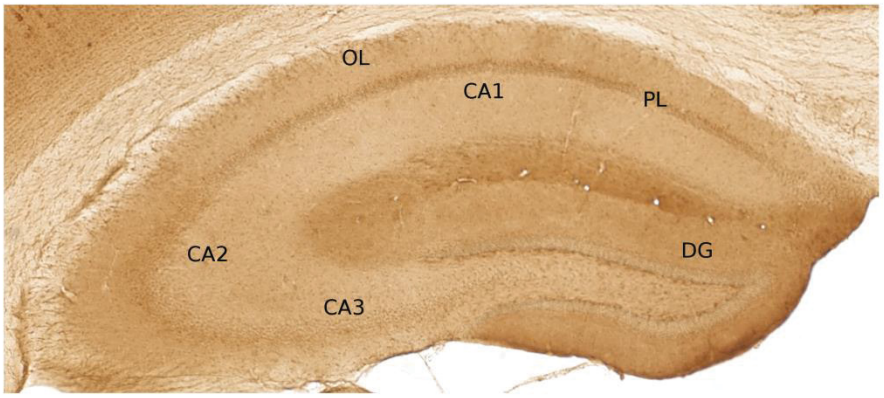

B. 7 Months

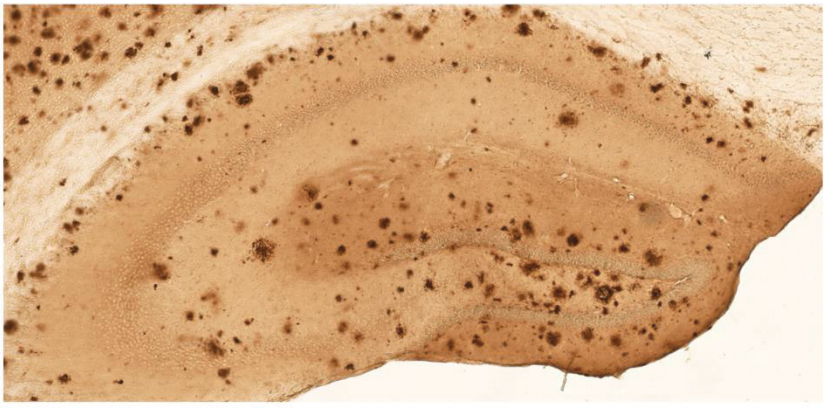

C. 13 Months

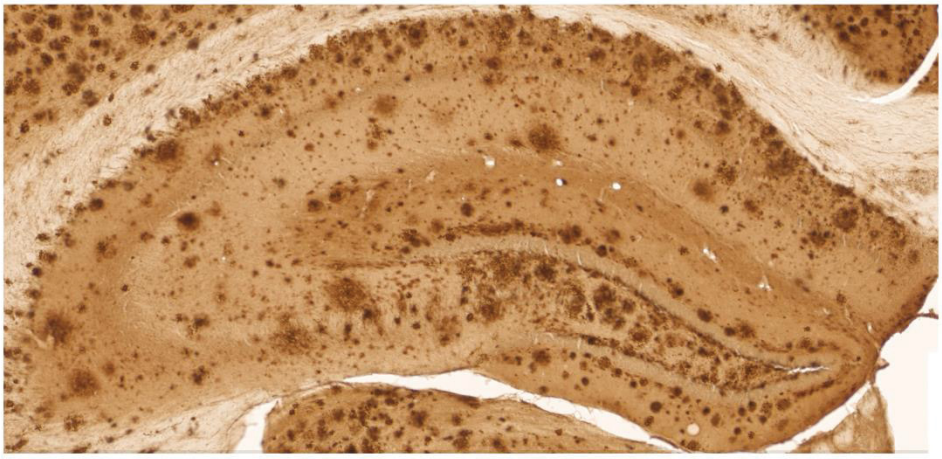

Figure 6.5. Aβ plaque pathology in the dorsal hippocampus within the 5XFAD mouse at 2 months (A), 7 months (B) and 13 months (C) of age. At 2 months of age, immunostaining was not observed within the hippocampus. At 7 months of age, Aβ staining was present primarily in the dentate gyrus (DG) and the oriens layer (OL) of the hippocampus, and to a lesser extent in the CA1, CA2, CA3 and pyramidal layer (PL). At 13 months of age, Aβ staining increased in all aforementioned regions, but was still found at higher levels in the DG and OL, than other hippocampal subregions. Images were obtained between -1.82 and -1.94 mm from bregma, at 100x magnification. Scale bar represents 200 μm.

present throughout the hippocampus, with a greater number in the dentate gyrus and oriens layer, relative to other hippocampal regions.

6.3.2 Aβ-pathology In Regions Involved In Motor Function

The regional distribution of plaque pathology was examined in the basal ganglia (caudate putamen and globus pallidus), primary motor cortex and cerebellum. At 2 months of age, no plaque deposits were observed in either the caudate putamen or globus pallidus of the basal ganglia (Figure 6.6A-C). At 7 months of age, plaque deposits were present in the caudate putamen but were largely absent from the globus pallidus. Plaque load increased in the caudate putamen at 13 months, but remained at low levels in the globus pallidus.

In the motor cortex, intra-cellular staining of Aβ was present in layer 5 (Figure 6.7A-C), similar to the parietal cortex. The amount of intra-cellular immunostaining in the motor cortex, however, appeared to be greater than in the parietal cortex (Figure 6.4D). Plaque load increased at 7 and 13 months of age, and a greater number of deposits were present in layers 5-6 than in layers 1-4.

In the cerebellum, plaque deposits were not present at 2 months of age (Figure 6.8A). Although present at 7 and 13 months, very few plaque deposits were present in the cerebellum. Within the brain-stem, deposits were present in the reticular nucleus as early as 2 months of age. Plaque load increased in the brainstem with age, but was found primarily in the reticular nucleus and the spinal trigmenial nucleus, with low levels present in the pyramidal tract and vestibular nucleus.

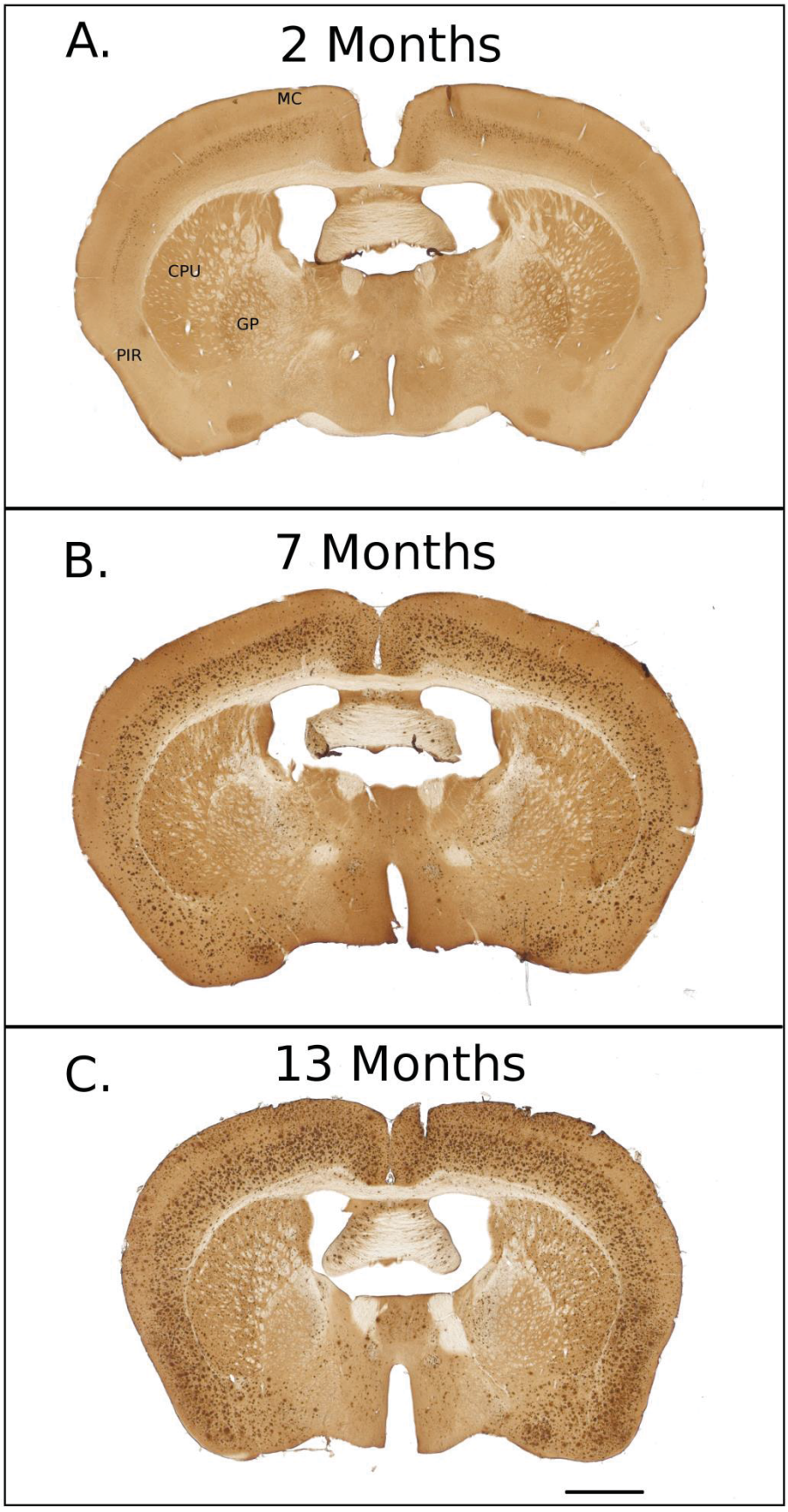
A.
2 Months
MC
CPU
GP
PIR
B.
7 Months
C.
13 Months

Figure 6.6. Aβ-plaque pathology within the cortex and basal ganglia of 5XFAD mice at 2 months (A), 7 months (B) and 13 months (C) of age. At 2 months of age, intra-cellular immunostaining was again found in the motor cortex, but was absent in both the caudate putamen (CP) and globus pallidus (GP) of the basal ganglia. Intra-cellular immunostaining in the pyriform cortex (PIR) was absent at this age, suggesting that intra-cellular accumulation of Aβ may progress in a dorsal to ventral fashion throughout the cortex, as was also shown in figure 6.1. At 7 months of age, immunostaining was found in CP, but was absent in the GP. At 13 months of age, plaque load increased in the CP, but was observed a much lower levels in the GP. Images were obtained between -0.22 to -0.46 mm from bregma, at 25x magnification. Scale bar represents 1mm.

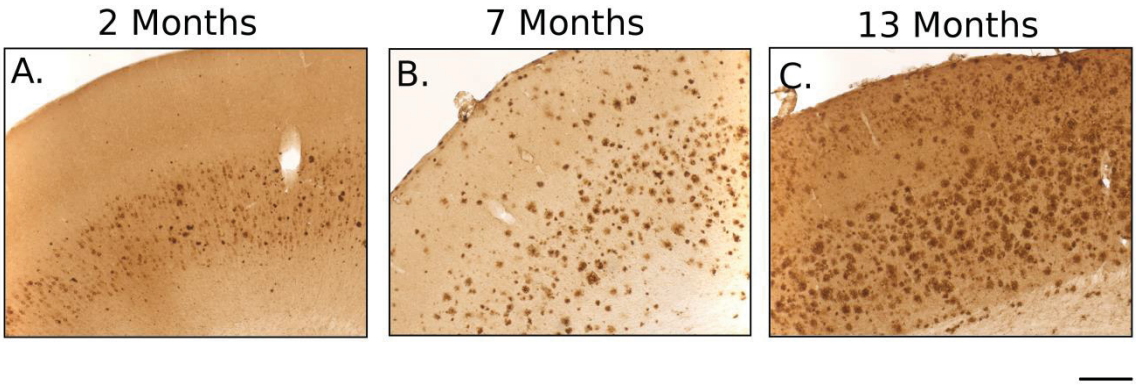

Figure 6.7. Aβ plaque pathology in the motor cortex of 5XFAD mice at 2 months (A), 7 months (B) and 13 months (C) of age. Intra-cellular labeling of Aβ is present within layer 5 of the motor cortex, and the amount of labeling is greater than that observed in the parietal cortex in Figure 6.3. At 7 and 13 months of age, plaque deposits increase in all layers, but are more abundant in layers 5 and 6, than 1-4. Images were obtained between 1.54 to 1.34mm from bregma at 100x magnification. Scale bar represents 200μm.

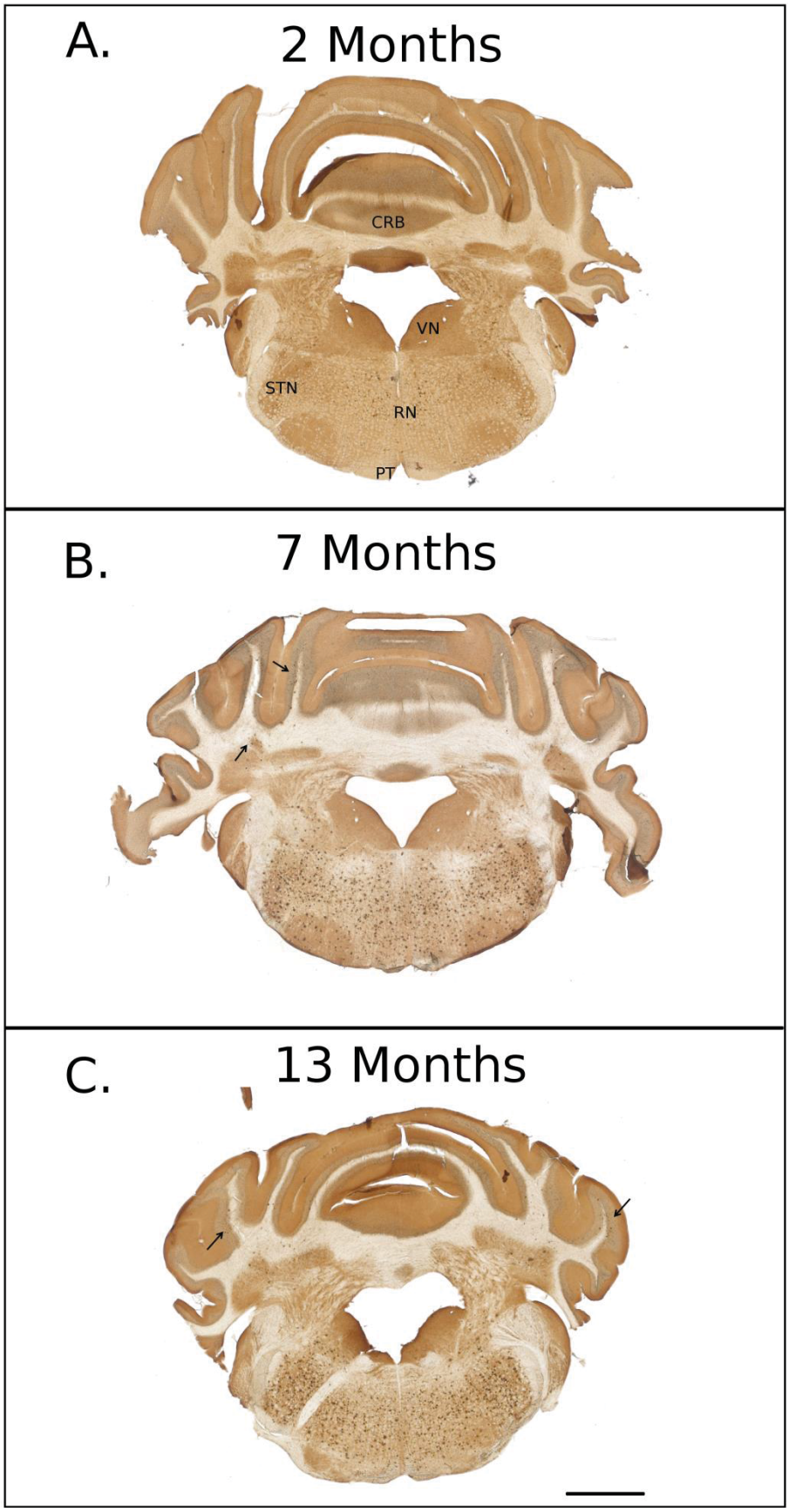
A.
2 Months
CRB
VN
STN
RN
PT
B.
7 Months
C.
13 Months

Figure 6.8. Aβ plaque pathology in the brain-stem and cerebellum of 5XFAD mice at 2 months (A), 7 months (B) and 13 months (C) of age. At 2 months of age no immunoreactivity for Aβ was observed in the cerebellum (CRB), but staining was observed within the reticular nucleus (RN). At 7 months small amounts of staining for Aβ was present in the CRB (indicated by arrows), while Aβ staining increased in the RN and was now observed in the spinal trigmenial nucleus (STN). Staining was largely absent in the vestibular nucleus (VN) and the pyramidal tract (PT) at this age. At 13 months of age Aβ, staining remained at low levels in the CRB, VN and PT, but increased further in the RN and STN. Images were obtained between -5.80 and -5.88 mm from bregma, at 25x magnification. Scale bar represents 1mm.

6.3.3 Aβ-pathology In Regions Involved In Olfactory Learning And Memory

Plaque pathology in olfactory regions with the MOB, anterior olfactory bulb and frontal cortex were examined to determine the extent of Aβ-pathology despite the lack of olfactory memory deficits (Figure 6.9 A-C). In the main and anterior olfactory bulb, plaque deposits were present in the anterior olfactory nucleus, granular layer, and anterior commissure, but were absent from other regions such as the olfactory nerve layer, glomerular layer and mitral cell layer. In the frontal cortex (Figure 6.9C), robust plaque pathology was present in the piriform cortex, tenia tecta, and orbitofrontal cortex.

6.4 Discussion

The results of this study confirm the rapid and large amount of Aβ plaque formation previously shown in the 5xFAD mouse (Oakley et al., 2006). Age-related changes and the regional distribution of plaque deposits suggest that Aβ pathology first accumulates within layer 5 neurons of the neocortex. The intra-cellular staining indicates the miss-localization of Aβ from the synapse to the soma of the cell. We observed intra-cellular Aβ within multiple cortical regions, suggesting that it is not specific to certain cortical sub-regions. However, given that intra-cellular staining was greater in dorsal compared to ventral cortical regions at 2 months of age, it may be that intra-cellular Aβ originates in dorsal regions and later spreads to ventral cortical regions. These layer 5 pyramidal neurons show increased vulnerability with age, as significant loss in layer 5 neurons occurs at 9 months of age in the 5XFAD mice (Jawhar et al., 2012).

The reason for intra-cellular Aβ accumulation and cell death within the layer-5 pyramidal neuronal population is not known, but could reflect a specific

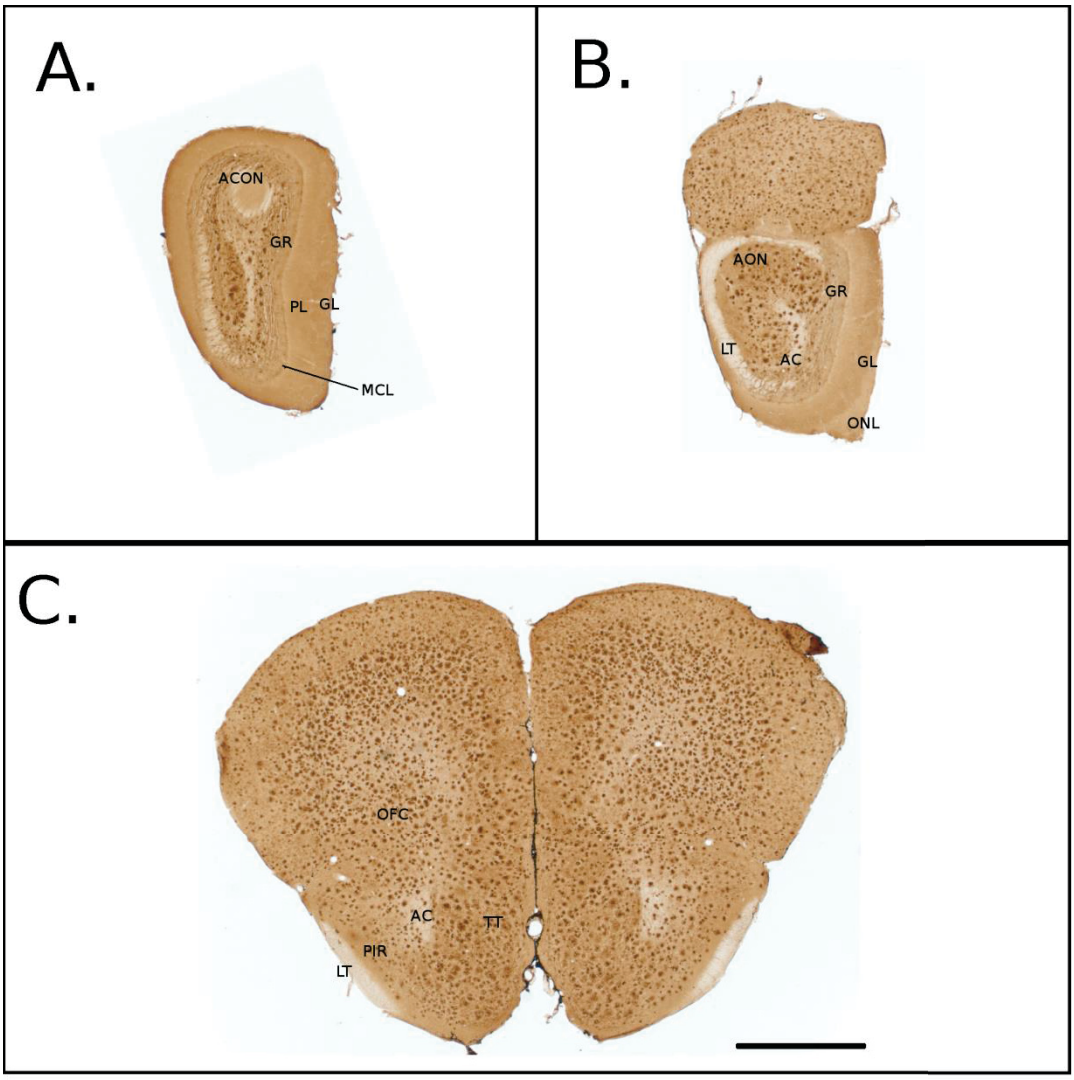

Figure 6.9. Aβ plaque pathology in the main olfactory bulb (A), anterior olfactory bulb (B) and frontal cortex (C) of 5XFAD mice at 15 months of age. In the main and anterior olfactory bulb (A and B), the greatest amount of Aβ staining was present in the anterior olfactory nucleus (AON), while less staining was present in the granular layer (GR) and anterior commissure (AC). No Aβ-immunoreactivity was present in the olfactory nerve layer (ONL), glomerular layer (GL), internal/external plexiform layers (PL), mitral cell layer (ML), or lateral olfactory tract (LT). In the frontal cortex (C), extensive Aβ staining was present in the piriform cortex (PIR), tenia tecta (TT), and orbitofrontal cortex (OFC). Images were obtained between 3.56 to 2.54 mm from bregma, at 25x magnification. Scale bar represents 1mm.

vulnerability/propensity of pyramidal neurons to accumulate intra-cellular Aβ. Indeed, research in humans has also implicated layer 3 and 5 pyramidal cells in AD pathogenesis, as a dramatic loss of pyramidal cells that are immuno-positive for neurofilament-heavy polypeptide (SMI-32 antibody) occurs (Thangavel et al., 2009). An alternative explanation is that layer 5 cells produce high levels of APP and Aβ, given that the endogenous Thy-1 expression in the mouse has been shown to be elevated within layer 5 of the cortex (Barlow and Huntley, 2000). Similar results have been shown with the APP/PS1KI transgenic mouse which also shows cell loss within cortical layers 5-6, and has transgenes regulated via the Thy-1 promoter (Lemmens et al., 2011). Regardless of the mechanism for cell loss, these pyramidal cells are proposed to form inter-regional cortico-cortical connections, and therefore cell loss leads to a disconnection and impaired integration of information from different cortical sub-regions. This "cortical-isolation" syndrome (Hof et al., 1990) may help explain the multiple systems dysfunction (i.e. motor and learning ability) observed in the 5XFAD mouse.

Aβ deposits were present in the subiculum, hippocampus, and parietal cortex, all of which are regions implicated in visuo-spatial learning and memory. This suggests that Aβ-induced dysfunction in each of these regions could contribute to learning impairment of 5XFAD mice at 6 months of age. However, the large number of Aβ deposits in the subiculum is unexpected given the lack of memory impairment in 5XFAD mice, and because lesions to the subiculum produce memory impairments on the MWM in rats (Morris et al., 1990). Therefore, this may suggest that although 5XFAD mice have impaired learning performance, a sufficient amount of training was provided for 5XFAD mice to learn the escape platform location as well as wild-type mice. Similar over-

training effects have been observed in fear conditioning experiments with the 5XFAD mice, where performance deficits are dependent on the number of context- and/or tone-shock pairings (see chapter 2). Together, this indicates that the amount of Aβ-deposits observed at 6-7 months in the hippocampus, subiculum and parietal cortex is only sufficient to produce moderate deficits in learning and memory in the 5XFAD mice.

Within motor regions, Aβ deposits were present in primary motor cortex, and the basal ganglia, but were found in very small amounts in the cerebellum. Given the small plaque load in the cerebellum, it is also not surprising that previous studies have reported the absence of plaque deposits in this region (Oakley et al., 2006), and suggests that motor dysfunction in the 5XFAD mouse is not due to impaired cerebellar function. Interestingly, there was variation in plaque load within the basal ganglia, with a greater number of deposits in the caudate putamen then in the globus pallidus. Similar results are also found in the APPSswe/PS1dE9 mouse which has transgenes regulated by the mouse prion promoter, suggesting this difference between the caudate putamen and globus pallidus is not unique to thy-1 transgene cassette in 5xFAD mice (Darvesh et al., 2012). Extensive plaque deposits were also present in the primary motor cortex at 13 months of age, which may also contribute to motor impairment due to Aβ induced dysfunction and/or death of Betz cells in layer 5, which are large pyramidal cells that form the cortico-spinal tract. Further research is required to determine the relative contribution of basal ganglia and motor cortex pathology to motor dysfunction in 5XFAD mice.

Despite the absence of olfactory memory deficits in 5XFAD mice, extensive Aβ-pathology was found throughout the olfactory bulb and related structures. Plaque pathology was present within specific regions, including the anterior olfactory nucleus,

granular cell layer, anterior commissure, piriform cortex etc. The notable absence of Aβ-plaques in the olfactory nerve layer, glomerular layer and mitral cell layer was unexpected, as humans with AD show plaque pathology throughout the olfactory bulb, including these regions. It is not known whether the unimpaired performance of 5XFAD mice in olfactory memory was because extra-cellular Aβ pathology was absent in the glomerular, olfactory nerve, and mitral cell layers. Nevertheless, the lack of a correlation between Aβ-pathology within the olfactory bulb and olfactory memory performance indicates that the association between olfactory memory impairment and the severity of Aβ-pathology in the olfactory bulb was not sufficiently robust to be detected in the 5XFAD mouse.

CHAPTER 7 GENERAL DISCUSSION

The important findings from this thesis can be summarized through the answers to four questions related to the use of 5XFAD mice and other transgenic mouse models in AD research.

7.1 Are The Age-related Changes In Motor ability Of The 5XFAD Mouse Model Of AD Replicable?

The present study replicated the motor impairments previously shown in the 5XFAD mice (Jawhar et al., 2005), further establishing the replicability of these phenotypes across different genetic backgrounds (C57BL vs. C57BL x SJL F1) and laboratories. At 9-12 months of age, 5XFAD mice show decreased body-weight, accompanied by motor impairments within multiple domains of motor function, including locomotor activity, motor coordination, balance and grip-strength. We also demonstrated that motor learning is relatively spared at 9 months, but becomes impaired at 12 and 15 months of age. This thesis also identified novel age-related changes in locomotor behaviours, such as decreases in rearing on the open-field, which may provide a simple and rapid measure of motor ability in future studies.

7.2 Are Age-related Changes In Visuo-spatial Learning And Memory In 5XFAD Mice Replicable, And At What Age Does Motor Impairment Confound Performance On The MWM?

5XFAD mice was showed small or moderately sized impairments in visuo-spatial learning at 6 and 9 months of age, replicating previous learning impairments at 4-6 months of age (Ohno et al 2006). Memory performance of 5XFAD mice, however, was not impaired suggesting that either 5XFAD were able to learn the location of the escape platform given training, or that a specific deficit is present in the ability to use extra-maze

cues to navigate to the escape platform. Motor dysfunction in 12-15 month old 5XFAD mice produced impairments in swimming ability, thus confounding learning performance on the MWM. This indicates that a limited window of time (6-9 months of age) is available for the valid assessment of visuo-spatial learning and memory in 5XFAD mice using the MWM. Although land-based tasks such as the Barnes maze and 8-arm Radial maze may be useful alternatives to the MWM, the learning impairment in the 5XFAD mice has yet to be replicated on these tests, and it is not clear if impaired locomotor activity at 12-15 months of age will also confound performance on these tests. Therefore, additional research is needed in characterizing the learning and memory of 5XFAD mice on land-based tasks, so that measurements of cognitive function can be obtained to complement measures of motor dysfunction after 9 months of age.

7.3 Is Olfactory Memory Impaired In 5XFAD Mice Given Neuropathology In The Olfactory Bulb?

Despite the development of Aβ-pathology in the olfactory system of the 5XFAD mouse, no impairments were observed in olfactory learning and memory. Given that age-related decline was not observed on this test in either wild-type or 5XFAD mice, this may suggest that the conditioning paradigm used was too simple. However, it may also suggest that the association between Aβ-pathology in the olfactory system and memory deficits in humans is not robust and/or does not extend to mice, given species differences. Regardless, these results indicate that the olfactory conditioning test should not be used in pre-clinical research given the lack of memory impairment, and caution should be exercised in the use of other olfactory memory tests with the 5XFAD mouse until it can be demonstrated that they have age-related deficits.

7.4 Do Background Genetic Factors Modulate The Expression Of AD-related Behaviours In The 5XFAD Mouse?

The 5XFAD mouse and other transgenic AD-mouse models are typically maintained on a hybrid genetic background consisting of two different inbred mouse strains. These strains often have mutant alleles that produce deleterious behavioural phenotypes and have the potential to interact with AD-transgenes to determine the expression of behavioural phenotypes. We show that when the retinal degeneration mutation is controlled, deficits of 5XFAD mice on the MWM are smaller than previously reported. In addition, both sex and albinism influence learning performance on the MWM, in addition to the learning impairment produced by the APP and/or PS1 transgenes. The mutant *D*ysf^{im} allele, however, did not generally impair performance of mice on tests of motor function. We propose that when uncontrolled, background factors increase the variability of the size of AD-related behavioural impairments in transgenic AD-model mice. Control of these factors will increase the replicability of behavioural phenotypes in AD-model mice, by preventing the overestimation or underestimation of AD-related transgene effects which is expected to occur when the number of mice with deleterious background mutations is larger in the AD-model and wild-type samples, respectively. Likewise, control of background mutations will prevent over- or under-estimation of the efficacy of novel compounds in ameliorating AD-related phenotypes, which can occur when the number of mice with deleterious background mutations is greater in the control or treatment groups, respectively.

7.5 What Are The Benefits And Limitations Of The 5XFAD Mouse?

The 5XFAD mouse is a valuable model of AD, due to the recapitulation of many disease phenotypes including Aβ-pathology, neuroinflammation, cell loss and cognitive impairment. Furthermore, the 5XFAD mouse shows a more rapid development of Aβ-pathology within the brain relative to other mouse models, suggesting that this model may be especially useful for high-throughput screening of novel compounds in reducing plaque load. Furthermore, these mice reliably develop cognitive impairment at 4-6 months of age, and motor impairments at 9-15 months, which can be used as end-points in pre-clinical research, and in the investigation of disease mechanism underlying the changes in cognitive and motor function.

There are several limitations of the 5XFAD mouse model, however, that must be considered in future research. First, the development of Aβ-pathology in the brain follows a very aggressive course, and therefore treatments with subtle effects may not be observed due to the rapid and extensive accumulation of Aβ-pathology. This is especially the case in regions such as the subiculum, where plaque load appears to saturate at 7 months of age at very high levels. Secondly, the rapid development of extra- and intra-cellular Aβ during early life (<2 months of age) may interfere with normal neurodevelopment of this strain, leading to pervasive changes in neural and behavioural phenotypes, thus reducing validity of this mouse as a model for neurodegeneration. Thirdly, cognitive dysfunction in this model was small to moderate in size, suggesting that a considerable number of animals may be needed to detect subtle treatment effects on cognition. Lastly, severe motor impairments may confound the assessment of cognitive

function after 12 months of age, and reduce the longevity of this strain, thus causing considerable attrition of sample size for long-term aging studies.

7.6 Conclusion

Given the predicted epidemic of AD in the growing global population, there is an urgent need to better understand disease mechanism and to develop disease-modifying treatments. Currently, transgenic mice are the most commonly used animal models in AD research, and are used extensively in the pre-clinical assessment of the efficacy of novel therapeutics. The ability to reliably detect the effects of a novel treatment is dependent on the validity of the animal model, and the careful control of potentially confounding factors associated with its use. This thesis provides an extensive characterization of age-related changes in the behavioural phenotype of 5XFAD mice, and confirms that background genetic factors can confound results when not controlled. Therefore, this research provides information needed for the rationale design of experiments that assess the efficiency of novel treatments with 5XFAD mice and other mouse models of AD. To this end, we hope that this research will help accelerate the development of novel treatments for AD.

REFERENCES

Alexandrov PN, Pogue A, Bhattacharjee S, Lukiw WJ (2011) Retinal amyloid peptides and complement factor H in transgenic models of Alzheimer's disease. NeuroReport, 22: 623-627.

Allan LM, Ballard CG, Burn DJ, Kenny RA (2005) Prevalence and severity of gait disorders in Alzheimer's and non-Alzheimer's dementias. Journal of the American Geriatrics Society 53: 1681-1687.

Allen Institute for Brain Science. Allen Mouse Brain Atlas [Internet]. 2012. Available at: http://mouse.brain-map.org. Accessed Nov 1, 2012.

Alzheimer's Association (2013) Alzheimer's Disease Facts and Figures, Alzheimer's & Dementia, Volume 9, Issue 2.

Alzheimer's Society of Canada (2010) Rising Tide: The Impact of Dementia on Canadian Society.

Balducci C, Forloni G (2011) APP transgenic mice: their use and limitations. Neuromolecular Medicine 13: 117-137.

Barlow JZ, Huntley GW (2000) Developmentally regulated expression of Thy-1 structures of the mouse sensory-motor system. Journal of Comparative Neurology 421: 215-233.

Bartus RT (2000) On neurodegenerative diseases, models, and treatment strategies: Lessons learned and lesson forgotten a generation following the cholinergic hypothesis. Experimental Neurology 163: 495-529.

Beermann F, Orlow SJ, Lamoreux ML (2004) The Tyr (albino) locus of the laboratory mouse. Mammalian Genome 15: 749-758.

Bittner RE, Anderson LBB, Burkhardt E, Bashir R, Vafiadaki E, Ivanova S, Raffelsberger T, Maerk I, Höger H, Jung M, Karbasiyan M, Storch M, Lassman H, Moss JA, Davison K, Harrison R, Bushby KMD, Reis A (1999) Dysferlin deletion in SJL mice (SJL-Dysf) defines a natural model for limb girdle muscular dystrophy 2B. Nature Genetics 23: 141-142.

Block ML, Zecca, L, Hong JS (2007) Microglia-mediated neurotoxicity: uncovering the molecular mechanisms. Nature Reviews Neuroscience 8: 57-69.

Braak H, Braak E (1997) Frequency of stages of Alzheimer-related lesions in different age categories. Neurobiology of Aging 18: 351-357.

Brookmeyer R, Corrada MM, Curriero FC, Kawas C (2002) Survival following a diagnosis of Alzheimer disease. Archives of Neurology 59: 1764-1767.

Brookmeyer R, Johnson E, Ziegler-Graham K, Arrighi HM (2007) Forecasting the global burden of Alzheimer's disease. Alzheimer's and Dementia 3: 186-191.

Cai Y, Xue ZQ, Zhang XM, Li MB, Wang H, Luo XG, Cai H, Yan XX (2012) An age-related axon terminal pathology around the first olfactory relay that involves amyloidogenic protein overexpression without plaque formation. Neuroscience 215: 160-173.

Campion D, Flaman J-M, Brice A, Hannequin D, Dubois B, Martin C, Moreau V, Charbonnier F, Didierjean O, Tardieu S, Penet C, Puel M, Pasquier F, Le Doze F, Bellis G, Calenda A, Heilig R, Martinez M, Mallet J, Bellis M, Clerget-Darpoux F, Agid Y, Frebourg T (1995) Mutations of the presenilin 1 gene in families with early-onset Alzheimer's disease. Human Molecular Genetics 4: 2373-2377.

Campsall KD, Mazerolle CJ, Repentingy YD, Kothary R, Wallance VA (2002) Characterization of transgene expression and cre recombinase activity in a panel of Thy-1 promoter-Cre transgenic mice. Developmental Dynamics 224: 135-143.

Christen-Zaech S, Kraftsik R, Pillevuit O, Kiraly M, Martins R, Khalili K, Milkossy J (2003) Early olfactory involvement in Alzheimer's disease. The Canadian Journal of Neurological Sciences 30: 20-25.

Craig-Schapiro R, Fagan AM, Holtzman DM (2009) Biomarkers of Alzheimer's disease. Neurobiology of Disease 35: 128-140.

Dal Forno G, Palermo MT, Donohue JE, Karagiozis H, Zonderman AB, Kawas CH (2005) Depressive symptoms, sex, and risk for Alzheimer's disease. Annals of Neurology 57: 381-387.

Darvesh S, Cash MK, Reid GA, Martin E, Mitnitski A, Geula C (2012) Butyrylcholinesterase is associated with β-Amyloid plaques in the transgenic APP_{SWE}/PSEN1dE9 mouse model of Alzheimer Disease. Journal of Neuropathology and Experimental Neurology 71: 2-14.

Daviglus ML, Plassman BL, Pirzada A, Bell CC, Bowen PE, Burke JR, Connolly ES Jr, Dunbar-Jacob JM, Granieri EC, McGarry K, Patel D, Trevisan M, Williams JW Jr (2011) Risk factors and preventive interventions for Alzheimer disease: state of the science. Archives of Neurology 68: 1185-1190.

Devi L, Ohno M (2010a) Genetic reductions of β-site amyloid precursor protein cleaving enzyme 1 and amyloid-β ameliorate impairment of conditioned taste aversion memory in 5XFAD Alzheimer's disease model mice. European Journal of Neuroscience 31: 110-118.

Devi L, Ohno M (2010b). Phospho-eIF2a level is important for determining abilities of BACE1 reduction to rescue cholinergic neurodegeneration and memory defects in 5XFAD mice. PLoS One 5: e12974.

Devi L, Alldred M, Ginsberg SD, Ohno M (2010c) Sex- and brain region-specific acceleration of β-amyloidogenesis following behavioural stress in a mouse model of Alzheimer's disease. Molecular Brain 3: 34.

Devi L, Ohno M (2012a) 7,8-Dihydroxyflavone, a small-molecule TrkB agonist reverses memory deficits and BACE1 elevation in a mouse model of Alzheimer's disease. Neuropsychopharmacology 37: 434-444.

Devi L, Ohno M (2012b) Mitochondrial dysfunction and accumulation of the β-secretase-cleaved C-terminal fragment of APP in Alzheimer's disease transgenic mice. Neurobiology of Disease 45: 417-424.

Dickerson, B.C. and Eichenbaum, H. (2010). The Episodic Memory System: Neurocircuitry and Disorders. Neuropsychopharmacology, 35: 86-104.

Dickson TC, Vickers JC (2001) The morphological phenotype of β-amyloid plaques and associated neuritic changes in Alzheimer's disease. Neuroscience 105: 99-107.

Djordjevic J, Jones-Gotman M, De Sousa K, Chertkow H (2008) Olfaction in patients with mild cognitive impairment and Alzheimer's disease. Neurobiology of Aging 29: 693-706.

Dubal DD, Broestl L, Worden K (2012) Sex and gonadal hormones in mouse models of Alzheimer's disease: what is relevant to the human condition. Biology of Sex Differences 3: 24.

Eckman CB, Mehta ND, Crook R, Perez-tur J, Prihar G, Pfeiffer E, Graff-Radford N, Hinder P, Yager D, Zenk B, Refolo L, Prada CM, Younkin SG, Hutton M, Hardy J (1997) A new pathogenic mutation in the APP gene (I716V) increases the relative proportion of Aβ42(43). Human Molecular Genetics 6: 2087-2089.

Feldman HH, Jacova C, Robillard A, Garcia A, Chow T, Borrie M, Schipper HM, Blair M, Kertesz A, Chertkow H (2008) Diagnosis and treatment of dementia: 2. Diagnosis. Canadian Medical Association Journal 178: 825-836.

Ferri CP, Prince M, Brayne C, Brodaty H, Fratiglioni L, Ganguli M, Hall K, Hasegawa K, Hendrie H, Yueqin H, Jorm A, Mathers C, Menezes PR, Rimmer E, Scazufca M (2005) Global prevalence of dementia: a Delphi consensus study. The Lancet 366: 2112-2117.

Fleminger S, Oliver DL, Lovestone S, Rabe-Hesketh S, Giora A (2003) Head injury as a risk factor for Alzheimer's disease: the evidence 10 years on; a partial replication. Journal of Neurology, Neurosurgery & Psychiatry 74: 857-862.

Franklin KBJ, Paxinos G (2008) The Mouse Brain in Stereotaxic Coordinates: 3rd Ed. San Diego, CA: Academic Press

Galimberti D, Scarpini E (2011) Disease-modifying treatments for Alzheimer's disease. Therapeutic Advances in Neurological Disorders 4: 203-216.

Galimberti D, Ghezzi L, Scarpini E (2013) Immunotherapy against amyloid pathology in Alzheimer's Disease. In press.

Gallagher M, Burwell R, Burchinal M (1993) Severity of spatial learning impairment in aging: development of a learning index for performance in the Morris water maze. Behavioral Neuroscience. 107: 618-626.

Galvin J, Palamand D, Strider J, Milone M, Pestronk A (2006) The muscle protein dysferlin accumulates in the Alzheimer brain. Acta Neuropathologica 112: 665-671.

Games D, Adams D, Alessandrini R, Barbour R, Borthelette P, Blackwell C, Carr T, Clemens J, Donaldson T, Gillespie F, et al. (1995) Alzheimer-type neuropathology in transgenic mice overexpressing V717F β-amyloid precursor protein. Nature 373: 523-527.

Geerlings MI, den Heijer T, Koudstaal J, Hofman A, Breteler MMB (2008) History of depression, depressive symptoms, and medial temporal lobe atrophy and the risk of Alzheimer disease. Neurology 70: 1258-1264.

Girard SD, Baranger K, Gauthier C, Jacquet M, Bernard A, Escoffler G, Marchetti E, Khestchatisky M, Rivera S, Roman FS (2013) Evidence of early cognitive impairment related to frontal cortex in the 5xFAD mouse model of Alzheimer's disease. Journal of Alzheimer's Disease 33: 781-796.

Goate A, Chartier-Harlin M-C, Mullan M, Brown J, Crawford F, Fidani L, Giuffra L, Haynes A, Irving N, James L, et al. (1991) Segregation of missense mutation in the amyloid precursor protein gene with familial Alzheimer's disease. Nature 349: 704-706.

Green KM, Billings LM, Roozendaal B, McGaugh JL, LaFerla FM (2006) Glucocorticoids increase amyloid-β and tau pathology in a mouse model of Alzheimer's disease. The Journal of Neuroscience 26: 9047-9056.

Guérin O, Andrieu S, Schneider SM, Milano M, Boulahssass, Brocker P, Vellas B (2005) Different modes of weight loss in Alzheimer disease: a prospective study of 395 patients. The American Journal of Clinical Nutrition 82: 435-441.

Hall AM, Roberson ED (2012) Mouse models of Alzheimer's disease. Brain Research Bulletin 88: 3-12.

Hardy JA, Higgins GA (1992) Alzheimer's disease: The amyloid cascade hypothesis. Science 256: 184-185.

Hardy JA, Higgins GA (2002) The amyloid hypothesis of Alzheimer's disease: Progress and problems on the road to therapeutics. Science 297: 353-356.

Hensley K (2010). Neuroinflammation in Alzheimer's Disease: Mechanisms, Pathologic Consequences, and Potential for Therapeutic Manipulation. Journal of Alzheimer's Disease 21: 1-14.

Hillmann A, Hahn S, Schilling S, Hoffman T, Demuth HU, Bulic B, Schneider-Axmann T, Bayer TA, Weggen S, Wriths O (2012) No improvements after chronic ibuprofen treatment in the 5xFAD mouse model of Alzheimer's disease. Neurobiology of Aging 33: 833.e39-833.e50.

Hof PR, Morrison JH, Cox K (1990) Quantitative analysis of a vulnerable subset of pyramidal neurons in Alzheimer's disease: I. Superior frontal and inferior temporal cortex. Journal of Comparative Neurology 301: 44-54.

Hongpaisan J, Sun MK, Alkon DL (2011) PKC ε Activation Prevents Synaptic Loss, Aβ Elevation and Cognitive Deficits in Alzheimer's Disease Transgenic Mice. The Journal of Neuroscience 31: 630-643.

Hsiao K, Chapman P, Nilsen S, Eckman C, Harigaya Y, Younkin S, Yang F, Cole G (1996) Correlative memory deficits, Aβ elevation, and amyloid plaques in transgenic mice. Science 274: 99-102.

Hu X, Hicks CW, He W, Wong P, Macklin WB, Trapp BD, Yan R (2006) Bace1 modulates myelination in the central and peripheral nervous system. Nature Neuroscience 9: 1520-1524.

Igoudjil A, Magrané J, Fischer LR, Kim HJ, Hervias I, Dumont M, Cortez C, Glass JD, Starkov AA, Manfredi G (2011) In vivo pathogenic role of mutant SOD1 localized in the mitochondrial intermembrane space. The Journal of Neuroscience 31: 15826-15837.

Iordanescu G, Venkatasubramanian PN, Wyrwicz AM (2011) Automatic segmentation of amyloid plaques in MR images using unsupervised support vector machines. Magentic Resonance in Medicine 67: 1794-1802.

Jankowsky JL, Fadale DJ, Anderson J, Xu GM, Gonzales V, Jenkins NA, Copeland NG, Lee MK, Younkin LH, Wagner SL, Younkin SG, Borchelt DR (2004) Mutant presenilins specifically elevate the levels of the 42 residue beta-amyloid peptide in vivo: evidence for augmentation of a 42-specific gamma secretase. Human Molecular Genetics 13: 159-170.

Jawhar S, Trawicka A, Jenneckens C, Bayer TA, Wriths O (2012) Motor deficits, neuron loss, and reduced anxiety coinciding with axonal degeneration and intraneuronal Aβ aggregation in the 5XFAD mouse model of Alzheimer's disease. Neurobiology of Aging 33: 196.e29-40.

Jawhar S, Wirths O, Schilling S, Graubner S, Demuth HU, Bayer TA (2011) Overexpression of glutaminyl cyclase, the enzyme responsible for pyroglutamate Aβ formation, induces behavioural deficits, and glutaminyl cyclase knock-out rescues the behavioural phenotype in 5xFAD mice. The Journal of Biological Chemistry 286: 4454-4460.

Johansson L, Guo X, Waern M, Östling S, Gustafson D, Bengtsson C, Skoog I (2010) Midlife psychology stress and risk of dementia: A 35-year longitudinal population study. Brain 133: 2217-2224.

Jonasson Z (2005) Meta-analysis of sex differences in rodent models of learning and memory: a review of behavioural and biological data. Neuroscience & Biobehavioral Reviews 28: 811-825.

Joyashiki E, Matsuya Y, Tohda C (2011) Sominone improves memory impairments and increases axonal density in Alzheimer's disease model mice, 5XFAD. International Journal of Neuroscience 121: 181-190.

Kaczorowski CC, Sametsky E, Shah S, Vassar R, Disterhoft JF (2009) Mechanism underlying basal and learning intrinsic excitability in a mouse model of Alzheimer's disease. Neurobiology of Aging 32: 1452-1465.

Kaduszkiewicz H, Zimmermann T, Beck-Bornholdt HP, van den Bussche H. (2005) Cholinesterase inhibitors for patients with Alzheimer's disease: systematic review of randomised clinical trials. British Medical Journal, 331: 321.

Kalinin S, Polak PE, Lin SX, Sakharkar AJ, Pandey SC, Feinsein DL (2012) The noradrenaline precursor L-DOPS reduces pathology in a mouse model of Alzheimer's disease. Neurobiology of Aging 33: 1651-1663.

Kaskie B, Storandt M (1995) Visuospatial deficit in dementia of the Alzheimer type. Archives of Neurology 52: 422-425.

Kaufer DL, Cummings JL, Christine D, Bray T, Castellon S, Masterman D, MacMillan A, Ketchel P, DeKosky ST (1998) Assessing the impact of neuropsychiatric

symptoms in Alzheimer's disease: the Neuropsychiatric Inventory Caregiver Distress Scale. Journal of the American Geriatrics Society 46: 210-215.

Kimura R, Ohno M (2009) Impairments in remote memory stabilization precede hippocampal synaptic and cognitive failures in 5XFAD Alzheimer mouse model. Neurobiology of Disease 33: 229-235.

Kimura R, Devi L, Ohno M (2010) Partial reduction of BACE1 improves synaptic plasticity, recent and remote memories in Alzheimer's disease transgenic mice. Journal of Neurochemistry 113: 248-261.

Kovács T, Cairns NJ, Lantos PL (1999) β-Amyloid deposition and neurofibrillary tangle formation in the olfactory bulb in ageing and Alzheimer's disease. Neuropathology and Applied Neurobiology 25: 481-491.

Kovács T (2013) The olfactory system in Alzheimer's disease: Pathology, pathophysiology and pathway for therapy. Translational Neuroscience 4:34-45.

Langa KM, Chernew ME, Kabeto MU, Herzog AR, Ofstedal MB, Willis RJ, Wallace RB, Mucha LM, Straus WL, Fendrick AM (2001) National estimates of the quantity and cost of informal caregiving for the elderly with dementia. Journal of General Internal Medicine 16: 770-778.

Lemmers MAM, Sierksma ASR, Rutten BPF, Dennissen F, Steinbusch HWM, Lucassen PJ, Schmitz C (2011) Age-related changes of neurons numbers in the frontal cortex of a transgenic mouse model of Alzheimer's disease. Brain Structure and Function 216: 227-237.

Larner AJ, Doran M (2006) Clinical phenotypic heterogeneity of Alzheimer's disease associated with mutations of the presenilin-1 gene. Journal of Neurology, 253: 139-158.

Lindsay J, Laurin D, Verreault R, Hébert R, Helliwell B, Hill GB, McDowell I (2002) Risk factors for Alzheimer's disease: A prospective analysis from the Canadian Study of Health and Aging. American Journal of Epidemiology 156: 445-453.

Maei HR, Zaslavsky K, Teixeira CM, Frankland PW (2009) What is the most sensitive measure of water maze probe test performance? Frontiers in Integrative Neuroscience 3: 4.

Mandillo S, Tucci V, Hölter SM, Meziane H, Al Banchaabouchi M, Kallnik M, Lad H, Nolan PM, Abdel-Mouttalib O, Coghill E, Gale K, Golini E, Jacquot S, Krezel W, Parker A, Riet F, Schneider I, Marazziti D, Auwerx J, Brown SDM, Chambon P, Rosenthal N, Tocchini-Valentini G, Wurst W (2008) Reliability, robustness, and reproducibility in mouse behavioral phenotyping: a cross-laboratory study. Physiological Genomics 34: 243-255.

Maurer K, Voik S, Gerbaldo H. (1997) Auguste D and Alzheimer's disease. The Lancet 349: 1546-1549.

Mesholam RI, Moberg PJ, Mahr RN, Doty RL (1998) Olfaction in neurodegenerative disease: A meta-analysis of olfactory functioning in Alzheimer's and Parkinson's diseases. Archives of Neurology 55: 84-90.

McFadyen MP, Kusek G, Bolivar VJ, Flaherty L (2003) Differences among eight inbred strains of mice in motor ability and motor learning on a rotorod. Genes Brain Behavior 2: 214-219.

McKhann GM, Knopman DS, Chertkow H, Hyman BT, Jack CR Jr, Kawas CH, Klunk WE, Koroschetz WJ, Manly JJ, Mayeux R, Mohs RC, Morris JC, Rossor MN, Scheltens P, Carrillo MC, Thies B, Weintraub S, Phelps CH (2011) The diagnosis of dementia due to Alzheimer's disease: recommendations from the National Institute on Aging-Alzheimer's Association workgroups on diagnostic guidelines for Alzheimer's diease. Alzheimers & Dementia 7: 263-269.

Minati L, Edington T, Bruzzone MG, Giaccone G (2009) Current concepts in Alzheimer's Disease: A multidisciplinary review. American Journal of Alzheimer's Disease & Other Dementias 24: 95-121.

Mitchell SL (1999) Extrapyramidal features in Alzheimer's disease. Age and Ageing 28: 401-409.

Moechars D, Lorent K, De Strooper B, Dewachter I, Van Leuven F (1996) Expression in brain of amyloid precursor protein mutated in the alpha-secretase site causes disturbed behavior, neuronal degeneration and premature death in transgenic mice. The European Molecular Biology Organization Journal 15: 1265-1274.

Monacelli AM, Cushman LA, Kavcic V, Duffy CJ (2003) Spatial disorientation in Alzheimer's disease: the remembrance of things passed. Neurology 61: 1491-1497.

Morris RGM, Schenk F, Tweedle F, Jarrard LE (1990) Ibotenate lesions of hippocampus and/or subiculum: dissociating components of allocentric spatial learning. European Journal of Neuroscience 2: 1016-1028.

Mouton PR, Martin LJ, Calhoun ME, Dal Forno G, Price DL (1998) Cognitive decline strongly correlates with cortical atrophy in Alzheimer's dementia. Neurobiology of Aging 19: 371-377.

Mucke L, Masliah E, Yu GQ, Mallory M, Rockenstein EM, Tatsuno G, Hu K, Kholodenko D, Johnson-Wood K, McConlogue L (2000) High-level neuronal expression of abeta 1-42 in wild-type human amyloid protein precursor transgenic

mice: synaptotoxicity without plaque formation. The Journal of Neuroscience 20: 4050-4058.

Mullan M, Crawford F, Axelman K, Houlden H, Lilius L, Winbalt B, Lannfelt L (1992) A pathogenic mutation for probably Alzheimer's disease in the APP gene at the N-terminus of β-Amyloid. Nature Genetics 1: 345-347.

Müller UC, Zheng H (2012) Physiological functions of APP family proteins. Cold Spring Harbour Perspectives Medicine 2: a006288.

Oakley H, Cole SL, Logan S, Maus E, Shao P, Craft J, Guillozet-Bongaarts A, Ohno M, Disterhoft J, Van Eldik L, Berry R, Vassar R (2006) Intraneuronal β-amyloid aggregates, neurodegeneration, and neuron loss in transgenic mice with five familial Alzheimer's disease mutations: Potential factors in amyloid plaque formation. The Journal of Neuroscience 26: 10129-10140.

O'Connor T, Sadleir KR, Maus E, Velliquette RA, Zhao J, Cole SL, Eimer WA, Hitt B, Bembinster LA, Lammich S, Lichtenthaler SF, Hébert SS, Strooper BD, Haas C, Bennett DA, Vasser R (2008) Phosphorylation of the translation initiation factor elF2α increases BACE1 levels and promotes amyloidogenesis. Neuron 60: 988-1009.

Oddo S, Caccamo A, Shepherd JD, Murphy MP, Golde TE, Kayed R, Metherate R, Mattson MP, Akbari Y, LeFerla FM (2003) Triple-Transgenic model of Alzheimer's disease with plaques and tangles: Intracellular Aβ and synaptic dysfunction. Neuron 39: 409-421.

Ohno M, Chang L, Tseng W, Oakley H, Citron M, Klein W, Vassar R, Disterhoft J (2006) Temporal memory deficts in Alzheimer's mouse models: rescue by genetic deletion of BACE1. European Journal of Neuroscience 23: 251-260.

Ohno M, Cole S, Yasvonia M, Zhao J, Citron M, Berry R, Disterhoft J, Vassar R (2007) BACE1 gene deletion prevents neuron loss and deficits in 5XFAD APP/PS1 transgenic mice. Neurobiology of Disease 26: 134-145.

Ohno M (2009) Failures to reconsolidate memory in a mouse model of Alzheimer's disease. Neurobiology of Learning and Memory 92: 455-459.

O'Leary TP, Brown RE (2009) Visuo-spatial learning and memory deficits on the Barnes maze in the 16-month-old APPswe/PS1dE9 mouse model of Alzheimer's disease. Behavioral Brain Research 201: 120-127.

O'Leary TP, Brown RE (2012) The effects of apparatus design and test procedure on learning and memory performance of C57BL/6J mice on the Barnes maze. Journal of Neuroscience Methods 203: 315-324.

O'Leary TP, Brown RE (2013) Optimization of apparatus design and behavioural measures for the assessment of visuo-spatial learning and memory of mice on the Barnes maze. Learning and Memory 20: 85-96.

Österman H (2010) Neuropathology and olfactory performance of Tg6799 strain of Alzheimer's disease model mice. Masters Thesis, Molecular Genetics and Physiology 2010, Department of Neurobiology, Yale University School of Medicine.

Pallier PN, Drew CJ, Morton AJ (2009) The detection and measurement of locomotor deficits in a transgenic mouse model of Huntington's disease are task- and protocol-dependent: influence of non-motor factors on locomotor function. Brain Research Bulletin 78: 347-355.

Pearson RC, Esiri MM, Hiorns RW, Wilcock GK, Powell TP (1985) Anatomical correlates of the distribution of the pathological changes in the neocortex in Alzheimer disease. Proceedings of the National Academy of Sciences 82: 4531-4534.

Phillips M, Boman E, Osterman H, Willhite D, Laska M (2011) Olfactory and visuo-spatial learning and memory performance in two strains of Alzheimer's disease model mice – A longitudinal study. PLoS One 6: e19567

Poncet C, Rossier J, Antonietti JP, Von Gunten A (2012) Personality traits and behavioral and psychological symptoms in patients at an early stage of Alzheimer's disease. International Journal of Geriatric Psychiatry 28: 276-283.

Porter VR, Buxton WG, Fairbanks LA, Strickland T, O'Connor SM, Rosenberg-Thompson S, Cummings JL (2003) Frequency and characteristics of anxiety among patients with Alzheimer's disease and related dementias. Journal of Neuropsychiatry and Clinical Neuroscience 15: 180-186.

Rayavarapu S, Van der meulen JH, Gordish-Dressman H, Hoffman EP, Nagaraju K, Knoblach SM (2010) Characterization of dysferlin deficient SJL/J mice to assess preclinical drug efficacy: Fasudil exacerbates muscle disease phenotype. PLoS One, 5: e12981.

Rebsam A, Bhansali P, Mason CA (2012) Eye-specific projections of retinogeniculate axons are altered in albino mice. The Journal of Neuroscience 32: 4821-4826.

Reed MN, Peng L, Kotilinek L, Ashe KH (2010) Effect size of reference memory deficits in the Morris Water Maze in Tg2576 mice. Behavioral Brain Research 212: 115-120.

Roddick K (2010) Assessing olfactory learning and memory in the 5XFAD mouse model of Alzheimer's disease. Masters Thesis, Psychology and Neuroscience 2012, Department of Psychology and Neuroscience, Dalhousie University.

Rogaev EI, Sherrington R, Rogaeva EA, Levesque G, Ikeda M, Liang Y, Chi H, Holman K, Tsuda T, et al. (1995) Familial Alzheimer's disease in kindreds with missense mutations in a gene on chromosome 1 related to the Alzheimer's disease type 3 gene. Nature 376: 775-778.

Rogers J, Morrison JH (1985) Quantitative morphology and regional and laminar distribution of senile plaques in Alzheimer's disease. The Journal of Neuroscience 5: 2801-2808.

Rosemblat S, Durham-Pierre D, Gardner JM, Nakatsu Y, Brilliant MH, Orlow SJ (1994) Identification of a melanosomal membrane protein encoded by the pink-eyed dilution (type II oculocutaneous albinism) gene. Proceedings of National Academy of Science 91: 12071-12075.

Rustay NR, Waahlsten D, Crabbe JC (2003) Influence of task parameters on rotarod performance and sensitivity to ethanol in mice. Behavioral Brain Research 141: 237-249.

Ryman D, Lamb BT (2006) Genetic and environmental modifiers of Alzheimer's disease phenotypes in the mouse. Current Alzheimer Research 3: 465-473.

Sadleir KR, Vasser R (2012) Cdk5 protein inhibition and Aβ42 increase BACE1 protein level in primary neurons by a post-transcriptional mechanism. Journal of Biological Chemistry 287: 7224-7235.

Schellinck HM, Forestell CA, LoLordo VM (2001) A simple and reliable test of olfactory learning and memory in mice. Chemical Senses 26: 663-672.

Schilling S, Zeitschel U, Hoffmann T, Heiser U, Francke M, Kehlen A, Holzer M, et al. (2008). Glutaminyl cyclase inhibition attenuates pyroglutamate A[beta] and Alzheimer's disease-like pathology. Nature Medicine: 14, 1106–1111.

Schneider JA, Arvanitakis Z, Bang W, Bennet DA (2007) Mixed brain pathologies account for most dementia cases in community-dwelling older persons. Neurology 69: 2197-2204.

Seo JS, Leem YH, Lee KW, Kim SW, Lee JK, Han PL (2010) Severe motor neuron degeneration in the spinal cord of the Tg2576 mouse model of Alzheimer's disease. Journal of Alzhiemers Disease 21: 263-276.

Serby M, Larson P, Kalkstein D (1991) The nature and course of olfactory deficits in Alzheimer's disease. American Journal of Psychiatry 148: 357-360.

Shao CY, Mirra SS, Sair HBR, Sacktor TC, Sigurdsson EM (2011) Post-synaptic degeneration as revealed by PSD-95 reduction occurs after Aβ and tau pathology in transgenic mouse models of Alzheimer's disease. Acta Neuropathologica 122: 285-292.

Sherrington R, Rogaev EI, Liang Y, Rogaeva EA, Levesque G, Ikeda M, Chi H, Lin C, Li G, Holman K, Tsuda T, Mar L, Foncin JF, Bruni AC, Montesi MP, Sorbi S, Rainero I, Pinessi L, Nee L, Chumakov I, Pollen D, Brookes A, Sanseau P, Polinsky RJ, Wasco W, Da Silva HA, Haines JL, Perkicak-Vance MA, Tanzi RE, Roses AD, Fraser PE, Rommens JM, St George-Hyslop PH (1995) Cloning of a gene bearing missense mutation in early-onset familial Alzheimer's disease. Nature 375: 754-760.

Shukla V, Zheng YL, Mishra SK, Amin ND, Steiner J, Grant P, Kesavapany S, Pant HC (2013) A truncated peptide from p35, a Cdk5 activator, prevents Alzheimer's disease phenotypes in model mice. Federation of American Societies for Experimental Biology Journal 27: 174-186.

Stewart S, Cacucci F, Lever C (2011) Which memory task for my mouse? A systematic review of spatial performance in the Tg2576 Alzhiemer's mouse model. Journal of Alzheimer's Disease 26: 105-126.

Stover KR, Brown RE (2012) Age-related changes in visual acuity, learning and memory in the APPswe/PS1dE9 mouse model of Alzheimer's disease. Behavioral Brain Research 231: 75-85.

Strittmatter WJ, Saunders AM, Schmechel D, Pericak-Vance M, Enghild J, Salvesen GS, Roses AD (1993) Apolopoprotein E: High-avidity binding to β-amyloid and increased frequency of type 4 alelle in late-onset familial Alzheimer's disease. Proceedings of National Academy of Science 90: 1977-1981.

Tanzi RE (2012) The genetics of Alzheimer's disease. Cold Spring Harbour Perspectives Medicine 2: a006296.

Terry RD, Masliah E, Salmon DP, Butters N, DeTeresa R, Hill R, Hansen LA, et al. (1991) Physical basis of cognitive alterations in Alzheimer's disease: Synapse loss is the major correlate of cognitive impairment. Annals of Neurology 30: 572-580.

Thal DR, Rüb U, Orantes M, Braak H (2002) Phases of Aβ-deposition in the human brain and its relevance for the development of AD. Neurology 58: 1791-1800.

Thangavel R, Sahu SK, Van Hoesen GW, Zaheer A (2009) Loss of nonphosphorylated neurofilament immunoreactivity in temporal cortical areas in Alzheimer's disease. Neuroscience 160: 427-433.

Tohda C, Nakada R, Urano T, Okonogi A, Kuboyama T (2011) Kamikihi-to (KKT) rescues axonal and synaptic degeneration associated with memory impairment in a mouse model of Alzheimer's disease, 5xFAD. International Journal of Neuroscience 121: 641-648.

Urano T, Tohda C (2010) Icariin improves memory impairment in Alzheimer's disease model mice (5XFAD) and attenuates amyloid β-induced neurite atrophy. Phytotherapy Research 24: 1658-1663.

Vafiadaki E, Reis A, Keers S, Harrison R, Anderson LVB, Raffelsberger T, Ivanova S, Hoger H, Bittner RE, Bushby K, Bashir R (2001) Cloning of the mouse dysferlin gene and genomic characterization of the SJL-Dysf mutation. NeuroReport 12: 625-629.

Van Vilet D, de Vugt ME, Aalten P, Bakker C, Pijnenburg YA, Vernooij-Dassen MJ, Koopmans RT, Verhey FR (2012) Prevalence of neuropsychiatric symptoms in young-onset compared to late-onset Alzhiemer's disease – Part 1: Findings of the two-year longitudinal NeedYD-Study. Dementia and Geriatric Cognitive Disorders 34: 319-327.

Vlad SC, Miller DR, Kowall NW, Felson DT (2008) Protective effects of NSAIDs on the development of Alzheimer disease. Neurology 70: 1672-1677.

Wadsworth LP, Lorius N, Donovan NJ, Locascio JJ, Rentz DM, Johnson KA, Sperling RA, Marshall GA (2012) Neuropsychiatric symptoms and global functional impairment along the Alzheimer's continuum. Dementia and Geriatric Cognitive Disorders 34: 96-111.

Wahlsten D (2011) Mouse behavioural testing: How to use mice in behavioural neuroscience. Elsevier Inc., Burlington MA, pp 75-105.

Walsh DM, Klyubin I, Fadeeva JV, Cullen WK, Anwyl R, Wolfe MS, Rowan MJ, Selkoe DJ (2002) Naturally secreted oligomers of amyloid beta protein potently inhibit hippocampal long-term potentiation in vivo. Nature 416: 535-539.

Weintraub S, Wicklund AH, Salmon DP (2012) The neuropsychological profile of Alzheimer Disease. Cold Spring Harbor Perspectives in Medicine 2: a006171.

Wesson DW, Levy E, Nixon RA, Wilson DA (2010) Amyloid-β burden in an Alzheimer's disease mouse model. The Journal of Neuroscience 30: 505-514.

West MJ, Kawas CH, Stewart WF, Rudow GL, Troncoso JC (2004) Hippocampal neurons in pre-clinical Alzheimer's disease. Neurobiology of Aging 25: 1205-1212.

Whishaw IQ, Cassel JC, Jarrad LE (1995) Rats with fimbria-fornix lesions display a place response in a swimming pool: dissociation between getting there and knowing where. The Journal of Neuroscience 15: 5779-5788.

Whittnam JL, Portelius E, Zetterberg H, Gustavsson MK, Schilling S, Koch B, Demuth HU, Blennow K, Wirths O, Bayer TA (2012) Pyroglutamate amyloid β (Aβ) aggravates behavioural deficits in transgenic amyloid mouse model for Alzheimer disease. The Journal of Biological Chemistry 287: 8154-8162.

Wilson RS, Arnold SE, Schneider JA, Boyle PA, Buchman AS, Bennett DA (2009) Olfactory impairment in presymptomatic Alzheimer's disease. Annals of the New York Academy of Sciences 1170: 730-735.

Wong AA, Brown RE (2007) Age-related changes in visual acuity, learning and memory in the C57Bl/6J and DBA/2J mice. Neurobiology of Aging 28: 1577-1593.

Woo DC, Lee SH, Lee DW, Kim SY, Kim GY, Rhim HS, Choi CB, Kim HY, Lee CU, Choe BY (2010) Regional metabolic alteration of Alzheimer's disease mouse brain expressing mutant human APP-PS1 by HR-MAS. Behavioural Brain Research 211: 125-131.

World Health Organization and Alzheimer's Disease International (2012). Dementia: A Public Health Priority.

Yassine N, Lazaris A, Dorner-Ciossek C, Després O, Meyer L, Maitra M, Mensah-Nyagan AG, Cassel JC, Mathis C (2013) Detecting spatial memory deficits beyond blindness in tg2576 Alzheimer mice. Neurobiology of Aging 34: 716-730.

Zhao J, Fu Y, Yasvoina M, Shao P, Hitt B, O'Connor T, Logan S, Maus E, Citron M, Berry R, Binder L, Vasser R (2007) β-Site amyloid precursor protein cleaving enzyme 1 levels become elevated in neurons surrounding amyloid plaques: Implication for Alzheimer's disease pathogenesis. The Journal of Neuroscience 27: 3639-3649.

Zhang XM, Cai Y, Xiong K, Cai H, Luo XG, Feng JC, Clough RW, Struble RG, Patrylo PR, Yan XX (2009) β-Secretase-1 elevation in transgenic mouse models of Alzheimer's disease is associated with synaptic/axonal pathology and amyloidogenesis: implications for neuritic plaque development. European Journal of Neuroscience 30: 2271-2283.